THESIS FOR THE DEGREE OF DOCTOR OF PHILOSOPHY

ROLES OF INTERMOLECULAR INTERACTIONS IN AMYLOID FIBRIL FORMATION MECHANISMS

TONY ERIK ROGER WERNER

Department of Biology and Biological Engineering

CHALMERS UNIVERSITY OF TECHNOLOGY

Gothenburg, Sweden 2020

ROLES OF INTERMOLECULAR INTERACTIONS IN AMYLOID FIBRIL FORMATION MECHANISMS

TONY ERIK ROGER WERNER

ISBN 978-91-7905-388-8

Doktorsavhandlingar vid Chalmers tekniska högskola

Ny serie nr 4855

ISSN 0346-718X

Department of Biology and Biological Engineering

Chalmers University of Technology

SE-41296 Gothenburg

Sweden

Telephone + 46 (0)31-772 1000

Cover:
High-resolution NMR structures of Ca^{2+}-bound Atlantic cod β-parvalbumin (*G. morhua*, PDB: 2MBX, blue) and rat apo-β-parvalbumin (PDB: 2NLN, red), depicting the ligand loss-induced structural change that results in the buried thiol becoming exposed to the environment, thus triggering amyloid fibril formation through disulfide bond formation. Ca^{2+} is depicted as green spheres, and the yellow stick represents the cysteine sidechain. Molecular graphics performed with UCSF Chimera.

Chalmers digitaltryck
Gothenburg, Sweden 2020

ROLES OF INTERMOLECULAR INTERACTIONS IN AMYLOID FIBRIL FORMATION MECHANISMS

TONY ERIK ROGER WERNER

Department of Biology and Biological Engineering
Chalmers University of Technology

Abstract

Amyloid fibrils, a major pathological feature of several neurodegenerative disorders, are highly stable, insoluble aggregates of misfolded proteins. The formation of such aggregates involves a complex equilibrium between protein monomers, different on- and off-pathway transient oligomeric species, and amyloid fibrils. Amyloid fibril formation *in vivo* may be induced by a myriad of factors, including oxidative stress and alteration of metal ion homeostasis.

The work in this thesis involves biophysical studies of the amyloid fibril formation mechanisms of the natively folded Ca^{2+}-binding fish protein, β-parvalbumin (β-PV); and how it is modulated by cell conditions including macromolecular crowding and stabilizing osmolytes, both of which tend to stabilize compact folded protein conformations through an excluded volume- or osmophobic effect, respectively. It was found that when β-PV aggregation is triggered, as occurs upon Ca^{2+} removal from the protein, spontaneous cystine formation between β-PV monomers initiates the process, whereafter the dimers template monomers into the amyloid conformation, resulting in polymerization. Furthermore, it was discovered that both excluded volume and the osmophobic effect promote the overall aggregation of β-PV, likely by facilitating protein dimerization. Together, these results highlight the potentially detrimental effects of ligand loss and oxidative stress on proteins, whose destabilization might induce amyloid fibril formation that is further exacerbated by otherwise protective in-cell conditions.

Amyloid fibril formation by fish β-PV at acidic pH is thought to confer protection against proteolytic degradation in the human gut. In addition, since recent evidence suggests that many incidences of the neurodegenerative disorder Parkinson's disease (PD) might originate from the gut, a putative interaction between β-PV and α-synuclein (αS), which forms amyloid fibrils in PD, was tested *in vitro*. Amyloid fibrils of β-PV block αS aggregation, likely by sequestering αS monomers onto the surface, thus potentially implying a protective effect of a diet rich in fish against PD. Lastly, in light of the fact that copper is reduced in affected brain regions of PD patients, as well as the presence of copper binding sites on αS, aggregation of αS in the presence of the endogenous cytoplasmic copper chaperone, Atox1, was studied. It was found that copper-Atox1 interacts with αS and can prevent its aggregation, while apo-Atox1 is ineffective, indicating a copper dependent interaction. The reduced copper levels associated with PD might thus play a role in PD progression by abolishing this protective interaction.

Keywords: Amyloid fibrils, aggregation, Atox1, α-synuclein, β-parvalbumin, disulfide-bonds, macromolecular crowding, osmolytes, Parkinson's disease, protein interactions

List of publications

This thesis is based on the work contained in the following papers:

I. **Amyloid formation of fish β-parvalbumin involves primary nucleation triggered by disulfide-bridged dimers**
Tony E. R. Werner, David Bernson, Elin K. Esbjörner, Sandra Rocha, Pernilla Wittung-Stafshede, *Proc. Natl. Acad. Sci. U. S. A.* **117** (45), 27997-28004 (2020). Doi: 10.1073/pnas.2015503117

II. **Response to crowded conditions reveals compact nucleus for amyloid formation of folded protein**
Tony Werner, Istvan Horvath, Pernilla Wittung-Stafshede. *Manuscript*.

III. **Abundant fish protein inhibits α-synuclein amyloid formation**
Tony Werner, Ranjeet Kumar, Istvan Horvath, Nathalie Scheers, Pernilla Wittung-Stafshede, *Sci. Rep*, **8**, 5465 (2018). Doi: 10.1038/s41598-018-23850-0

IV. **Copper chaperone blocks amyloid formation via ternary complex**
Istvan Horvath, Tony Werner, Ranjeet Kumar, Pernilla Wittung-Stafshede, *Q. Rev. Biophys*, **51**, E6 (2018). Doi: 10.1017/S0033583518000045

Additional paper not included in this thesis:

V. Crosstalk Between Alpha-Synuclein and Other Human and Non-Human Amyloidogenic Proteins: Consequences for Amyloid Formation in Parkinson's disease
Tony Werner, Istvan Horvath, Pernilla Wittung-Stafshede, *J. Parkinsons Dis.*, **10** (3), 819-830 (2020). Doi: 10.3233/JPD-202085

Contribution report

I. Conceived the idea (together with D.B.), designed and performed the experiments (except AFM), and contributed to the data analysis and paper writing.

II. Contributed to the design of the experiments and performed the experiments (except AFM). Contributed to the analysis of the data and paper writing.

III. Contributed to the design of the experiments and performed the experiments (except TEM). Contributed to the analysis of the data and paper writing.

IV. Contributed to the design, execution, and data analysis of the experiments.

Preface

This thesis was submitted for the partial fulfilment for the degree of Doctor of Philosophy. It is based on work carried out between May 2016 and December 2020 at the department of Biology and Biological Engineering, Chalmers University of Technology, under the supervision of Professor Pernilla Wittung-Stafshede. The research was funded by Knut and Alice Wallenbergs Foundation and the Swedish Research Council.

Tony Werner
December 2020

1. Introduction

Prior to the emergence of the germ theory of disease, which resulted in improved public health and hygiene, as well as the invention of vaccines and antibiotics, infections were the biggest challenge to human health (1). However, with the epidemiological transition after the industrial revolution, together with medical advances, followed an increasing number of chronic, noncommunicable and recurrent diseases, *e.g.* cancer and neurodegenerative diseases (1). Neurodegenerative diseases pose a major burden on the well-being of the afflicted, their family and friends, and both private and national economy, with the latter being expected to increase nearly five-fold from 2016 to 2050 for dementia related diseases alone (2). A common thread among many neurodegenerative diseases is the appearance of highly stable protein deposits known as amyloids that occurs concomitantly with loss of neurons (3). Although, amyloids are not restricted to neuronal environments. For example, they have been found to form in the pancreas in type 2 diabetics (4), and may even be systemic as in the case of AL amyloidosis (5). While amyloids have historically been viewed through the lens of pathogenicity, it has become increasingly apparent that organisms from all kingdoms of life exploit the amyloid structure for function. For example, amyloids have been found to be components of human melanosome ultra-structures (6) and bacterial biofilms (7).

Despite being detected as far back as 1854 by Rudolf Virchow and proven to be protein deposits in 1859 (8-10), it was not until 1959 and onwards that amyloids were structurally characterized, and experimental detection methods were developed (10, 11). Despite these advances and tremendous efforts into understanding the mechanisms of amyloid formation in the recent decades, no cure exists (12). Part of the reason why it has been so difficult to treat these protein deposits is the sheer complexity of the amyloid formation mechanism, where amyloid fibril formation may be induced from a myriad of factors, that are not necessarily mutually exclusive, such as oxidative stress (13, 14), chemical insult (15) and alterations to various homeostases, *e.g.* dysregulation of ion homeostasis (16) or proteostasis (17). In addition, the pathway to forming amyloid fibrils generally involves complex equilibria between monomers and different oligomer and fibril species (17). However, the complexity of amyloid fibril formation and propagation is not only limited to molecular mechanisms and local cellular environments. Recent understanding of Parkinson's disease (PD) has revealed a significant involvement of the enteric nervous system in the development of the disease, as researchers have found that disconnecting the vagus nerve connecting the gastro-intestinal system to the brain results in a major reduction of PD incidences (18-20). Additionally, amyloid fibrils of the protein central to PD, α-synuclein (αS), have been found in the gut and along the vagus nerve (21-23). Several factors may thus influence the initiation of PD, including gut microbiota and compounds ingested through diet (20).

The aim of the work in my thesis has been to provide a deeper understanding into amyloid formation mechanisms, and to study the interaction of an exogenous (fish β-parvalbumin) and endogenous (Atox1) protein with the protein central to PD, αS. The observations presented in the thesis are based on work described in four research papers (denoted **paper I-IV**). **Paper I** shows that folded β-parvalbumin (β-PV) monomers form disulfide-bridged dimers, when the Ca^{2+} is absent, in an enzyme-independent manner, resulting in highly amyloidogenic species capable of forming nuclei that may recruit monomers. Traditionally, investigations into the kinetics of amyloid fibril formation have been conducted in pure, dilute, solutions. While necessary to build the foundation of our understanding, several factors present in cells are absent, such as the excluded volume effect by macromolecular crowding, and protein interactions that may modulate this behavior. In order to simulate more cell-like environments, macromolecular crowding agents were employed, and it was observed that the excluded volume effect drastically promotes amyloid fibril formation of the folded protein, β-PV (**paper II**). Furthermore, investigating the interaction of fish β-PV with αS showed that β-PV in an amyloid form is capable of inhibiting αS amyloid fibril formation *in vitro* (**paper III**). Lastly, studying the interaction between the copper chaperone, Atox1, and αS, showed that copper loaded Atox1 is capable of interacting with αS and delaying its amyloid fibril formation (**paper IV**).

2 Protein folding, misfolding and amyloid formation

The body is composed of trillions of heterogenous cells working together to achieve a functioning human (24). In order to build such a complex machine, four macromolecules are integral to the function. These are polysaccharides, lipids, nucleic acids and proteins. Lipids, unlike the other examples, are non-polymeric macromolecules, which are responsible for energy storage, signaling and structural components. Polysaccharides, in the form of glycogen, are a rapidly mobilizable energy reserve. Nucleic acids, which include DNA and RNA, are primarily responsible for coding and translating the blueprint for the linear protein building block sequence. Lastly, proteins are molecular machines that are capable of a wide array of activities based on their sequence. Among their many functions, they may act as structural support, signal relaying, catalysts, cellular gates and molecular motors; interacting in a massively intricate proteomic network. However, since proteins are responsible for most of the active functions within the body, they also become the primary culprit of non-infectious diseases when they malfunction. Modification to a building block, or altered sequence, may have effects that are usually either neutral or detrimental (25). Examples include relay proteins becoming permanently activated, as may occur in proto-oncogenes driving cancer (26), or structurally destabilized proteins, which may induce amyloidogenic diseases (27).

2.1 Protein folding

Protein function is encoded in the sequence of its building blocks, known as amino acids, of which humans are known to utilize 21. Amino acids are organic compounds that have a carboxylic acid and an amine group, whose bonding links amino acids together, and they are differentiated by a side chains with varying functional groups (Figure 1). Humans only use α-amino acids, which means that the three groups are connected to the central carbon, and amino acids can be grouped based on polarity and charge at physiological pH. It is thus the sequence of functional groups along the peptide backbone that encodes the protein fold, structure, and activity, as the peptide chain has an optimal conformation where a stable local free energy minimum is met, based on carefully tuned entropic and enthalpic contributions (28).

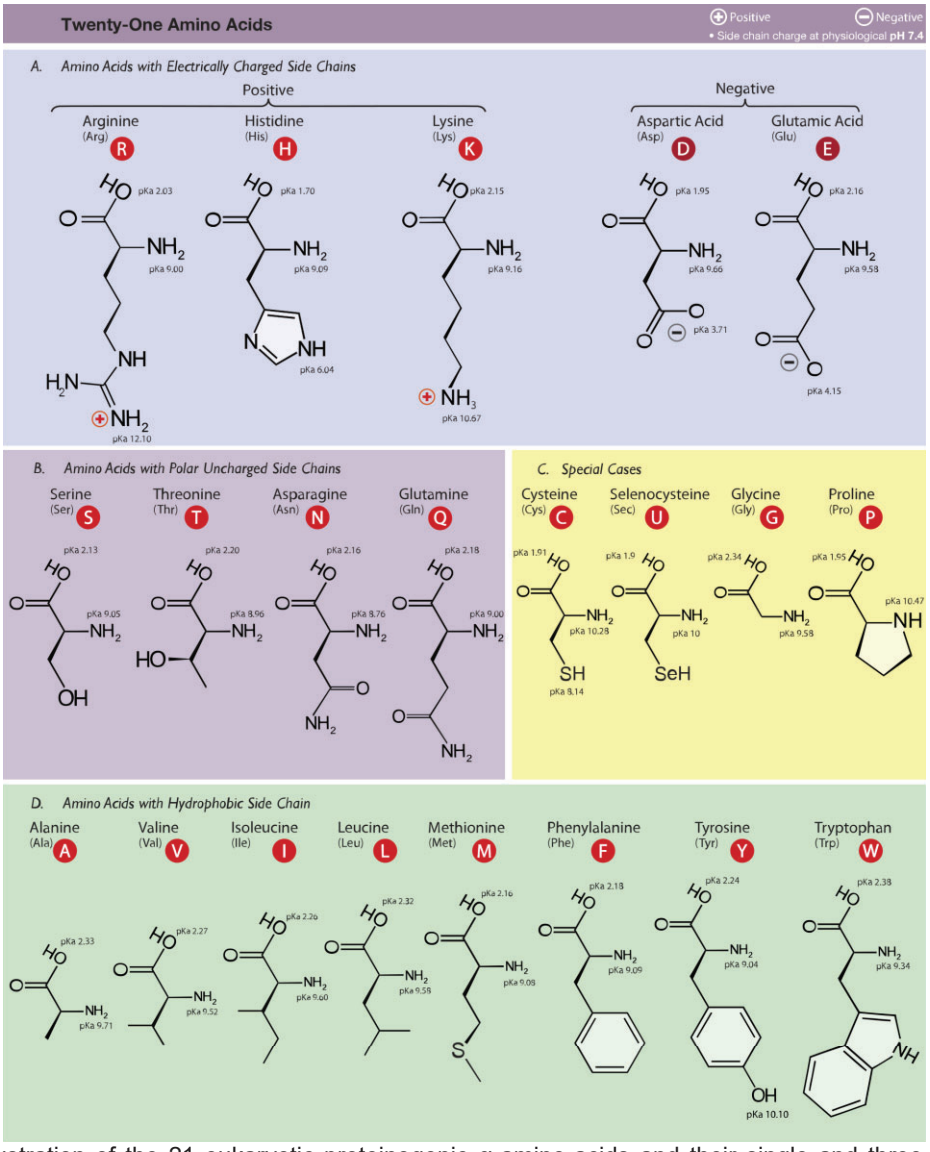

Figure 1 Illustration of the 21 eukaryotic proteinogenic α-amino-acids and their single and three letter code, grouped by charge, polarity and pK_a values at physiological pH (7.4).[1]

[1] Amino acids (https://commons.wikimedia.org/wiki/File:Amino_Acids.svg) by Don Cojocari (https://commons.wikimedia.org/wiki/User:Dancojocari), licensed by CC-BY-SA 3.0 (https://creativecommons.org/licenses/by-sa/3.0/legalcode).

Protein structures are described at four different levels; primary, secondary, tertiary and quaternary. Primary structure denotes the sequence of amino acids, secondary structure describes the local sub-structure of the protein, which forms primarily due to hydrogen bonds between the amide groups, whereas the tertiary structure refers to the three-dimensional structure of the whole peptide chain. Lastly, quaternary structure describes a multimeric complex between two or more individual peptide chains. As mentioned, it is the primary structure that imposes the final structure onto the protein, which is due to several interactions and constraints (28). A major constraint to possible protein conformations comes from the co-planar nature of the amide bond connecting the amino acids. Hence, bond rotation may only occur at the bonds around the α-carbon (29). Beside the steric constraints, enthalpic interaction occurs within the protein chain in several ways. The backbone amide groups may form hydrogen bonds, *i.e.* between carboxyl oxygens and amino hydrogens, which give rise to local structures, most commonly α-helices and β-sheets. The structure of α-helices is a twist of the peptide chain into a helix, with 3.6 residues per turn, whereas β-sheets result from an interaction between two adjacent chain segments forming a flat sheet (30). Lastly, the side chains and backbone amide groups contribute to the tertiary and quaternary structure through different interactions. Proteins can be stabilized by ionic bonds (*e.g.* between glutamate and lysine), hydrogen bonds (*e.g.* between serine, glutamine and backbone amide groups), van der Waals interactions, and even covalent bonds in the form of cysteine disulfide bridges. However, protein structure is not only dependent on interactions within its own or other peptide chains, but also through interactions with the aqueous environment. Major examples include hydrogen bonding and ion-dipole interactions with H_2O, as well as exclusion of hydrophobic residues from the aqueous environment, contributing to hydrophobic core packing. The latter is often known as the “hydrophobic effect”, as it increases the entropy of the water, which together with hydrogen bonds contribute the most to protein folding (31). The major force that counteracts these contributions towards the native state is the conformational entropy, as the peptide chain becomes restricted to fewer states.

Despite the fact that the peptide chain may, in theory, have an unfathomable amount of conformations that it requires to sample in order to finally acquire the native state, while avoiding local energy minimum traps, proteins are capable of folding in very short time scales, from microseconds to seconds (32-34). To elucidate this apparent paradox, dubbed “Levinthal’s paradox” (35), Monte Carlo simulations were employed wherein folding of randomized amino acid sequences was investigated. It was found that only a fraction of these randomized sequences was fast-folding, and the sequences that were folding fast exhibited distinct energy minima (36, 37). Thus, the current hypothesis speculates that proteins initiate folding by obtaining a few key interactions, yielding a “native-like structural nucleus”, and subsequent native-like intermediates (38). This is typically considered the process for proteins that go through one or more stable intermediate states, that are separated from the unfolded and native state by one or more rate-determining kinetic barriers. Thus, as the protein gains more native-like interactions, the search for correct folding becomes more constrained, guiding the protein towards the native state (38). However, it might occur for the two-

state folding proteins as well, where the unfolded protein passes an energy barrier to the native state in a seemingly single step, and thus only exists at an equilibrium of unfolded and folded states (38). In addition, it has also been observed that parallel pathways may exist depending on the protein, where multiple different intermediates converge to the native state (38, 39). A common representation of this folding process is the funnel-shaped energy landscape diagram, initially depicted by Wolynes, Onuchic and Thirumalai, which illustrates an energetically favorable process of folding that constricts the available conformational states as it progresses. The aforementioned intermediate rate-determining kinetic barriers are depicted as ruggedness and traps, and deep wells for the major intermediary species (Figure 2) (38, 40). However, not all proteins have an ordered three-dimensional structure, as is the case of intrinsically disordered proteins (IDPs). This flexible conformation allows IDPs to interact with many different partners by adopting compatible conformational states, which also include secondary structure elements such as α-helices (41). While the protein structure is encoded by the primary sequence and may readily adopt the fold *in vitro*, especially for small single-domain proteins, the conditions *in vivo* pose other issues. Such issues include folding during synthesis, with steric constraints within the ribosome, high concentration of nascent chains and initial long-range contact cannot be made as the protein is polymerized. To solve these issues, the cells employ protein chaperones (42). Chaperones bind folding intermediates in order to prevent aggregation, which may occur when *e.g.* hydrophobic patches are exposed and may be excluded from the aqueous environment through association with other proteins, resulting in *e.g.* amorphous aggregates (43).

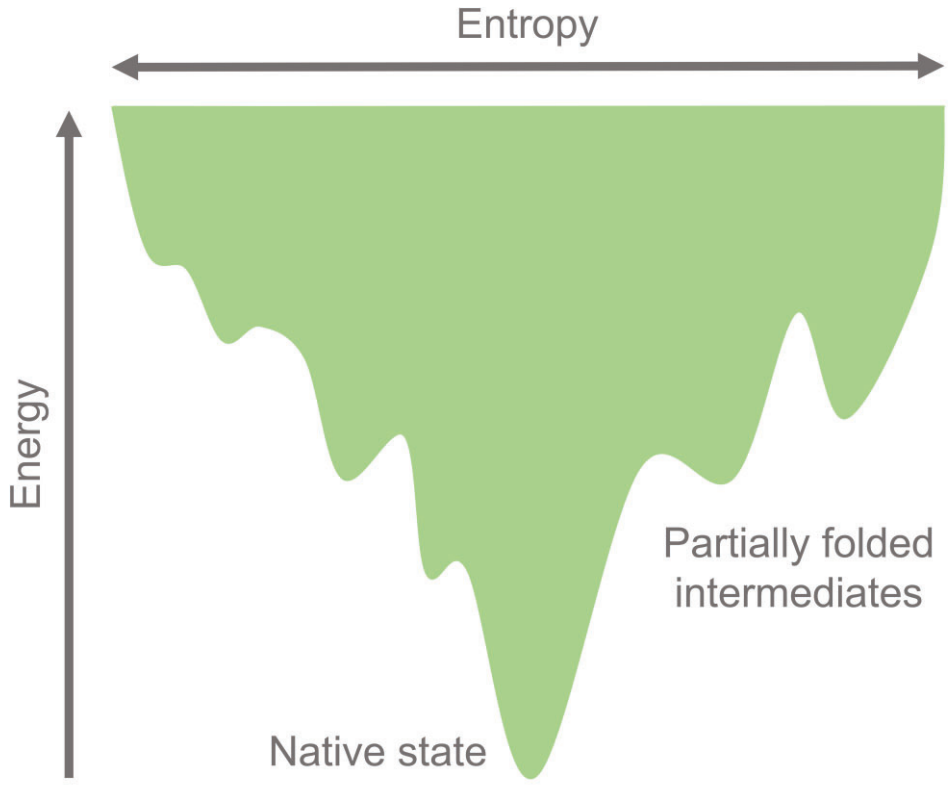

Figure 2 Simplified illustration of the energy landscape of protein folding.

2.2 Protein misfolding and amyloids

As proper protein function within the proteome is crucial for survival, the cell employs a highly sophisticated set of tools that are capable of dynamically regulating a balanced and functional system. This “proteostasis” is ensured at several levels, from regulation of the peptide synthesis, utilization of chaperones to fold or rescue misfolded proteins, to the degradation network (44, 45). Nevertheless, despite such an extensive control system, proteins may still misfold, both spontaneously or by environmental induction, *e.g.* thermal, chemical or oxidative stress (45). Misfolded proteins, by themselves or in amorphous aggregates, can typically be rescued or degraded. Nevertheless, there are situations when the proteostasis network becomes overburdened, resulting in impaired clearance of misfolded protein species (45), which happens when *e.g.* oxidative stress becomes too great, as may occur with age (46). Formation of highly degradation resistant misfolded species such as aggregates in the form of fibrils is also a possible outcome, and of particular concern. Appearance of these species results in diseases known as “amyloidoses”, where the proteins form highly stable β-sheet rich fibrillary aggregates (Figure 3) (17). Diseases that are associated with the formation of amyloid fibrils vary greatly. They can be local, as in the case of islet amyloid polypeptide aggregating in the pancreas of type 2 diabetic patients, or systemic, as displayed by amyloid light-chain amyloidosis. They are, however, most often considered in the context of neurological disorders, *e.g.* Alzheimer’s disease and PD (17).

Amyloid fibrils are a type of supramolecular polymers, consisting of proteins in β-sheet rich conformations, with the β-strands aligned perpendicularly to the fibril axis, known as the “cross-β fold” (17, 47). The amyloid fibrils are typically 7-13 nm in diameter and composed of 2-8 protofilaments, where each filament has an approximate diameter of 2-7 nm and they either associate laterally or twist around each other, although, mono-protofilaments have also been observed (17). At an atomic

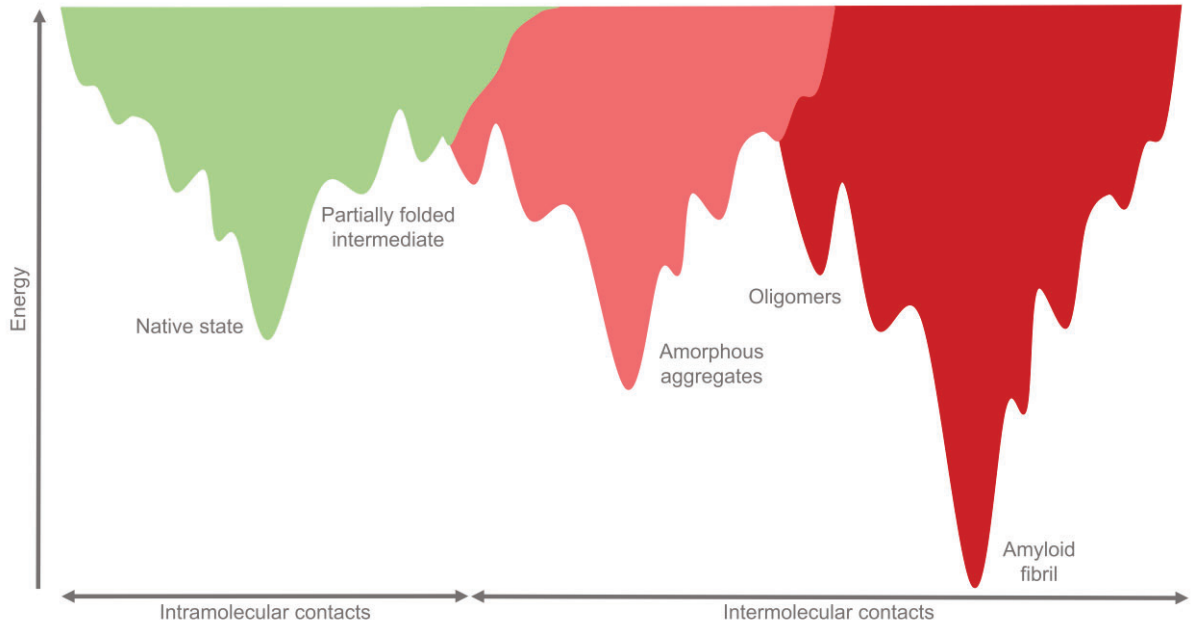

Figure 3 Simplified illustration of the protein energy landscape, with aggregates included.

level, studied by X-ray diffraction, two distinct reflections can be observed independently of the protein, at ~4.7 Å and 10-11 Å (48). These reflections correspond to the distance between the β-strands, and the distance between β-sheet layers, respectively. The β-sheet structure is stabilized by extensive hydrogen bonding between the amide groups of each chain, and this property is inherent in all proteins regardless of the side chains. In fact, this generic property is likely one reason that several pathological amyloid fibrils have been shown to be capable of “cross-seeding”, a process where an amyloid fibril of one protein can act as a template for monomers of another protein, thereby creating heterogeneous amyloid fibrils (49, 50). Furthermore, most proteins have high amyloid forming propensity sequences (51). The amino acid side chains are also involved in fibril stabilization, where they stabilize β-sheet layer interactions by interdigitating side chains (“steric zipper”) as well as intermolecular stabilization (52, 53). Together, these forces create an exceptionally stable protein species that, instead of occupying a local free energy minimum as the native fold does, are often considered to be the global minimum (Figure 3) (54). Interestingly, amyloid fibrils are often not homogenous species. A substantial degree of polymorphs has been identified from fibrils formed by a single protein, even in a single reaction mixture, in respect to protofilament count, arrangement and substructure (55). However, the field is currently shifting focus more towards the study of the pre-fibrillar oligomeric species. It has been discovered that these species appear to be the primary reason for cell toxicity, and some even speculate that the formation of fibrils is a last resort in order to reduce the oligomeric load, as inclusion bodies have been positively correlated with cell health (56-58). Albeit, oligomeric species are far more difficult to study than amyloid fibrils, due to their transient nature and significantly heterogeneous population.

2.3 α-synuclein and Parkinson's disease

PD is a neurodegenerative disease that results in symptoms such as bradykinesia, rigidity and tremor, and is characterized by deterioration of dopaminergic neurons in *substantia nigra* (59). Concomitant with neuronal deterioration comes the appearance of Lewy bodies, that are considered the hallmark of PD, of which a major constituent is the protein αS in an amyloid conformation (60, 61). The vast majority of PD cases are idiopathic in nature, although there are rare familial forms (20). Furthermore, while PD is commonly thought of in the perspective of the central nervous system, accumulating evidence implicates the gut-brain axis to play a major role, where misfolded αS has been implicated to spread along the vagus nerve (18-20). In order for clinical symptoms to manifest, it is estimated that approximately 30 % of neurons are lost in *substantia nigra* (62), the trigger of which is thought to have occurred decades prior in the case of idiopathic PD (20, 63). While these triggers are largely unknown, there are indications as to of what nature they may be, through inference from the functions of PD risk genes and experimental animal work (20). Triggers that have been implicated include altered gut microbiota (64, 65), pathogens (66-68), air pollution (69), pesticides (70), heavy metals (71) and head trauma (72). These triggers may result in long-term gut dysfunction through impaired intestinal barrier (73), chronic inflammation (74) or pathogenic misfolding events as a result of direct interaction with αS (75). However, while misfolding of αS is typically considered a pathogenic event, it was recently speculated that it may also be part of a normal physiological response to infections (20, 67). Reasoning behind this includes healthy people displaying αS aggregates in the gut (21, 22), as well as an observed upregulation of αS in response to gastrointestinal infection of norovirus, including neutrophil and monocyte response to both monomeric and oligomeric αS (67). It was instead proposed that PD requires temporary or permanent facilitating events, concomitant with or following the triggers (20). These facilitators would allow triggers access, or aid in the pathological spread, into the central nervous system. For example, pesticides could trigger mitochondrial dysfunction, resulting in chronic production of reactive oxygen species, which in turn facilitate misfolding of αS (76, 77). Another example is irritable bowel syndrome, which is correlated with increased PD incidences (78-81), where inflammation results in impaired intestinal barrier function (82, 83), potentially facilitating the entry or spread of misfolded α-synuclein or other triggers to the nervous system (21, 22), as well as inducing oxidative stress (84).

α-synuclein

It was not until 1997 that αS was identified as a central protein in PD pathogenesis, as a mutation in the gene was observed in families with susceptibility to the disease (85). Significant efforts into understanding αS, its function and its involvement in the disease subsequently ensued, but the functions of the protein remain unclear (86). The function is primarily studied in a neuronal context, where it has been observed that there is an abundant expression of αS in various brain regions, *e.g. substantia nigra*, cerebellum, hippocampus, thalamus and neocortex (87, 88). Within the central nervous system, αS

is primarily concentrated at the presynaptic terminals (89), where it has been shown to associate with synaptic vesicles and is thought to be involved in neurotransmission and synaptic plasticity (90, 91). Several observations have been made in regards to the effect of αS on synaptic vesicles, including the regulation of synaptic vesicle pools, facilitating vesicular cell membrane docking, recycling and clustering, as well as acting as a chaperone by aiding the SNARE complex assembly (91-97). However, despite all the observations that have been procured over the last decades, there are still disagreements as to whether αS facilitates or prevents neurotransmitter release (98). Additionally, these observations appear to only scratch the surface of the true and complex nature of αS. Several observations indicate that αS is a pleiotropic protein, as it has been observed to *e.g.* regulate gene expression, apoptosis, neuronal differentiation, immune system response and modulating glucose and calmodulin levels (20, 99, 100). Expression of αS throughout a wide array of tissues has also been reported, as it has been observed in the peripheral nervous system, circulating blood cells, hematopoietic cells of the bone marrow, kidney, lungs, liver, heart, enteroendocrine cells and muscles (98, 101-103).

αS is an IDP whose sequence can be divided into three domains, comprising the amphipathic N-terminal, non-amyloid-β component (NAC) and the acidic C-terminal, together making up the 140 amino acid short protein (100). The amphipathic N-terminal allows α-synuclein to form an alpha-helix when binding to lipid vesicles with acidic head groups (Figure 4) (104, 105), with the first 25 residues binding tightly to the membrane, whereas the residues 26-97 have a weaker affinity but are inferred to regulate the affinity (106). The NAC region, comprising residues 61-95, is essential for the amyloid fibril formation of αS (107, 108). Interestingly, the highly homologous β-synuclein protein does not form amyloid fibrils, and it has been implied that the reason for that is the absence of sequence homology in the NAC domain (109). The acidic C-terminal, on the other hand, does not typically interact with vesicles. However, in the presence of Ca^{2+}, whose influx at the presynapse occurs with electrical depolarization, the polarity of the C-terminal is reduced and it appeared to anchor vesicles to each other, and/or the plasma membrane (110). In addition, αS has also been shown to have a copper binding affinity, with binding constants (K_a, M^{-1}) of 10^5-10^6 for Cu^+, and 10^7 for Cu^{2+} (111-114). Several residues have been identified as the binding site of Cu^{2+}, primarily located in the N-terminal (residue 1-9), where Met1-Asp2 amide bond together with the Asp2 carboxylate and either H_2O or His50, is a strongly proposed

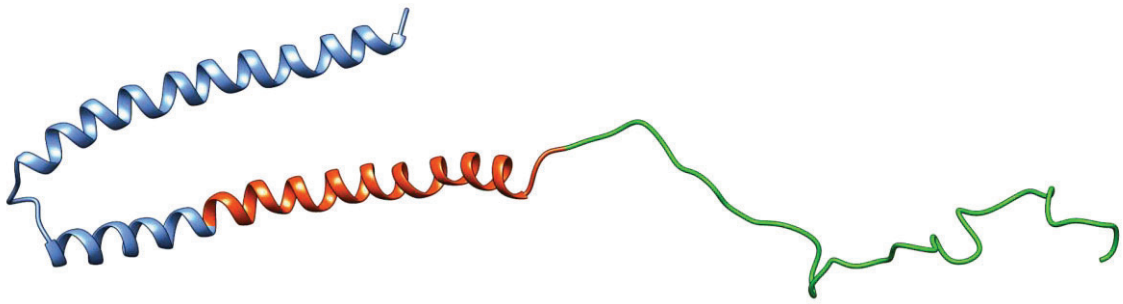

Figure 4 NMR solution structure of micelle bound αS (PDB: 1XQ8), with the N-terminal (blue), NAC region (red) and C-terminal (green) color coded.

complex (114). Cu^{+}, on the other hand, has been shown to exhibit a preference for the sulfur atoms of Met1 and Met5, together with the Asp2 carboxyl group and H_2O, creating a tetrahedral complex (114). While several studies have been performed on αS, less is known about the more physiologically relevant N-terminal acetylated variant, ^{NAc}αS (114-116). It was found that whereas Cu^{+} coordination remained unaffected by the acetylation (117), N-terminal coordination of Cu^{2+} was lost, and the ion was instead coordinated by the lower affinity His50 and Asp121 (118, 119). For this variant, the binding constant was reduced to 10^4-10^5 for Cu^{+} and 10^4 for Cu^{2+} (the latter, provided in (118) but taken from the value of His50 given in (111)) (118, 120). Additionally, the C-terminal appears to bind both Cu^{+} and Cu^{2+} around the same region as Ca^{2+}, *i.e* around residue 120 (110, 117, 118). However, there is no free copper in the cytosol, which is instead regulated by high affinity copper binding proteins (121). Nevertheless, there are some indications that it may have copper dependent interactions *in vivo*. From cell work it could be seen that removing copper results in an increased cell membrane localization, whereas cells expressing C-terminally truncated αS were unaffected by copper levels (122). Copper bound αS has also been implicated in acting as a ferrireductase (123). Furthermore, free copper stored in neuronal vesicles is released into the synaptic cleft during electrical depolarization, resulting in a minimal concentration of 100 μM (124), in addition to the release of αS (125).

2.4 Fish β-parvalbumin and dietary amyloids

Since close to all proteins share the feature of containing amyloid competent sequences (51), it is not surprising that food proteins can form amyloids as well (126). In fact, amyloid fibril formation of dietary proteins has been explored to provide favorable qualities to food, *e.g.* transparent gelation properties (127), biodegradable and anti-oxidant colloidal stabilizer of iron-particles to treat iron-deficiency anemia (128), foam stabilizing antioxidant properties (129), and even food grade antibacterial hydrogels (130). Although, concerns of food protein amyloid fibrils are being raised due to the generic nature of amyloid fibrils, connection to pathogenicity and evidence of pathogenic spread from the gut of some proteins. Modified κ-casein amyloid fibrils displayed toxicity to PC12 cells *in vitro*, and feeding mice with amyloid fibrils of the disease-related apolipoprotein A-II, or *in vivo* extracted serum albumin A, resulted in significantly accelerated misfolding throughout different organs of a mouse disease model, or deposition in organs of healthy mice, respectively (126, 131-133). Additionally, the major fish allergen, β-parvalbumin (β-PV), has been shown to form amyloid fibrils. These amyloid fibrils have been suggested to be the main conformational culprit of fish allergies, as human antibodies from fish allergic people bind a thousand-fold more strongly to the amyloid fibril conformation than to the monomeric one (134). Currently, apart from the modified κ-casein and β-PV, food protein amyloids have not been shown to have any adverse effects. In fact, some of the treatments to produce the amyloid fibrils are already in use in the food industry today, albeit not for purposes of amyloid fibril formation but rather food processing (126). While many food proteins have been identified to form amyloid fibrils, they typically do not do so under physiological conditions. Instead, low pH, low ionic strength and harsh heating (~80-90 ˚C) together with stirring are usually employed (126). Low pH results in two effects: hydrolysis of peptide bonds (135), and modulation of the amino acid charge distribution that significantly destabilizes the protein due to *e.g.* loss of salt bridges, protonation of aspartate and glutamate, resulting in loss of repulsion, or protonation of histidines causing repulsion of lysines and arginines (136-138). For β-lactoglobulin and ovalbumin it was found that at low ionic strength and pH, the resulting fibrils become long and semi-flexible, whereas higher ionic strength results in faster assembly but shorter and curly fibrils, which has been observed for β_2-microglobulin as well (139-142). Faster assembly with higher ionic strength appears to be a typical characteristic of fibril polymerization, and appears to be due to the electrostatic repulsion reducing the rate of assembly (140, 141, 143). However, in the case of ovalbumin it was found that the short flexible fibrils formed at higher ionic strength lacked a well-defined specific secondary structure, unlike the β-sheet rich fibrils formed at low ionic strength (143). Although, this effect of ionic strength on the fibril morphology and substructure may be less general. Amyloid-β peptide was found to form mature fibrils with higher ionic strength compared to low ionic strength that produced off-pathway immature fibrils, whereas αS and islet amyloid polypeptide displayed small or no differences at either low or higher ionic strength conditions, and some food protein amyloid fibril formation protocols make use of high ionic strength

(126, 144-147). Lastly, the high temperature disrupts the internal bonds and facilitates hydration of the buried residues (148, 149), resulting in denaturation of the protein, as well as facilitating pH induced hydrolysis of peptide bonds (150), thus exposing aggregation prone sequences. While the majority of dietary proteins require such harsh treatments, a food protein that readily forms amyloid fibrils under mild conditions is fish β-PV (151).

Parvalbumin

Parvalbumins are small ~12 kDa Ca^{2+} binding proteins (152). They belong to the EF-hand family, which also includes calbindins, calretinin and calmodulin, among others (152). The term EF-hand stems from early X-ray structure investigations, of which parvalbumin isolated from carp muscles was the first one. It was found that parvalbumin contains three helix-loop-helix motifs: AB, CD and EF (Figure 5). The conformation of a single EF-hand domain is reminiscent of a hand with an extended thumb and index finger, with a curled middle finger (153, 154). The EF-hand domain has a 12 residue conserved motif (Table 1), which when searched for in the human genome reveals 242 proteins (155). Of all the EF-hand proteins, most have domains organized in pairs, an exception of which includes the parvalbumin family, that contains three domains (152). Two parvalbumin paralogues exist in mammals, α-parvalbumin (α-PV) and β-PV (152, 156). While both PV paralogues contain three Ca^{2+} binding

Table 1 Conserved EF-hand domain motif. X, Y, Z and -Z are side-chain oxygen ligands, -Y denotes the backbone carbonyl ligand, whereas -X corresponds to a water ligand hydrogen-bonded to a loop residue. The most conserved residues and positions are bolded.

1	2	**3**	4	**5**	**6**	7	**8**	9	10	11	**12**
X		Y		Z		-Y	I	-X			-Z
Asp		**Asp**		Asp	**Gly**		**Thr**	Asp			**Glu**
		Asn		Asn	Pro		Leu	Ser			
		Glu		Ser			Val	Glu			

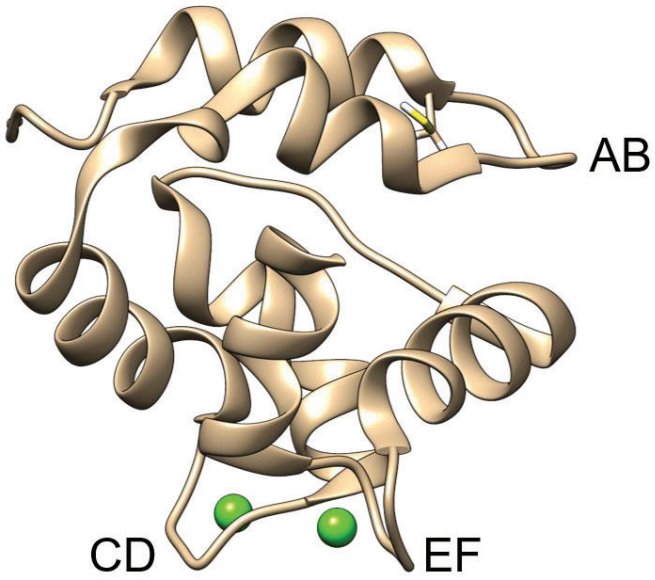

Figure 5 NMR solution structure of Ca^{2+} bound Atlantic cod (*G. morhua* PDB: 2MBX) with the respective EF-hand domains denoted. Ca^{2+} is displayed as green spheres, and the cysteine shown as a stick representation.

loops, the AB domain is inactive. However, it nonetheless fulfills a purpose of structural integrity, as well as to increase the Ca^{2+} binding affinity of PV, as shown by studies on the rat orthologues (157, 158). The AB domain does so by exposing its own hydrophobic sides toward the hydrophobic sides of the remaining EF-hands, thus acting reminiscent to that of Ca-calmodulin-peptide complex, but with an intramolecular C-terminal bound peptide instead (157, 158). In fact, remodeling the AB domain into a canonical EF-hand loop does not restore Ca^{2+} binding and destabilizes the overall structure, particularly in its apo-form, and it also increased the cooperativity of the two active Ca^{2+} binding domains (157). Furthermore, PV is not only capable of binding Ca^{2+}, but also Mg^{2+} (152). Based on work with rat orthologues, it was shown that the CD- and EF-domains are capable of binding both ions in α-PV, whereas the CD-domain of β-PV acts as a Ca^{2+} specific loop (159, 160). In addition, while rat α-PV is relatively unaffected in its conformational state as it transitions between apo- and Ca^{2+} bound forms (161), rat β-PV undergoes significant structural reorganization of the hydrophobic core when Ca^{2+} is removed from the Ca^{2+} specific CD-domain (160). It should, however, be noted that the literature has often treated lower vertebrate β-PV (*e.g.* fish and frog) as direct orthologues to mammalian β-PV (also known as oncomodulin), due to many shared essential features. However, with more refined phylogenic analysis, it has recently been shown that while mammalian α-PV has a closely shared phylogeny with lower vertebrates, β-PV does not (162). Indeed, some evidence can be observed in the literature, where it has been reported that lower vertebrate β-PV does in fact bind Mg^{2+} at two sites (163). Additionally, tissue expression of β-PV differs greatly between lower vertebrates and mammals, where it has been shown that lower vertebrates express β-PV in muscles (152, 164), whereas mammals only express α-PV (165, 166). Expression of β-PV in mammals has instead been shown to be limited to the outer hair cells, vestibular hair cells, placenta, and secreted by macrophages (167-170). It was initially assumed that PV only acts as intracellular Ca^{2+}/ Mg^{2+} buffers (159), due to the slow exchange rate (171) and two high affinity Ca^{2+}/Mg^{2+} mixed sites (163, 172), where it would return Ca^{2+} from the myofibrils to the sarcoplasmic reticulum (173-175). However, single Ca^{2+} binding properties, as displayed by mammalian β-PV, are usually characteristic of Ca^{2+} binding proteins that have signal transduction characteristics, as they allow fast and dramatic conformational changes. Therefore mammalian β-PV was also speculated to be a signal transduction protein (159). Additionally, and not mutually exclusive to the latter hypothesis, it was also suggested that the conformational change induced by Ca^{2+} binding to the CD domain is designed so to impart an energetic penalty upon Ca^{2+} binding, resulting in a modulation of Ca^{2+} binding affinity (160, 176). In terms of amyloid fibril formation, fish β-PV has specifically been shown to readily form amyloid fibrils under physiological conditions (151). It was shown that under simulated gastric fluid, *i.e.* pH 2, or addition of EDTA at pH 7.4, fish β-PV readily formed amyloid fibrils that conferred a protection against proteolytic attacks (151). It was thus speculated that the low pH of the gut protonates the coordinating ligands of β-PV, resulting in a release of Ca^{2+}, and thus destabilizing the protein (151), and it was further shown that chelating Ca^{2+} from β-PV results in an expanded conformational state (177). Additionally,

antibody reactive epitopes could be observed in the blood following a meal of fish, insinuating that it may traverse the intestinal barrier (178). Mechanistically, it was identified that the highly conserved cysteine of β-PV may play a key role in the amyloid fibril formation, as a C19S mutant resulted in an increased lag time before forming non-fibrillar Thioflavin T reactive aggregates, with an incomplete β-sheet transition and reduced stability (177).

2.5 Amyloid fibril formation mechanisms

During amyloid fibril formation proteins go through a thermodynamically unfavorable process, leading to the formation of nuclei. Nuclei may be regarded as the smallest species capable of initiating fibril elongation, but can also be regarded as the smallest aggregates where addition of monomers occurs at a faster rate than dissociation (17, 179), the latter definition of which will be used henceforth. The process leading to nuclei differs depending on whether the native protein is an IDP or folded (Figure 6A). For IDPs, disordered or partially disordered monomers may convert directly into elongation competent nuclei, or they may go into highly disordered or partially structured transient oligomers, followed by internal reorganization into a more stable β-sheet containing structure (Figure 6C). These oligomers are then capable of further growth by monomer addition or oligomeric self-association, eventually forming fibrils (17, 180). The process is, as stated, slightly different for natively folded proteins. While it is hypothesized by some that close to all proteins can form amyloid fibrils under the right conditions (54), the amyloid competent sequences have been estimated to be exposed at the surface of folded proteins in only 5.3 % of the cases, and less than 0.1 % of these comprise geometrical compatibility with self-complementary β-sheets (51). In line with this, it has been observed that folded proteins initiate amyloid fibril formation by exposing aggregation prone sequences as a result of thermal fluctuations, ligand release, or local unfolding, thus circumventing the major energy barrier of unfolding (181). These partially folded intermediates may then form nuclei directly, go into partially structured oligomers followed by, as for IDPs, structural conversion to β-sheet rich oligomers, or associate into native-like aggregates that are capable of converting into amyloid-like oligomers and fibrils (17). However, further complicating matters is the typically heterogenous population of different types of oligomers. They may be on- or off-pathway towards amyloid fibril formation, and they are meta-stable and transient in nature, thus difficult to study (17). In addition to the formation of the primary nucleus, secondary processes that increase the aggregation rate through formation of growth competent species may also take place for both IDPs and folded proteins, depending on the protein and physicochemical conditions. For example, fragmentation of the fibrils increases the number of growth competent species, and secondary nucleation wherein the surface of the fibrils catalyzes the formation of new oligomers and nuclei can occur (17, 182) (Figure 6B).

Amyloid fibril formation typically follows sigmoidal kinetics, with an initial lag phase, followed by an exponential phase and lastly an equilibrium phase (Figure 6B) (17, 182). During the lag phase the aforementioned processes described above occur in a highly dynamic fashion, where metastable oligomers associate and dissociate in multiple competing pathways (180), with a rate-limiting step being either the direct conversion to a nucleus, or the structural reorganization into a β-sheet containing oligomer (180). This does not mean that nuclei do not exist during the lag time. In fact, for amyloid-β peptide, with a lag time of 33 minutes, it was estimated that the first nucleus appears after 3 μs (179). Thus, fibrils form already in the lag phase, where the length of the phase also depends on the elongation rate, and secondary processes if

they exist in the system. Furthermore, monomers or fibrils will always be the dominant species in the solutions, with only few oligomers at any given time point (179). As enough nuclei have formed, or fibrils in systems with secondary processes (where the fibril surface catalyzes formation of new nuclei, or fragmentation events form new ends), the kinetics transitions to the exponential phase, where fibril mass formation increases to its maximum rate. Following this phase comes the equilibrium phase. Since all the processes occur continually independent of the phase, the fibril mass is at an equilibrium in respect to protein association, nuclei formation and dissociation (17, 179).

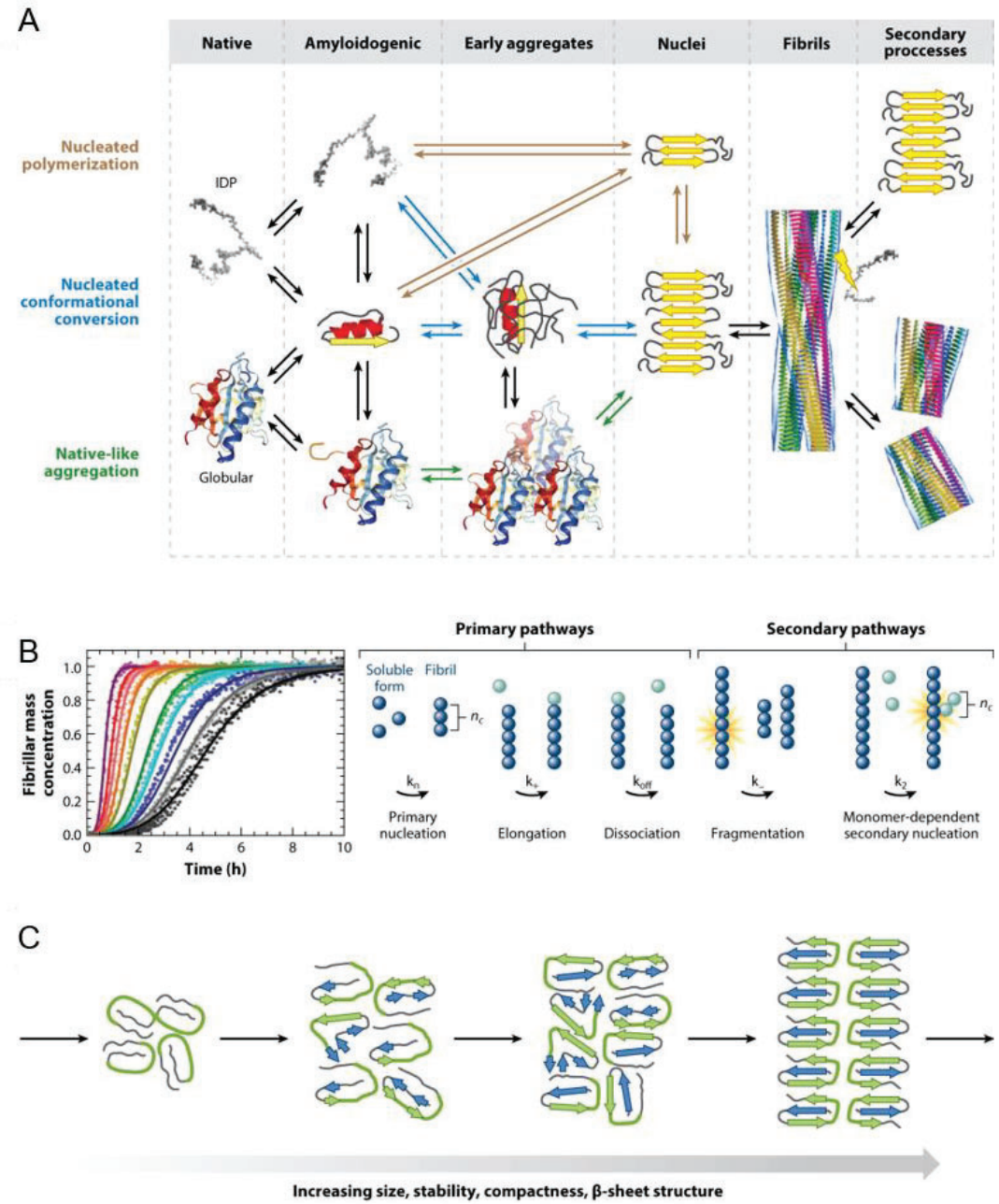

Figure 6 Proposed amyloid fibril formation mechanisms. (A) Nucleus formation of IDPs and folded proteins, with vertical boxes representing different stages of the amyloid fibril formation process. (B) Typical sigmoidal amyloid fibril formation kinetics (represented by amyloid-β in this graph) (left), and the different key microscopic steps involved in amyloid fibril formation (right). (C) Illustration of the structural reorganization during oligomer formation. Adapted with permission from ref (17).

2.5.1 Modulation of amyloid fibril formation by protein and ligand interactions

Amyloid fibril formation can be modulated at all the stages, from the monomeric to the fibrillary stage. Monomeric proteins can either be stabilized from progression towards oligomers or guided towards either off- or on-pathway oligomers. Oligomers themselves can be disassembled into monomers, structurally reorganized into non-toxic off-pathway species, or can be prevented from forming nuclei. Lastly, fibrils can seed and cross-seed amyloidogenic proteins by templating them into the amyloid conformation, resulting in fibril elongation, or guide them towards nuclei by means of surface catalysis. Surprisingly, amyloid fibrils of different protein species have even been shown to prevent amyloidogenic proteins from aggregating. A few examples will be described henceforth, of both endogenous and exogenous sources.

Naturally occurring endogenous modulators of amyloid fibril formation are, as has been touched upon, chaperones. Chaperones consist of many different proteins, often working together, and they may stabilize the native fold of amyloidogenic proteins during *de novo* folding or prevent the aggregation when the native state is destabilized (183). As such, chaperones have been shown to interact with several species in the amyloid fibril formation chain. They may inhibit formation of both oligomers and amyloid fibrils by stabilizing the monomeric state or, interestingly, direct the protein into amorphous aggregates (58, 184). Chaperones have also been found to be capable of binding oligomers, thus interfering with primary nucleation, as well as binding to the ends and surfaces of fibrils, resulting in reduced elongation and secondary nucleation rates (185, 186). Notably, while amyloid fibrils have long been considered dead end species that the cell is unable to clear, recent findings suggest that this may not be the case. The chaperone heat shock protein (Hsp) 104, found in *Saccharomyces cerevisiae* in 1990, is known as a “disaggregase”. It is capable of solubilizing large protein aggregates, including amyloid fibrils (187, 188), and together with Hsp40 and Hsp70, may even rescue enzymes (189). While Hsp104 is highly conserved in eubacteria and eukaryotes, it has no homolog nor ortholog in metazoa (190). However, in 2011 it was found that Hsp110, together with Hsp40 and Hsp70 was capable of disaggregating and reactivating proteins in amorphous aggregates, but with little effect on amyloids (188). Following this it was found that heat shock cognate 71 kDa protein, Hsp40 and Hsp110 were capable of rapidly disassembling αS fibrils *in vitro* (191). This highlights how the cells have a wide array of chaperones that achieve different tasks depending on the circumstance, and work together in a fascinatingly modular fashion.

While homologous seeding is straightforward, heterologous seeding is less so. However, as the amyloid fibril is a supramolecular polymer that shares structural features and interactions independent of protein species (48), it is not surprising that some can cross-seed (49, 50). It may occur from endogenous sources, as it does for amyloid-β peptide, islet amyloid polypeptide, and tau monomers co-aggregating with α-synuclein (192-195), or acceleration of αS aggregation in the presence of the respective fibrils. It may occur by exogenous sources, as was shown with the functional bacterial amyloid CsgA monomers and fibrils accelerating αS aggregation (64). A

potential explanation of these differences may stem from structural similarity of the formed fibrils, rather than sequence similarity (49). Albeit, cross-seeding may not occur at all, or, interestingly, it may in some cases occur cross-inhibitory, or even unidirectionally (49). Examples of inhibitory reactions include pro-islet amyloid polypeptide that is, in both monomeric and fibrillar form, capable of preventing amyloid fibril formation of α-synuclein (192). Unidirectional cross-seeding, on the other hand, may be a result of the protein fibrils conformational plasticity, as observed by the myriad of polymorphs (55). Therefore, a protein (A) with a set of conformational polymorphs, where one or more conformations can adopt the structure of another amyloidogenic protein (B), then A may be seeded by B. However, if the conformational state of B is not preferred by A, and thus not propagated when A is aggregated in isolation, the converse might not occur, therefore leading to unidirectional cross-seeding (196, 197). Intriguingly, secondary nucleation has been indicated to impart the structure of the parent fibril, as was shown when different amyloid-β peptide mutants were cross-seeded. Different mutants formed different morphologies, and only the mutants with the same polymorphs were capable of cross-seeding, independent of hydrophobic patches (198). It should, however, be noted that the fibril substructure was not resolved.

As described, the amyloid competent sequence is generally buried in the core of folded proteins (51), and exposure of it may occur, or be prevented, due to ligand release or binding, respectively (17). This has been observed in several cases, *e.g.* transthyretin (TTR), superoxide dismutase 1, acylphosphatases and β-PV (151, 199-202). In the case of TTR, a primary carrier of thyroxine, both hormone analogues and small aromatic molecules were found to stabilize the quaternary native state by binding the thyroxine binding sites (199). Acylphosphatases from *Sulfolobus solfataricus* and *Drosophila melanogaster* have been shown to form amyloid-like aggregates in the absence of initial unfolding. However, it was observed that a competitive enzyme inhibitor (inorganic phosphate) was capable of stabilizing the native state of the protein and prevent amyloid-like aggregate formation (202). More general examples are polyphenols. They are well known to interact with amyloidogenic proteins, where (-)-Epigallocatechin-gallate (EGCG) is especially well studied, and has been shown to prevent amyloid fibril formation of both natively folded proteins and IPDs (203). EGCG is capable of binding both monomeric and oligomeric species, directing the monomers towards off-pathway β-sheet poor aggregates, and even remodels pre-formed toxic oligomers (204, 205). It appears to do so in a complex manner, where it forms hydrogen bonds with both the amide groups and side chains, in addition to hydrophobic interactions (206). However, EGCG has also been shown to covalently modify proteins, which may be a contributing factor to the inhibitory effect (207). Superoxide dismutase 1, involved in amyotrophic lateral sclerosis, is a homodimeric metalloprotein primarily known for disproportionation of superoxide into oxygen and hydrogen peroxide (200). It requires Cu^{2+} for enzymatic activity and Zn^{2+} for structural stability (208, 209), where demetalation of superoxide dismutase 1 has been shown to destabilize the protein, and mutations in the zinc-binding loop have been correlated with enhanced hydrophobicity and misfolding (200). In addition, small molecules have

been shown to bind to the dimer interface cavity, at a position where introduced disulfide bonds resulted in dimer stabilization and misfolding prevention (201). However, it should be noted that *in vivo* amyloid fibril formation of superoxide dismutase 1 is still contested, despite *in vitro* formed aggregates showing a negative circular dichroism peak at 220 nm and reactivity by the amyloid binding fluorescent dyes, congo red and Thioflavin T (210, 211).

Several metal ions have been implicated in the progression of neurodegenerative amyloidoses, both due to long term environmental exposure and alterations in metal homeostasis (16). The effect of metal ions is a complicated relationship, where the effect may be on tissue and cellular level, *e.g.* increased oxidative stress, altered signaling and metabolic changes, or on a molecular level, *e.g.* direct interaction with amyloidogenic proteins (16). In the case of direct interaction, there are several ways metal ions may influence amyloid fibril formation. Metal ions may rearrange the peptide backbone, as was shown for Cu^{2+} induced cis-trans isomerization of proline in β_2-microglobulin, resulting in distal oligomerization interfaces that promote amyloid fibril formation (212). Inter-molecular protein association may also be induced through metal ion coordination complexes, *e.g.* several amyloid-β peptide molecules coordinating Zn^{2+} by histidine, thereby promoting oligomerization and amorphous aggregation rather than amyloid fibril formation (213-215). Chemical modification of proteins by metal ions is also a possibility, as was shown for N-terminally acetylated αS (^{NAc}αS) bound to Fe^{2+} under aerobic conditions, resulting in Schiff base formation and reversible intermolecular covalent bonds that lock the protein in an oligomeric state. In contrast, Fe^{3+} and anaerobic conditions prevented this from occurring and instead resulted in amyloid fibrils, leading the authors to conclude that Fe^{2+} may reductively activate O_2, that then may oxidize ^{NAc}αS or protein partners (216). While it did not occur in this study, such a reaction may also yield tyrosine hydroxylation, oxidation and/or dityrosine cross-linking (217), which is a feature of αS in Lewy bodies (218).

2.5.2 Effect of macromolecular crowding on protein aggregation

The intracellular environment is estimated to have 80-400 mg/ml macromolecules, which corresponds to a volume occupancy of 5-40 % (219, 220). Extracellular space also displays high concentrations of macromolecules, where *e.g.* blood has been shown to have a protein concentration of 60-80 mg/ml (221). This mixture of macromolecules results in many effects due to its heterogeneous nature, including non-specific chemical interactions (*e.g.* electrostatic and hydrophobic interactions) and an effect known as “excluded volume”. The latter is a major effect that arises from the inaccessibility of surrounding space. The excluded volume reduces the available space wherein the protein can conformationally rearrange, and thus the configurational entropy, resulting in more compact states. A similar effect can generally be observed by protein-protein interactions, whereby association reduces occupied space, thereby increasing the entropy of the system in both cases as a result of increased number of crowder configurations (219, 222). Excluded volume thus stabilizes natively folded

states (Figure 7), as well as interactions with other macromolecules, *e.g.* multimers. Yet, as the amyloid fibril state is a highly compact polymer, this would imply that the amyloid fibrils themselves should be favored, as well as the on-path association reactions into oligomeric states. It has been observed for many amyloidogenic IDPs, which occupy a larger volume compared to more structurally ordered proteins, that macromolecular crowding agents appear accelerate amyloid fibril formation (223-225). The effect is, however, less straightforward for natively folded proteins. While natively folded proteins exist in a local free energy minimum (226), and this energy minimum is further stabilized by macromolecular crowding agents (219), they do not necessarily need to cross the major energy barrier of unfolding to become amyloidogenic (17). Thus, rather than significant unfolding, association of these aggregation prone sequences during partially destabilizing events may initiate the misfolding, followed by entry into the misfolding funnel that is further exacerbated by macromolecular crowding. In accord, several folded proteins have shown increased stability against amyloid fibril formation under macromolecular conditions, *e.g.* bovine carbonic anhydrase (227), bovine core histones and insulin (225), with the latter two existing in multimeric states at physiological conditions. However, in destabilized native states, *i.e.* by low pH, an accelerated aggregation under macromolecular crowding conditions could be observed, which also held true for β_2-microglobulin (225, 227, 228). It was also speculated that since the multimeric states of bovine core histones and insulin prevent aggregation, macromolecular crowding facilitates multimers, whereas low pH shifts the equilibrium towards aggregation prone monomers (225). Additionally, another folded protein, apolipoprotein C-II, aggregates in the absence of lipids, and this was further facilitated by crowding (229). It can thus be observed that macromolecular crowding tends to stabilize folded proteins in their native states. Albeit, during destabilizing events the proteins may start to expose aggregation prone sequences that associate, which can be further exacerbated by macromolecular crowding agents directing them down the “misfolding funnel”.

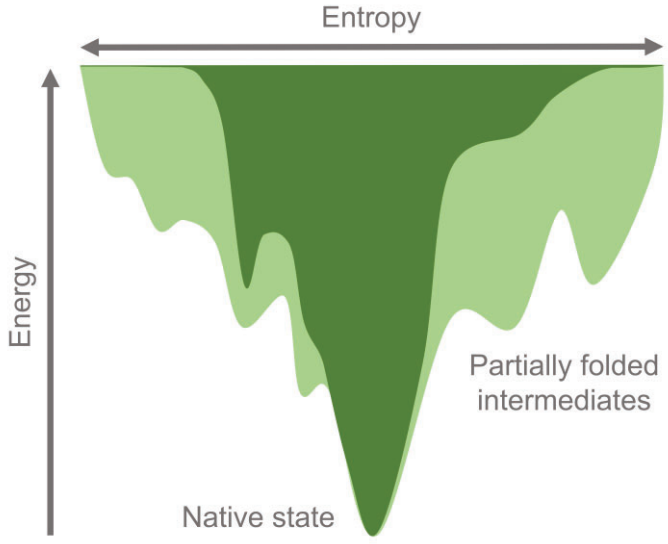

Figure 7 Simplified illustration of folding energy landscape of a protein in presence of macromolecular crowding. Light green represents without- whereas dark green represents with macromolecular crowding. Redrawn from ref (228).

However, macromolecular crowding does not necessarily alternate between stabilization of native protein states and facilitation of amyloid fibril formation. If several aggregation pathways exist, macromolecular crowding may trap the protein in an alternate thermodynamically stable, misfolded, conformation. (183). This was shown for αS in macromolecular crowding conditions together with various alcohols and trimethylamine-N-oxide, which, depending on concentrations, allows parallel aggregation species (225). In addition, when human islet amyloid polypeptide was incubated with macromolecular crowding agents, amyloid formation was attenuated. Instead, the authors noted an accumulation of off-pathway non-toxic oligomers, in place of the typically toxic end-products (230). However, while these studies have been made *in vitro*, it should be noted that a functioning proteostasis network would likely work to prevent the misfolding funnel *in vivo* for both IDPs and folded proteins.

2.5.3 Effect of osmolytes on amyloid fibril formation

Stabilizing osmolytes also play a role in the cell, where it has been shown that they are upregulated or imported during conditions of stress, thus promoting the proteins native fold (231-234). Such osmolytes include small polyols, sugars, amino acids and methyl amines, that induce and stabilize the protein fold through enthalpic contributions, rather than entropic contributions as displayed by macromolecular crowding (219, 220, 233, 235, 236). Through studies of 48 different proteins with several different osmolytes it has been found that interaction of stabilizing osmolytes with the protein backbone is unfavorable. Additionally, charged side chains have the most favorable interactions, whereas polar side chain contributions are smaller or negligible, and apolar side chains tend to be negligible or slightly unfavorable. Interestingly, while some osmolytes increase the solubility of proteins through favorable side chain interactions (*e.g.* glycine betaine and proline), others decrease solubility as the unfavorable interactions with the backbone outweigh the favorable side chain interactions, despite stabilizing the native state (*e.g.* trimethylamine N-oxide) (236). Thus, the strong aversion against the amide groups favors a compacted protein (known as the osmophobic effect), albeit with a preferential interaction with the charged side chains, which in turn favors the folding of proteins. Despite this, the mechanism of action of stabilizing osmolytes is not known, and several proposed models exist, although not mutually exclusive. For trimethylamine N-oxide alone, it has been proposed that it may stabilize compact conformations through direct interactions (237, 238), interact favorably with the heterogeneous surface of folded proteins as a surfactant (239), act as a crowding agent and thus contribute entropically (235, 240), or reduce the hydrogen bonding ability of water, thus favoring amide group hydrogen bonding, as occurs in the protein core (222, 234, 240, 241). As can be surmised, osmolytes will also modulate protein aggregation (242). For the folded amyloidogenic proteins, P39A cellular retinoic acid-binding protein, insulin and immunoglobulin light chain, it was shown that various osmolytes stabilized the native state, thus preventing amyloid fibril formation (231, 232, 243). However, for several IDPs it was shown that the osmolytes trimethylamine-N-oxide, glycerol and glycine betaine enhanced the amyloid fibril formation (244-246).

Furthermore, and akin to macromolecular crowding, the effect of osmolytes on IDPs was shown to alternate between facilitation and inhibition of amyloid fibril formation (242). At high concentrations, the effect of trimethylamine-N-oxide on αS displayed an off-pathway aggregation into alpha-helical oligomeric states (245). Furthermore, an extensive investigation into human islet polypeptide aggregation showed that osmolytes stabilize proto-fibrillary structures, rather than amyloid fibrils, without affecting the morphology of the mature fibrils (247). However, human islet polypeptide was, in the presence of proline, redirected into amorphous aggregates instead of protofibrils (248).

3 Methodology

This chapter is intended to give a brief description of the techniques used within this thesis. This section does, however, not aim to give detailed experimental methodology, which can instead be found in the respective papers.

3.1 Protein expression

Protein expression can be performed by a variety of organisms, all of which have different advantages and disadvantages (249). The work performed in this thesis was done with proteins expressed by the work horse, *E. coli*, and this section will therefore focus on this expression system. A highly popular *E. coli* expression system involves the T7 promoter, where the gene is inserted into a plasmid containing the promoter sequence recognized by the phage T7 RNA polymerase (250). The phage T7 RNA polymerize gene itself is commonly placed in the genome of the expression system under control of the lacUV5 promoter. Unlike the prototypical *lac* promoter, the lacUV5 displays reduced catabolite repression due to three point mutations, and protein expression may thus be induced by lactose, or the non-hydrolyzable analogue isopropyl β-D-thiogalactopyranoside, even in presence of glucose (249, 251). Addition of IPTG is then typically done mid log phase of *E. coli*, as the growth stage typically has the maximal protein translation, although early stationary phase can be used as well if *e.g.* formation of inclusion bodies is an issue (249). The plasmid containing the gene of interest typically includes a selection marker, where antibiotic resistance is commonly used (249). Thus, by growing *E. coli* in media containing the selected antibiotics, only bacteria with the resistance gene, *i.e.* plasmid, will survive. This

ensures that the plasmid is not lost, as plasmid-free bacteria are more metabolically competitive. After induction and protein expression the bacteria are typically lysed to extract the protein, followed by purification through various means, which often is fast protein liquid chromatography systems.

3.2 Fast protein liquid chromatography

For analytical scale protein preparations, the cell lysis homogenate is typically cleared by centrifugation, wherein the protein remains in the supernatant. After recovering the supernatant, several procedures can be used to purify the protein of interest, based on its properties. These include solvent, pH, ionic strength, charge, size and structural features. To purify based on these features, chromatography is typically employed. Chromatography is essentially a technique that is based on partitioning of a compound between two nonmiscible phases, consisting of a stationary phase and a mobile phase. For protein purification, the stationary phase is typically attached to an inert matrix, with a liquid mobile phase flowing through it, often with the aid of a pump system, hydrostatic pressure or gas pressure. The most common method is the fast protein liquid chromatography system, and a few of the available separation techniques will be covered in this section, based on the textbook by H.G Pontis (252).

Affinity chromatography

A powerful technique that employs a well-known and defined structural feature of the protein is the affinity chromatography, which may in a single step purify a target protein several thousand-fold from the crude lysate. In the technique, the stationary phase can include *e.g.* immobilized ligands, a cofactor, receptor or antibodies. A highly popular form of affinity chromatography is the immobilized ion affinity chromatography, wherein transition metals such as cobalt, nickel, copper and zinc are immobilized. This stationary phase can then selectively bind proteins with affinity towards the ions. Such a binding feature can be engineered onto recombinant proteins of interest, in the form of fusion proteins, where the his-tag is exceedingly common. The histidines readily form coordination complexes with nickel and cobalt, by binding with their imidazole groups. In order to elute the subsequently immobilized protein, increasing concentrations of free imidazole can be added, that will compete with the his-tag for binding of nickel or cobalt and thus release the protein. Another option is to decrease the pH, which will protonate the histidine and disturb the coordination with the ions. Lastly, the his-tag is typically connected by a short chain segment that is recognized by a specific protease, *e.g.* thrombin or tobacco etch virus protease. The his-tag can then be specifically removed upon addition of the protease and purified from the protein.

Ion-exchange chromatography

The charge of the target protein is another feature that is commonly exploited in the purification procedure. The principle is based on ionic interactions of the protein with the stationary phase, which depend on the isoelectric point and pH of the buffer, and may result in a 10-fold degree of purification. A pH below the isoelectric point results

in a positively charged protein, whereas above results in a negatively charged protein. Thus, depending on the pH, the protein will interact with different affinities towards the charged stationary phase. This is, however, a simplified picture, as discrete charges on the proteins, in particular the surface, play a role as well (253). The most common strategy to elute the protein involves an increasing ionic strength of the mobile phase, where proteins will elute depending on the cumulative strength of the ionic interaction.

Size-exclusion chromatography

Size-exclusion chromatography is a very useful technique in two ways. First, it provides further separation of proteins based on their sizes, as well as a complete buffer exchange into the buffer of interest. Thus, it may *e.g.* remove the large amount of imidazole following immobilized ion affinity chromatography, or the potentially highly ionic buffer after ion-exchange chromatography, both of which may interfere with subsequent studies or applications. Size-exclusion chromatography employs a matrix of porous beads, where size-compatible proteins are slowed down within the column by entering the porous networks, whereas proteins too large to enter pass by the beads. This results in a size-dependent elution distribution of proteins, with larger proteins eluting first, followed by smaller and smaller proteins. Depending on the protein of interest, the beads are cross-linked to different degrees, with a higher degree of cross-linking to resolve smaller proteins from each other.

3.3 SDS-PAGE

Sodium dodecyl sulphate-polyacrylamide gel (SDS-PAGE) is a common technique used to separate and analyze proteins. It works, in principle, by applying an electric field, resulting in migration of proteins through a cross-linked gel matrix. However, as proteins are molecules with varying charge and tertiary structures depending on species, they will not migrate uniformly throughout the gel. To achieve size-based separation, the anionic surfactant SDS is used, which denatures the proteins (often combined with heating) resulting in linearized proteins, thus avoiding the issue of the protein fold in gel migration. SDS also covers the protein with negative charges, resulting in an approximately equivalent charge-to-mass ratio independent of protein species, thus allowing separation of proteins based on mass. Reducing agents may also be used, that will cleave disulfide bonds. The protein in the gel can be analyzed after the electrophoresis by several techniques, including Coomassie staining, which binds and visualizes proteins, Western blot, in which antibodies are used for visualizing specifically the protein of interest, and mass-spectrometry.

3.4 UV-vis spectroscopy

Electromagnetic radiation can be described both as a wave, with the electric and magnetic field oscillating perpendicular to each other, and as an energy package with particle-like properties, known as a photon. The study of the interaction of matter with electromagnetic radiation as a function of wavelength or frequency is known as spectroscopy, which, in the case of ultraviolet-visible spectroscopy corresponds to

~200 nm – 800 nm. The textbooks about fluorescence (254) and circular dichroism (255) can be read for more in depth information.

3.4.1 Absorption spectroscopy

One mechanism in which UV-vis light interacts with matter includes absorption, wherein the matter absorbs the photon. In an atom or molecule, electrons only exist in quantized energy levels, determined by the electron configuration. Only when the energy of the photon matches the difference of these quantized energy levels (ΔE) may it be absorbed, resulting in a rearrangement of the electrons into an excited state. The absorption process can be described by Bohr's frequency condition ((1), which takes Plank's constant (h) and the frequency (v), speed (c) and wavelength of light (λ) into account.

$$\Delta E = hv = \frac{hc}{\lambda} \tag{1}$$

Thus, different atoms and molecules absorb different wavelengths of electromagnetic radiation, giving rise to absorption bands. Furthermore, the electronic wave function overlap between the two states determines whether the transition will occur or not, and the likelihood of transition. As a result, the intensity of absorption will vary with electromagnetic wavelength. This phenomenon can be applied by spectroscopy, by measuring the relative intensity of the light before (I_0) and after (I) interaction with the sample, thus measuring the absorption (A) (Equation 2).

$$A(\lambda) = log \frac{I_0(\lambda)}{I(\lambda)} \tag{2}$$

This can be further used to measure the concentration of the chromophore, as chromophores will have a molar extinction coefficient (ε), which is a measure of how strongly the chromophore absorbs light at a given wavelength. By knowing the molar extinction coefficient, the optical path length (l), one can apply Lambert-Beer law to calculate the concentration (c) (3). For proteins, the chromophore is usually the amino acid residues tryptophan, tyrosine and cystine measured at 280 nm, whose cumulative extinction coefficient can be used to measure the protein concentration. In addition, phenylalanine can also be used to measure the concentration, as it has a maximal extinction coefficient at 257.5 nm.

$$A(\lambda) = \varepsilon(\lambda) cl \tag{3}$$

Absorption spectrophotometers contain a light source, a monochromator (which only allows the selected wavelength to pass) and a beam splitter that diverts the electromagnetic radiation to both the reference detector and through the sample to the sample detector (Figure 8).

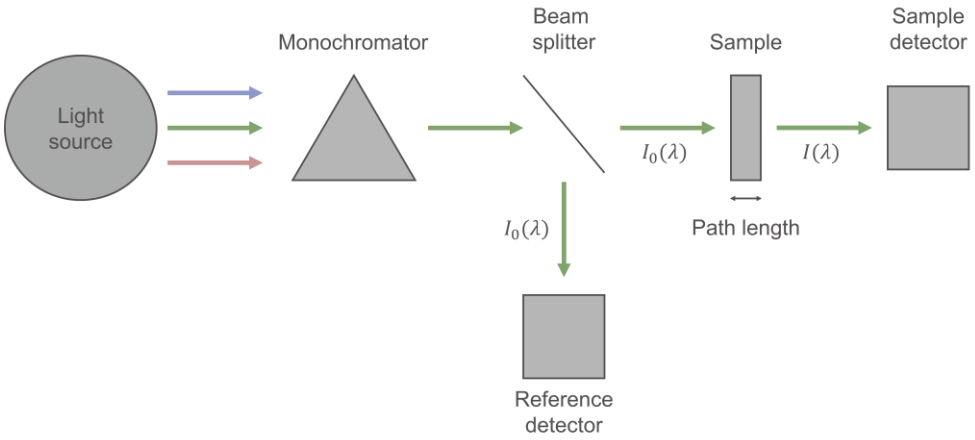

Figure 8 A schematic of an absorption spectrophotometer, where the incident light passes through a monochromator that only allows the specified wavelength through (I_0), which is then split to the reference detector and through the sample (I) to the sample detector.

3.4.2 Fluorescence spectroscopy

Upon absorption, the system may excite to either singlet (S_n) or triplet states, which are described relative to the ground state (S_0). Triplet states will, however, not be considered in this thesis. There are also several vibrational states for each electronic state (Figure 9).

As the singlet states are energetically unfavorable, they are typically short lived, and there are several ways the system relaxes. Vibrational relaxation to the lowest vibrational state of the excited state (S_{n+1}) occurs quickly, often followed by non-radiative internal conversion (S_{n+2} to S_{n+1}) and non-radiative relaxation (S_1 to S_0). While this represents the most common mode of system relaxation, there are also molecules known as fluorophores, whose relaxation is radiative. As the vibrational relaxation is the fastest regardless, emission of a photon as the system relaxes to S_0 typically occurs from the ground state of the excited state, thus resulting in a lower energy emission compared to the absorbed photon (redshift). In addition, as the emission almost always occurs from the ground state, the energy of the emitted photon is independent of the absorbed photon (Figure 9).

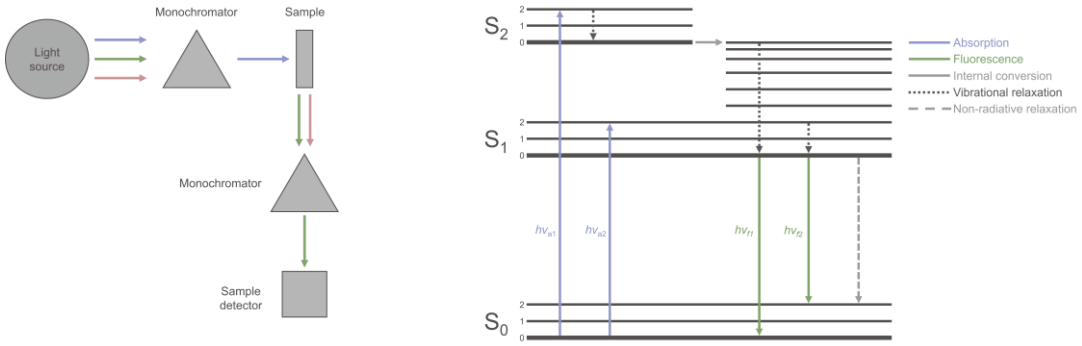

Figure 9 Left: Schematic of a fluorometer, where only the selected wavelength passes through the monochromator and reaches the sample. The sample is then excited, and subsequently emits photons that are further selected through a second monochromator before reaching the detector. Right: Simplified Jablonski diagram displaying the different modes of system relaxation following excitation, where hva1 and hva2 correspond to photons of different wavelengths exciting the system, and hvf1 and hvf2 to emitted photons.

A fluorometer is used to measure fluorescence and it is very similar to absorption spectrophotometers. The light passes through a monochromator and excites the sample, which then fluoresces omnidirectionally. This emitted light then passes through a second monochromator and into the detector, which is typically situated 90˚ from the initial light source, as to avoid measuring incident light (Figure 9). Both emission and excitation spectra can be measured with this instrument. To measure an emission spectrum, the incident light wavelength can be fixed, and the emitted light detected over a selected range. In converse, excitation spectra can be measured by fixing the excitation wavelength and exciting the fluorophore over a selected range.

A major technique used in this thesis employs the fluorescent amyloid fibril binding dye, Thioflavin T (ThT), whose fluorescence quantum yield increases drastically upon binding amyloid fibrils. This dye was used to monitor the bulk amyloid fibril formation kinetics discussed in section 2.5.

3.4.3 Circular dichroism spectroscopy

Circular dichroism (CD) is a technique that measures the differential absorption of left- and right-handed circularly polarized light. This phenomenon only occurs for chiral molecules, which includes amino acids (except glycine), and thus peptides and proteins. In the context of biophysical studies, CD is most often used to study the secondary structure of proteins. An optical transition shift or split into multiple transitions occur when the amide chromophores of the polypeptide backbone are aligned in arrays, resulting in different characteristic spectra depending on the structural element. The three prototypical structural elements are α-helix, β-sheets and intrinsically disordered structures, all of which have distinct far-UV CD spectra (Figure 10). The CD instrument typically gives a unit of degrees of ellipticity (θ), which, for proteins, is then converted into mean residue molar ellipticity. The degree of ellipticity per amino acid is reported through this conversion, which allows one to crudely compare the amount of secondary content between different proteins. Although this comparison becomes significantly unreliable when comparing proteins with mixed secondary structure.

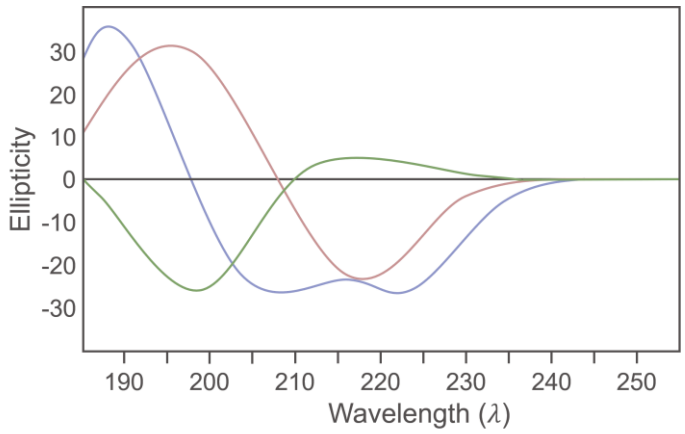

Figure 10 Schematic representation of the different characteristic CD spectra exhibited by α-helix (blue), β-sheet (red) and intrinsically disordered proteins (green).

3.5 Atomic force microscopy

Atomic force microscopy makes use of a sharp probe that scans across the surface of the object of interest. The set-up includes a movable stage, a scanning head onto which the probe is mounted and a response detecting laser. The probe itself is attached to a cantilever where the opposite side of the probe is highly reflective. Due to the high sensitivity of the technique it is necessary to have a nearly atomically flat substrate, which most commonly, for biomolecules, is mica. This silicate mineral gives an ultraflat negatively charged hydrophilic surface as it is cleaved, that readily adsorbs proteins to the surface. As the probe scans across the surface, interactions between the outermost atoms of the tip of the probe and the object occur as they are brought into proximity of each other, which results in a deflection of the probe, that is then recorded by laser reflections from the probe to the detector. This allows the creation of topographical images (256). AFM can be used in different modes, with the most common one for static topographical imaging being intermittent contact (or tapping) mode. The intermittent contact mode works by vertical oscillation of the cantilever with a fixed amplitude. However, as the cantilever is brought into proximity of the object, the interacting forces between the tip and the object will cause a change to the oscillation amplitude, which through a feedback loop alters the vertical position of the stage to maintain the fixed amplitude and this generates a topographic image of the sample. This technique can allow sub-nanometer vertical resolution, and approximately 1 nm lateral resolution, and is a common technique for imaging amyloid fibrils (257).

3.6 Electron microscopy

Optical and electron microscopes are similar in many ways. Both light and electrons can be described as particles, and in terms of wavelengths. While typical optical microscopes utilize the visible spectrum that has wavelengths of 400-700 nm, with a diffraction limit of about 150 nm, electron microscopes use electrons that have wavelengths in the range of 0.001 and 0.01 nm and are capable of separating two points with about 0.05 nm distance (258, 259). Benefits of electron microscopes over light microscopes include higher resolution, higher magnification, greater depth of field and versatility. However, disadvantages with electron microscopes exist as well. They are expensive to build and maintain, and as electrons are far more scattered by air than light, where they would barely penetrate a few mm at atmospheric pressure, the electron path has to be in a vacuum. This text will focus on the transmission electron microscope, although much is shared with the scanning electron microscope. The electron microscope has several parts, where the “illumination” source is an electron gun, which emits electrons that passes through two or more electromagnetic condenser lenses. These lenses fulfill much the same function as an optic condenser lens, by focusing the electrons onto the sample. Below the condensers is the sample chamber, where the sample scatters electrons depending on thickness and material (less than 100 nm), and the electrons that exit pass the objective and intermediate lenses. The image is finally created as the electrons hit the imaging device, often a

phosphor screen (258). This technique can be used to image amyloid fibrils, where heavy metal salts are adsorbed onto the fibrils, whereafter an electron image can be generated due to differential electron scattering as a result of the mass-thickness difference between the fibrils and the stain (260). Additionally, specific protein species can be detected through the use of immunogold staining, where primary antibodies recognize the protein, after which secondary antibodies with attached colloidal gold particles recognize the primary antibodies. The gold then scatters electrons, allowing one to detect the antigen binding location.

3.7 Surface plasmon resonance

A highly sensitive technique capable of quantitively detecting the dynamic binding of biomolecules is surface plasmon resonance (SPR). SPR can provide binding affinity, specificity and kinetics, and it does so by detecting changes on the surface upon binding. Essentially, the SPR detection system consists of a polarized and monochromatic light source, a prism with a thin metal film at the base, and a detector. A reaction flow-chamber is present on the other side, where biomolecules of interest can be immobilized. The incident light at the base of the prism is directed at a specific resonance angle, which results in excitation of surface plasmons by some photons, whereas the rest are reflected to the detector. An evanescent electromagnetic field is created at the metal-liquid interface as the surface plasmons become excited, which decays exponentially into the interfacing medium where immobilized biomolecules reside. The resonance angle depends on the refractive index, which in turn is dependent on the evanescent wave. As biomolecules are immobilized, or bind to immobilized biomolecules, the evanescent wave is affected, resulting in a changed refractive index and resonance angle, thus affecting the amount of photons reflected to the detector (261). In most instruments the change in resonance angle is converted into “response units” which is linearly proportional to the bound mass on the surface, thus allowing real-time observation of the binding and dissociation processes. This can be done either by analyzing the time dependent traces of the binding to obtain the rate constants, or by using the equilibrium binding data at different concentrations of the binding partner to calculate equilibrium constant for the binding.

4. Original work

This section of the thesis aims to summarize and discuss the work performed in the research papers; wherein further details can be gathered. The section will start with the explored amyloid fibril formation mechanism of β-PV, a study that was then expanded to investigate possible consequences of specific cell conditions, *i.e* macromolecular crowding and stabilizing osmolytes, on protein misfolding and amyloid fibril formation (**paper I-II**). Subsequently, the interaction of β-PV with αS will be discussed (**paper III**), followed by the interaction of αS with the endogenous copper chaperone, Atox1 (**paper IV**).

4.1 Amyloid fibril formation of fish β-parvalbumin

Amyloid fibril formation of fish β-PV was first described in 2015, when it was found that low pH or removal of Ca^{2+} resulted in protein aggregation (151). As it was later observed that the fibrillization at pH 7.5 appeared to require the single conserved cysteine (177), it was thus an intriguing system to explore mechanistically, to expand the current knowledge of oxidation induced cross-linking and subsequent aggregation of folded proteins (**paper I**). Furthermore, as multimerization is favored by macromolecular crowding, as well as the dehydration of hydrophobic residues by stabilizing osmolytes, the effect of these conditions on the aggregation of a folded protein whose amyloid fibril formation is catalyzed by an initial covalent dimerization step appeared as an interesting venue to expand on (**paper II**).

4.1.1 Disulfide-mediated nucleation and monomer recruitment by fibrils

Oxidative stress is a pathological hallmark of a number of amyloidoses, including Alzheimer's disease, PD and diabetes type 2 (262, 263). Oxidative stress can in turn modify proteins, with one possible outcome being different types of intra- and intermolecular cross-links, *e.g.* cystine and dityrosine (264). In fact, dityrosine cross-linking has been observed in both amyloid-β plaques (265) and Lewy bodies (218) *in vivo*, as well as implicated in facilitating dimerization and aggregation of amyloid-β and αS (265, 266). Additionally, the highly cross-linking prone residue cysteine is present in several amyloidogenic proteins, although current studies are limited in regard to the impact of intermolecular disulfide bonds in amyloidoses. Apo-SOD1 has been shown to become amyloidogenic upon reduction of the homo-dimeric disulfide bond at pH 7.4, with the reduced variant being capable of recruiting disulfide-intact apo-SOD1. Although, the reduced residues were implied to be necessary for initiating nucleation by subsequent intermolecular disulfide-bond formation (267). Transthyretin, which has two cysteine residues, has also been investigated, where disulfide bridges in the Tyr114Cys variant were observed to impaired the amyloid fibril formation (268), whereas the Cys10Ala/Tyr114Cys mutant could proceed to protofibrils (269). Lastly, the human tumor suppressor protein $p16^{INK4A}$, which has one cysteine residue, was found to form amyloid fibrils upon addition of excess oxidizing agents and agitation. In this case, the disulfide-bridged dimers could form amyloid fibrils that were destabilized and disassembled upon reduction of the disulfide-bridge (270). Synthetic variants of amyloidogenic proteins that do not have cysteine residues have also been created, and it has been observed that the amyloid-β Ser26Cys mutant aggregated more rapidly than the wild-type form, albeit halted at the protofibrillary stage (271). A cysteine introduced αS mutant showed increased or reduced aggregation depending on whether the residue was introduced at the C- or N-terminal (272). Lastly, recombinant introduction of Tyr39Cys or Tyr125Cys αS mutants to cells displayed increased intracellular triton X-100 insoluble inclusions, which was further exacerbated by oxidative stress (273). The modulation of amyloid fibril formation by intermolecular disulfide bonds has varying effects depending on the protein and the location of the cross-linking cysteine, but current knowledge is lacking in this area. A perfect protein model for further expanding the understanding of this phenomenon is thus β-PV, as it is highly stable and monomeric in its holo-form, and contains a single cysteine which is thought to be important in amyloid fibril formation as β-PV transitions to its apo-form; which in turn can be easily controlled and triggered. As mammalian β-PV transitions to its apo-form, the buried cysteine side-chain becomes exposed to the environment (158, 160). Only the holo-form of fish β-PV has been solved by NMR, but it agrees well with the high-resolution structures of human holo-β-PV (Figure 11) (274).

To investigate the mechanism by which β-PV forms amyloid fibrils, aggregation of β-PV at different concentrations was monitored. From these data it could be observed that the fluorescence half-time (*i.e.* the point at which fibril mass has reached

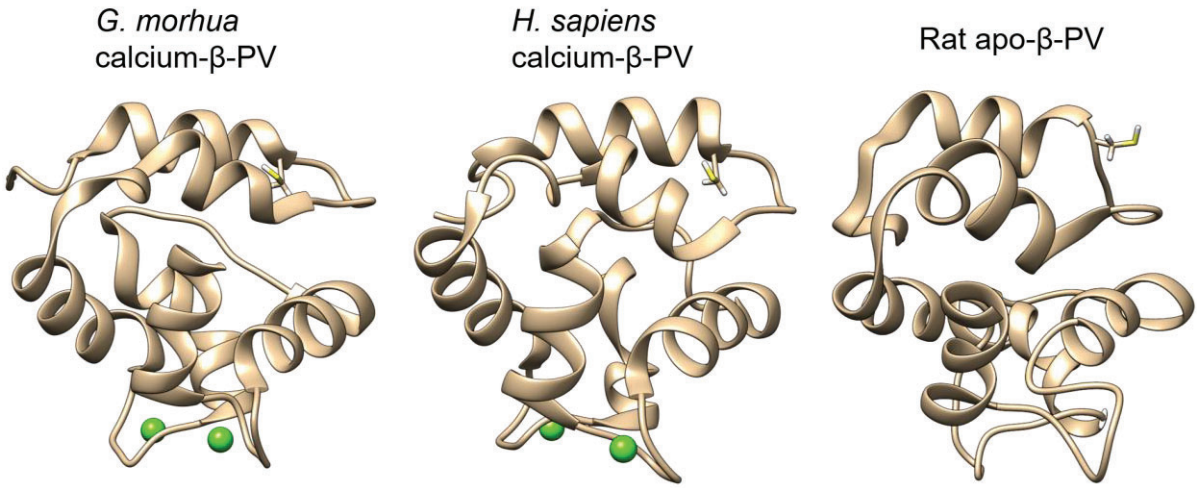

Figure 11 NMR solution structures of apo- and Ca^{2+}-β-PV of *G. morhua* (PDB: 2MBX), *H. sapiens* (PDB: 1TTX) and rat (PDB: 2NLN), with the green spheres representing Ca^{2+}. Cysteine is visualized as a stick representation and can be observed to be buried in the holo-form, whereas it is exposed in the apo-form.

50 % of its final mass) against protein concentration displayed a linear relationship on a double- logarithmic plot (Figure 12A). This suggests that the main mechanism does not change over the assayed range. In contrast, a negative curvature would suggest competition between processes and changes in the dominant process with concentration, whereas a positive curvature (*i.e.* flattening of the curve at higher concentrations) would suggest a saturation effect (182). Globally fitting mathematical models of amyloid fibril formation to the data through the use of the web-based Amylofit program (182) revealed that primary nucleation and elongation steps fitted well. To verify that secondary processes are not involved, non-sonicated fibrils were added to monomeric β-PV, and were found to be incapable of surface catalyzing nuclei formation, thus agreeing with the mathematical models (Figure 12B). Additionally, fibrils are incapable of recruiting holo-β-PV. To verify that the fibrils are elongation competent, as the model suggests, sonicated pre-formed fibrils were added, and elongation could be observed (Figure 12C).

To investigate whether the formed fibrils contain monomers, dimers, or both, they were sedimented by ultracentrifugation (100 000 *g*) and disaggregated by

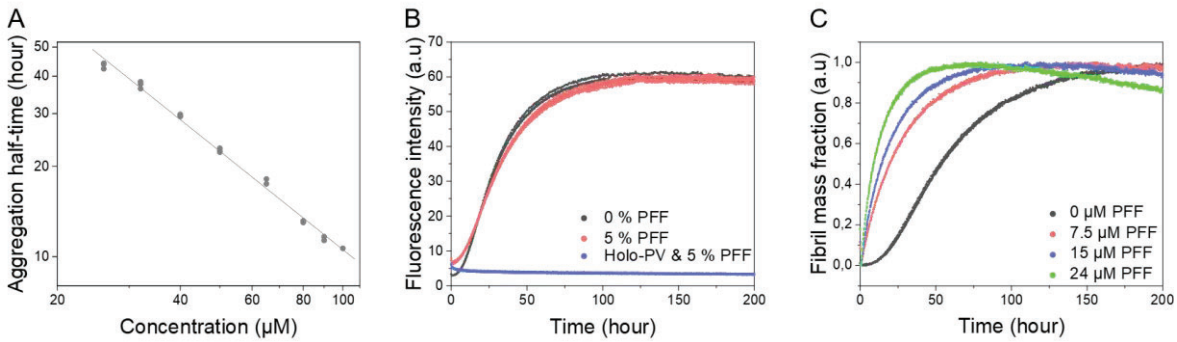

Figure 12 ThT aggregation kinetics of apo-β-PV under quiescent conditions at 37 ˚C (150 mM NaCl, 1 mM $CaCl_2$, 5 mM EDTA and 25 mM Tris-HCl, pH 7.4). (A) Double-logarithmic plot of fluorescence half-time against monomer apo-β-PV concentrations. (B) Aggregation kinetics of 50 μM apo- and holo-β-PV in the presence of 0 and 5 % pre-formed fibrils (PFF). (D) Aggregation kinetics of 30 μM apo-β-PV in the presence of varying amounts of sonicated PFF.

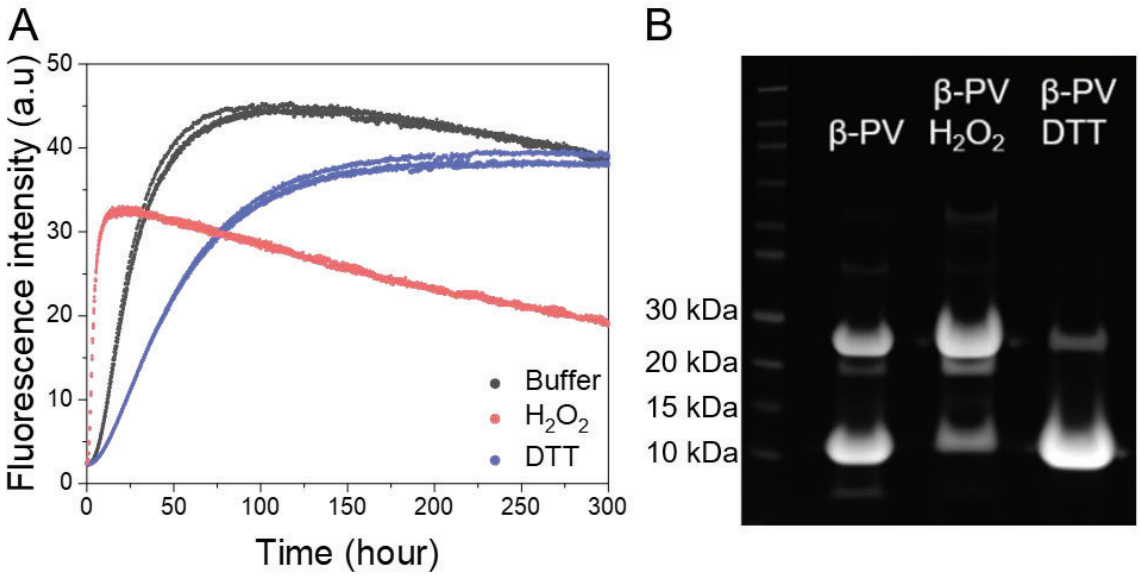

Figure 13 (A) ThT aggregation kinetics of apo-β-PV in the presence of 100 μM H_2O_2 or DTT, under quiescent conditions at 37 C˚ with 150 mM NaCl, 1 mM $CaCl_2$, 5 mM EDTA and 25 mM Tris-HCl (pH 7.4). (B) SDS-PAGE analysis of disaggregated apo-β-PV fibrils after incubation in (A).

hexafluoroisopropanol (HFIP). The disaggregated β-PV was then run on a non-reducing SDS-PAGE, which revealed an incorporation of ~40 % dimers (Figure 13B). As the dimers are the likely result of cysteine oxidation, the effect of oxidizing and reducing conditions on the apo-β-PV aggregation kinetics was investigated, and it could be observed that H_2O_2 accelerates the aggregation, whereas DTT retards it (Figure 13A). Furthermore, performing a non-reducing SDS-PAGE on the disaggregated fibrils after either conditions displayed that H_2O_2 and DTT result in an increased and decreased dimer content, respectively (Figure 13B).

To gain a deeper understanding of the dimer involvement in amyloid fibril formation of apo-β-PV, efforts to isolate them were undertaken. By incubating β-PV with increasing amounts of H_2O_2 at 4 ˚C, it could be observed that dimers formed in an H_2O_2-concentration dependent manner for apo-β-PV, but not in the case of holo-β-PV (Figure 14A). This further substantiates the notion that the cysteine is protected in the holo-form for fish β-PV, as it is for mammalian β-PV (158, 160, 274). The formed dimers could then be isolated from the monomers by size exclusion chromatography, even remaining in a stable non-aggregated state in the holo-dimer form. As they can be completely reduced to monomeric forms by DTT, it indicates that they are connected by a cystine (**paper I**). Interestingly, investigating the secondary structure of the β-PV dimers by CD, it becomes apparent that they retain a large degree of the native monomeric structure, and are capable of transitioning between the characteristic CD spectra of apo- and holo-β-PV (Figure 14BC).

After successful isolation of β-PV dimers, several kinetic aggregation assays were performed. Aggregation experiments over a concentration range of apo-β-PV dimers (4-15 μM monomer equivalents) showed a concentration dependency with a linear double-logarithmic half-time vs concentration plot, akin to the monomers (Figure 15A). Mathematical modeling with Amylofit could fit the nucleation-elongation model for the kinetic profiles of apo-β-PV dimers as well, although this time with a 20-fold

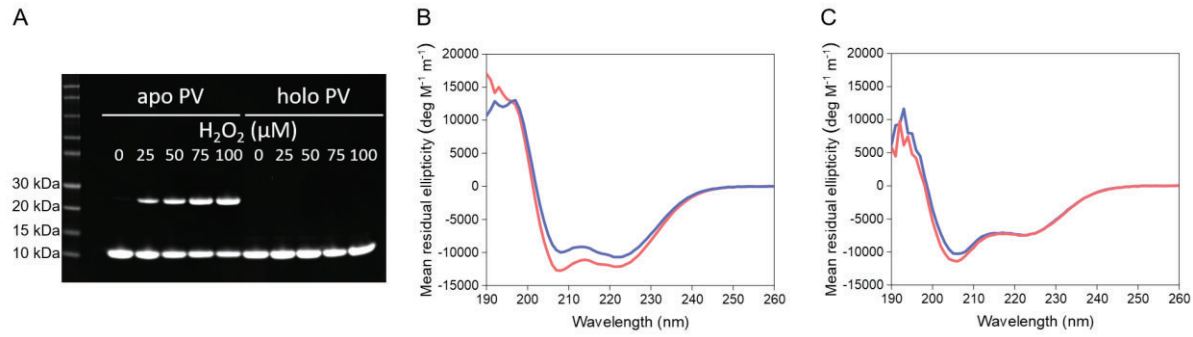

Figure 14 (A) SDS-PAGE of 50 μM β-PV incubated in the presence of 0-100 μM H_2O_2 over 20 h at 4 ˚C, in 1 mM $CaCl_2$, 5 mM EDTA (for apo) and 25 mM Tris-HCl (pH 8.22). (B and C) CD spectra of 15 μM β-PV (monomer equivalent) of monomers (blue) and dimers (red) at 21 C˚ in 1 mM $CaCl_2$, 5 mM EDTA (for apo) in Tris-HCl (pH 7.8) in Ca^{2+}- (B) or apo-β-PV state (C).

increased convoluted rate constant compared to the monomers (in monomer equivalents, **paper I**). In addition, Ca^{2+}-β-PV dimers did not form amyloid fibrils (**paper I**). To investigate whether the apo-β-PV dimers were capable of recruiting monomers, increasing amounts of dimers were added to monomers and the kinetics were followed. As can be seen, an increasing apo-β-PV dimer concentration above 1 % results in a concentration dependent acceleration of the monomeric aggregation rate, shortening the half-time from 21.7 ± 1.5 h to 13.6 ± 1.7 h for 5 % dimers (Figure 15B). Together with the fact that the fibrils are capable of recruiting monomers for elongation (Figure 12C), this shows that the dimers can act as nuclei alone, or possibly together with monomers if they are present, and the formed nuclei may then further recruit monomeric apo-β-PV, thus creating heterogeneous fibrils.

Investigating whether there is any detectable morphological difference by AFM showed that fibrils formed from monomer, monomers accelerated by dimers, and dimeric apo-β-PV starting material all shared the same curvilinear appearance, clustering preference and fibril heights (Figure 16A-C). Furthermore, analyzing the fibrils from both monomeric and dimeric starting material by CD displays that they

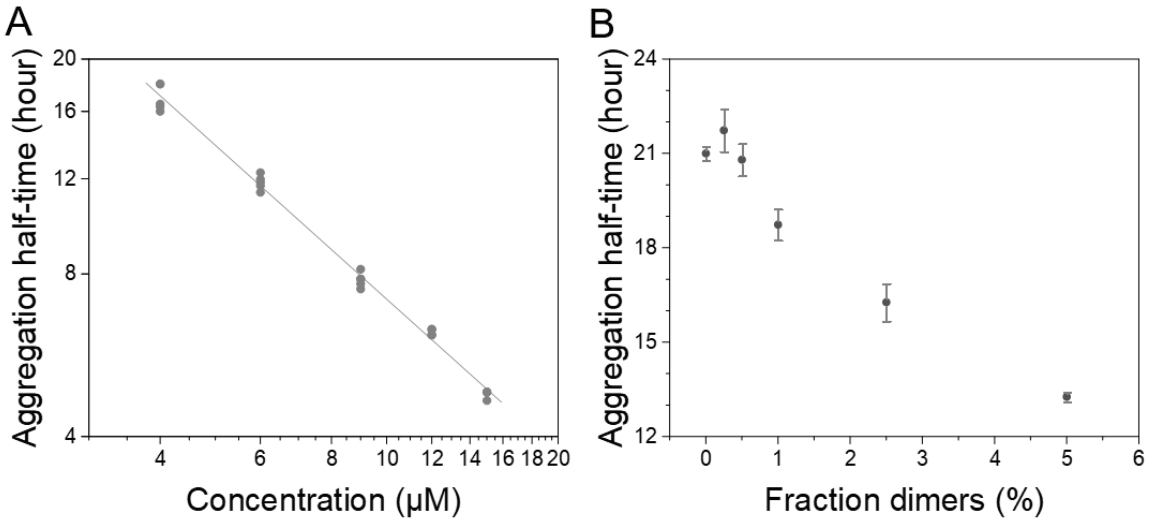

Figure 15 ThT assay of apo-β-PV under quiescent conditions at 37 ˚C (150 mM NaCl, 1 mM $CaCl_2$, 5 mM EDTA and 25 mM Tris-HCl, pH 7.4). (A) Double-logarithmic plot of fluorescence half-time against apo-β-PV concentrations. (B) Half-time plot of 50 μM total apo-β-PV, with increasing amounts of dimers (monomer equivalents).

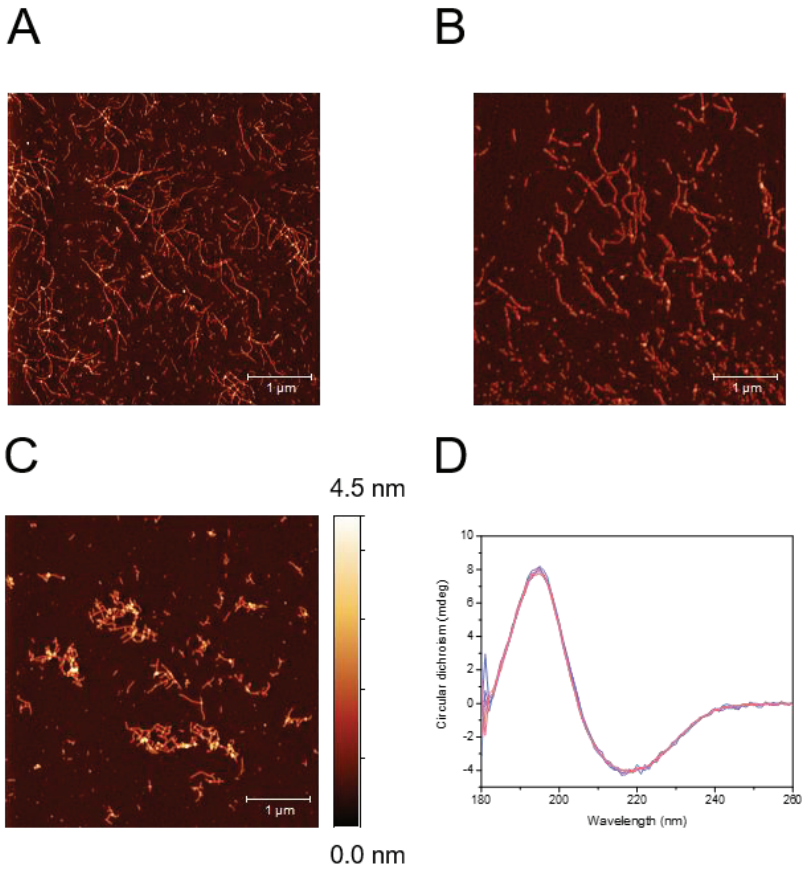

Figure 16 (A-C) AFM images of apo-β-PV fibrils created from monomeric (A), monomers accelerated by dimers (B) and dimeric (C) starting material. (D) CD spectra of apo-β-PV fibrils formed from monomeric (blue) and dimeric (red) starting material, signal matched at 222 nm (unknown concentration).

share an equal proportion of secondary structure content (Figure 16D). This thus further supports the notion that apo-β-PV fibrils share the same conformation regardless of monomeric or dimeric origin.

As discussed in section 2.4, fish β-PV and mammalian β-PV appear to be more different than how it has been described in the literature. The major structural reorganization displayed by mammalian β-PV, as it transitions from holo- to apo-form, occurs in the Ca^{2+} specific CD-domain (159, 160). However, fish β-PV has two Ca^{2+}/Mg^{2+} mixed sites, *i.e.* the CD-domain is a mixed binding site (163), and a fast and dramatic structural change is typically a characteristic of Ca^{2+} specific signal transduction proteins (159). This thus raises the question whether fish β-PV undergoes the same structural reorganization as mammalian β-PV, and if Mg^{2+} is capable of inducing the change as well. Several experiments were performed to probe this, albeit indirectly. ThT aggregation assay displayed that 2 mM $MgCl_2$ was capable of completely preventing β-PV from proceeding to amyloid fibrils (lower concentration was not tested) (Figure 17A). Furthermore, upon exposure of Mg^{2+}-β-PV to H_2O_2, it could be observed by SDS-PAGE that, in similarity to Ca^{2+}-β-PV, dimers did not form, whereas apo-β-PV readily formed dimers (Figure 17B). Ellman's assay, which quantifies sulfhydryl groups, was also employed, and showed that while apo-β-PV had instantaneous reaction of all its thiols, the thiols in Ca^{2+}- and Mg^{2+}-β-PV reacted far

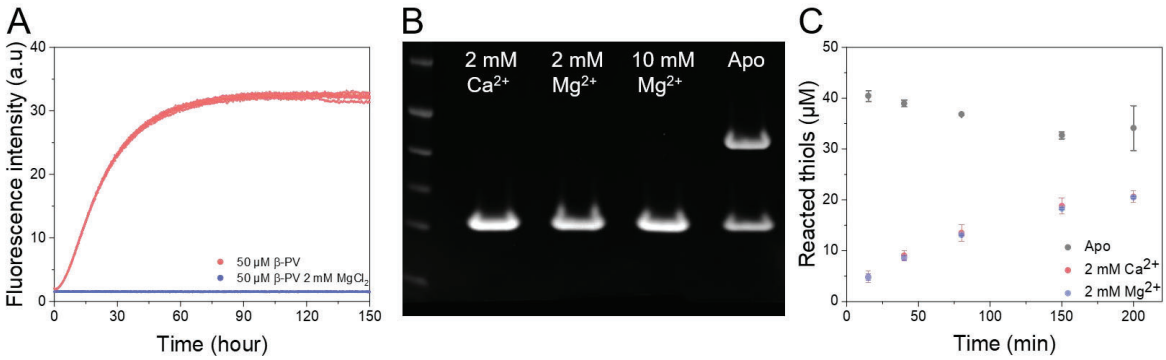

Figure 17 (A) ThT aggregation kinetics of apo- and Mg^{2+}-β-PV under quiescent conditions at 37 ˚C (150 mM NaCl, 2 mM $MgCl_2$, 25 mM Tris-HCl, pH 7.4, and 10 mM EDTA in the apo-β-PV sample). (B) SDS-PAGE of 50 μM β-PV incubated at under quiescent conditions at room temperature for 20 hours in 25 mM Tris-HCl (pH 7.8) and 50 μM H_2O_2. (C) Ellman's assay of 35 μM β-PV in 25 mM Tris-HCl, pH 7.8, 5 mM EDTA (for apo) incubated over 200 minutes at room temperature (duplicate).

slower, and did so with an identical response to Ellman's reagent regardless of the ion (Figure 17C). These data thus suggest that, similar to mammalian β-PV, fish β-PV also undergoes structural reorganization upon loss of ligands, resulting in an exposed cysteine. Whether the reorganization is as significant as for mammalian β-PV remains to be answered.

Taken together with the study performed by Castellanos et al. (177), which showed that substituting the conserved cysteine with a serine results in ThT reactive non-fibrillary aggregates with incomplete β-sheet transition, our results suggest that the cystine formation is required for the formation of initial nuclei and subsequent fibril growth through templating of either monomers and/or dimers. However, while enhanced ThT fluorescence does not necessitate an amyloid fibril conformation, it cannot be excluded that the non-fibrillary aggregates displayed by Castellanos et al. (177) do not contain partial regions within β-PV that adopt the amyloid conformation. Although that is a phenomenon that is more prevalent with larger proteins (17).

These results are similar to those obtained for the protein $p16^{INK4A}$, which also requires an intermolecular disulfide-bond between the sole cysteine of two protein to form amyloid fibrils. However, $p16^{INK4A}$ fibrils are also stabilized by this bond and incapable of recruiting monomers, as reduction of the bond results in disaggregation of the fibrils, and formation of the fibrils requires added oxidizing agents and agitation (270). Fibril formation by apo-β-PV, on the other hand, requires neither oxidizing agents nor agitation. Instead, spontaneous disulfide bonds may form *in vitro* in reaction with dissolved O_2 (275-277), which may facilitate the apo-β-PV fibrillization (Figure 18).

Interestingly, unlike the fish orthologue, mammalian β-PV is remarkably stable from forming cystines in its apo-form, despite an exposed cysteine thiol. Mammalian apo-β-PV does not form dimers after incubation at room temperature for 30 hours (278), and it remains in a monomeric state at concentrations as high as 4 mM (160). Fish β-PV, on the other hand, forms dimers detectable by SDS-PAGE after 20 hours at 4 ˚C (Figure 14A). If one may speculate, there may be several reasons for this difference. Lower vertebrate β-PV exists intracellularly in the muscles, and cycle between Ca^{2+}- and Mg^{2+}-bound forms (173), and should thus never be in an

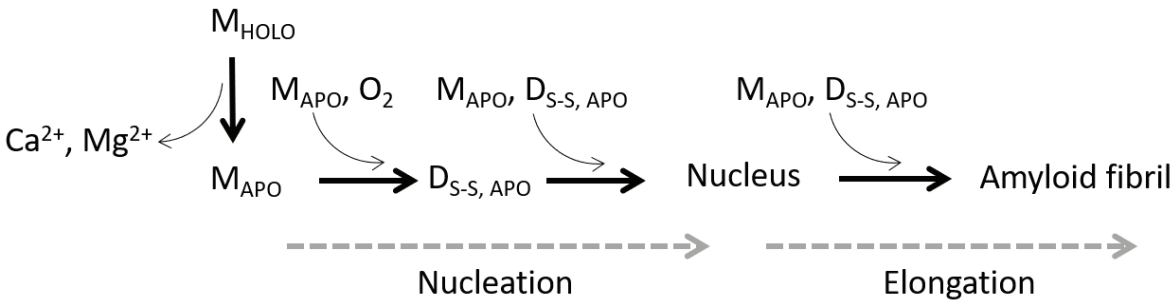

Figure 18 Proposed dominant apo-β-PV amyloid fibril formation mechanism, which is initially triggered by conformational change concomitant with cysteine exposure as the ligands release (*i.e.* Ca^{2+} and Mg^{2+}) from the holo-form (M_{HOLO}). The monomer in its apo-form (M_{APO}) then, in reaction with O_2, forms a disulfide bond with another monomer, thus creating covalent apo-dimers ($D_{SS,\ APO}$). These dimers may then proceed to nuclei and amyloid fibrils that can be elongated by both monomeric and dimeric apo-β-PV.

apo-state *in vivo*. Instead, the structural reorganization observed may be a feature to modulate the Ca^{2+}- and Mg^{2+} binding affinities, by imparting a penalty upon binding, thus lowering the affinity (160, 176). Mammalian β-PV, on the other hand, displays different tissue expression patterns. It is, for example, secreted by macrophages during intraocular inflammation (169), and activated macrophages reside in heavily oxidizing environments (*e.g.* inflammation). This may require mammalian β-PV to possess a stronger ligand independent stabilization of the native structure in this extracellular environment, possibly with additional features such as local charge repulsion preventing the thiols from approaching each other. In addition, *G. morhua* β-PV is not designed for the high temperatures of mammals, where 37 ˚C might thermally destabilize the protein structure. Combined with loss of ligands and thermal destabilization, a local unfolding and thus exposure of adhesive, hydrophobic, residues of *G. morhua* β-PV might occur, that in turn may bring the thiols into vicinity of each other and thus facilitate disulfide-bond formation. The formed dimer may then result in further destabilization and local unfolding, as well as increasing the chance of collision between two segments possessing, at the same time, the conformational compatibility for forming the initial intermolecular beta-sheets.

Another intriguing question arises as to the purpose of the metabolically expensive cysteine (279) that has been conserved between all the lower vertebrates. One possible answer might be that β-PV acts as a redox sensor, as cysteine is known to act as a redox sensor *in vivo*. The way cysteine does so is through oxidation to sulfenic or sulfinic acid, that in turn can be recognized by the cell (280). Muscles, in turn, produce a lot of reactive oxygen species during contraction that, at too high levels, result in contractile dysfunction and muscle fatigue (281). The Ellman's assay showed that while the thiol was more protected in Ca^{2+} and Mg^{2+} bound β-PV, it was, however, not inaccessible (Figure 17C). The levels of the muscle reactive oxygen species might thus be sensed by the abundantly expressed β-PV, resulting in adaptation of the antioxidant defenses. A similar function might also hold true for mammalian β-PV, where it might have a function in sensing the oxidative environment during *e.g.* inflammation.

4.1.2 Macromolecular crowding and stabilizing osmolytes accelerate aggregation of apo-β-parvalbumin

Another interesting aspect of amyloid fibril formation *in vivo* is how it is modulated by the steric effect of macromolecular crowding. As described in section 2.5.2, folded proteins in their native state become stabilized by macromolecular crowding (225, 227), but when they are partially destabilized, *i.e.* low pH (225, 228) or in the absence of a crucial ligand (229), macromolecular crowding might accelerate amyloid fibril formation. The effect of macromolecular crowding is thus interesting from the perspective of β-PV. As β-PV releases Ca^{2+} its conformation becomes expanded, although it still retains an α-helical fold. Thus, macromolecular crowding could, on one hand, potentially stabilize apo-β-PV by reducing its conformational space (219). On the other hand, as dimerization facilitates amyloid fibril formation, it is also possible that macromolecular crowding will promote multimerization of apo-β-PV, that can lead to amyloid fibril formation. Furthermore, if the intermediate species towards nuclei result in expanded conformational states, they may be prevented from forming amyloid fibrils, instead resulting in *e.g.* native-like aggregates. In a similar vein, and as discussed in 2.5.3, protective osmolytes might also stabilize the protein native monomeric state, or facilitate multimerization, due to osmophobic effect and unfavorable interaction with protein backbone, which in turn might either prevent or facilitate amyloid fibril formation, respectively.

The ThT aggregation assay was employed to monitor the amyloid fibril formation of apo-β-PV in the presence of the different macromolecular crowding agents and stabilizing osmolytes. Ficoll 70 was primarily used as a macromolecular crowding agent, as it is generally considered inert with little or no protein interactions (282-284). The aggregation rate of apo-β-PV in presence of 100 and 200 mg/ml Ficoll 70 displayed a significant acceleration compared to incubation in buffer alone, with a reduced half-time from 32 ± 3 h to 11 ± 1 h (100 mg/ml) and 4.5 ± 0.2 h (200 mg/ml), and drastically shortened lag time (Figure 19A). The increase in aggregation rate by Ficoll 70 is quite substantial, as 30 μM apo-β-PV in 100 mg/ml (6.5 % excluded volume) Ficoll 70 results in an aggregation half-time of ~10.5 h, which is what would be expected from ~100 μM β-PV (Figure 12A). AFM was utilized to visualize the sample at the plateau of the fluorescence ThT intensity, revealing fibrils that appear similar for both buffer and macromolecular crowding conditions (**paper II**). The data suggest that macromolecular crowding does not stabilize the monomeric β-PV state, thus allowing nuclei formation, and drastically accelerates either nucleation, elongation or both. To probe the apo-β-PV conformation in macromolecular crowding conditions, far-UV CD was used at 50 mg/ml Ficoll 70, as higher Ficoll 70 concentration induced aggregation at a too rapid pace. Since the holo-state of β-PV is a more compact state (177), one might speculate that any compaction and stabilization would result in a CD spectrum similar to that of the holo-state. However, at 50 mg/ml Ficoll 70, no immediate secondary structure content difference could be observed (Figure 19B). To investigate whether the effect can be replicated by another crowding agent, PEG 35,000 was used, which again resulted in an accelerated aggregation (Figure 19C).

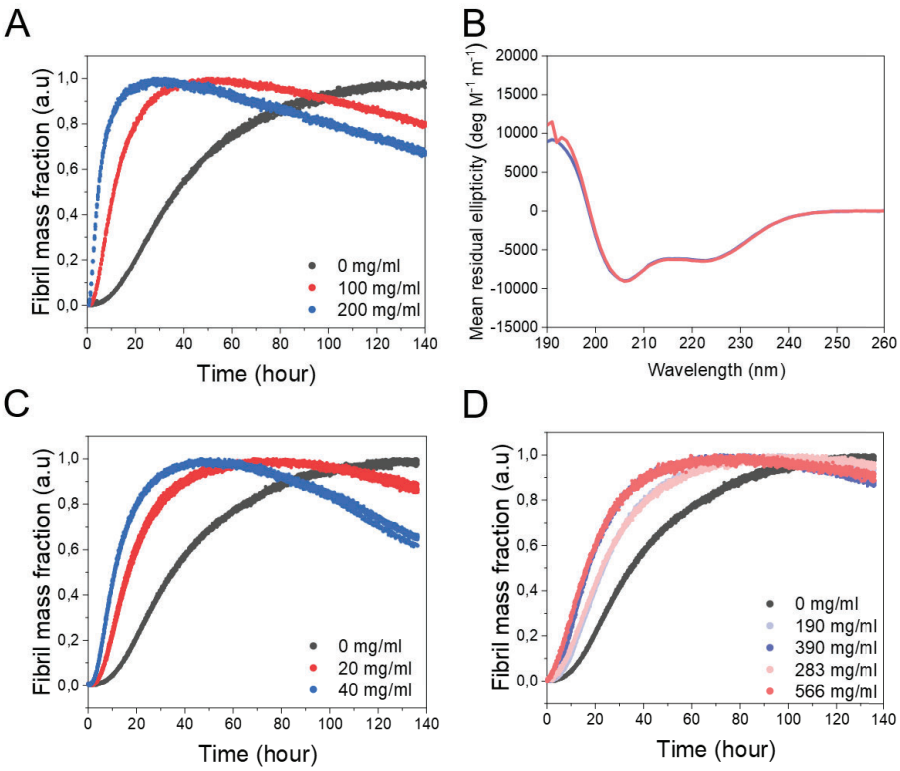

Figure 19 ThT aggregation kinetics of 30 µM apo-β-PV under quiescent conditions at 37 ˚C (150 mM NaCl, 1 mM $CaCl_2$, 5 mM EDTA and 25 mM Tris-HCl, pH 7.4) with 0-200 mg/ml Ficoll 70 (A), 0-40 mg/ml PEG 35,000 (C) or 0-390 mg/ml sucrose (blue) or 0-566 mg/ml glycerol (red) (D). (B) CD spectra of 15 µM apo-β-PV at 21 C˚ in 96 µM $CaCl_2$, 1 mM EDTA, 10 mM Tris-HCl (pH 7.8) with (red) or without (blue) 50 mg/ml Ficoll 70.

Sucrose and glycerol were then used to test the effect of stabilizing osmolytes. The results showed that both sucrose and glycerol accelerated apo-β-PV amyloid fibril formation in a concentration dependent manner, reducing the lag time (Figure 19D). The overall aggregation rate was not promoted as strongly as in the case of Ficoll 70 when considering the concentration (weight/volume) of the agent, where 380 mg/ml sucrose reduced the half-time by a factor of two, whereas 200 mg/ml Ficoll 70 reduced the half-time by a factor of seven (Figure 19AD). AFM shows the same curvilinear fibrils are formed in sucrose and glycerol as for buffer (**paper II**).

To delineate whether the elongation rate is affected, seeding experiments (7.5 µM sonicated pre-formed fibrils) were performed at Ficoll 70 and sucrose concentrations that still allowed for a lag-phase, *i.e.* 50 and 190 mg/ml, respectively. The initial linear slope of fibril mass increase corresponding solely to elongation was then investigated, and it could be seen that whereas Ficoll 70 accelerates the elongation rate of apo-β-PV, sucrose retards (Figure 21). Acceleration of the fibril elongation rate appears to be a generic effect of macromolecular crowding by high weight polymers (*e.g.* dextran 200 kDa) on IDPs and destabilized globular proteins, and was associated with the changes in volume available to the reactants and products (285). The stabilizing osmolyte, sucrose, instead has the opposite effect, delaying the fibril elongation rate. This might be due to the polymerization reaction requiring an expanded conformational transition of β-PV as it restructures from α-helices to β-sheets. As such, sucrose might prevent the transition due to the osmophobic effect, which is in line with previous results showing that glucose prevents globular proteins

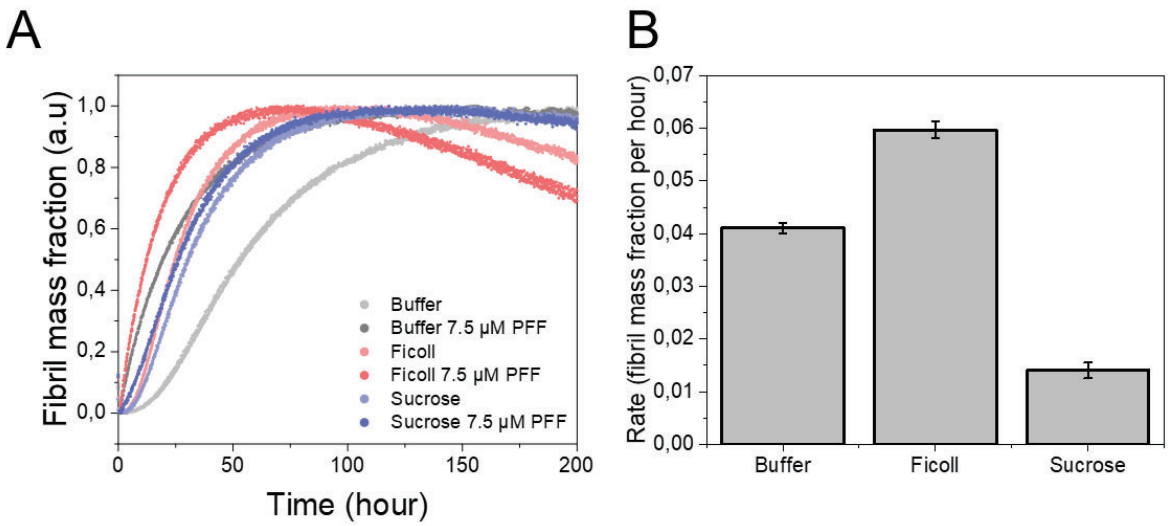

Figure 20 (A) ThT aggregation kinetics of 30 µM apo-β-PV under quiescent conditions at 37 ˚C (150 mM NaCl, 1 mM $CaCl_2$, 5 mM EDTA and 25 mM Tris-HCl, pH 7.4) with or without 7.5 µM sonicated pre-formed fibrils, either in buffer, 50 mg/ml Ficoll 70 or 390 mg/ml sucrose. (B) Elongation rate of (A) during the first 2.3 hours.

that retain a significant degree of their structure from polymerizing the fibril (285). However, there might also be increased diffusion limitation as a result of increased viscosity, thus retarding elongation, which cannot be delineated from these data (286). Furthermore, as sucrose reduces the elongation rate, while still accelerating the overall aggregation, it appears that stabilizing osmolytes facilitate nucleation of apo-β-PV.

Both macromolecular crowding conditions and presence of stabilizing osmolytes accelerate the overall aggregation of β-PV. Macromolecular crowding appears to do so sterically, by reducing occupied volume through multimer association, thus maximizing system entropy. While it can be observed that the excluded volume effect accelerates elongation, the data do not confirm whether nucleation is accelerated as well, as fibrils may have already formed in the lag phase. Stabilizing osmolytes, on the other hand, might accelerate aggregation through the osmophobic effect, thus facilitating multimerization in order to reduce the solvent accessible surface area and in turn facilitate disulfide bonds and subsequently nuclei formation.

4.2 Effect of fish β-parvalbumin amyloid fibrils on α-synuclein aggregation

As mentioned in section 2.3, diet is one implicated modulator of PD initiation; where *e.g.* the Mediterranean diet has been correlated with a reduced PD incidence (287). Fish in particular is generally considered beneficial against several age-related diseases, including dementia and Alzheimer's disease (288-290), which is typically assumed to be due to ω-3 fatty acids (291). However, direct evidence of such an effect by ω-3 is lacking (292), possibly due to the fact that the triggering event is thought to occur decades before clinical symptoms, thus making such studies difficult endeavors (20, 63). Nevertheless, there are multiple components to fish, with one being fish β-PV, which is expressed at a concentration as high as 0.2 g / 100 g muscle tissue depending on the fish species (293). Additionally, while most dietary proteins are proteolytically degraded as to recycle and utilize the individual building blocks (294), β-PV instead forms amyloid fibrils that confer a resistance against proteases (151). In fact, following a meal of fish, β-PV epitopes can be recognized in the blood (178), implying not only retained sequence and/or structure, but also transcellular transport. As αS appears to be a pleiotropic protein (20, 99, 100) with a wide tissue expression (98, 101-103), including in the gastric and enteric environment, *e.g.* enteroendocrine cells that sample the intestinal lumen (103), it is thus interesting to investigate whether β-PV interacts with αS.

To investigate whether β-PV is capable of modulating the amyloid fibril formation of αS, the ThT assay was employed. As can be observed, while the addition of 280 μM non-aggregating Ca^{2+}-β-PV to 70 μM αS has no effects on αS kinetics (Figure 21A), apo-β-PV appears to be capable of completely inhibiting αS aggregation, as the resulting kinetics in the samples with both proteins show identical aggregation curves to that of apo-β-PV alone, rather than co-aggregation of both (Figure 21A). As the apo-β-PV kinetics are completely unaffected by αS, this suggests that it is not the monomers but rather the formed fibrils that prevent αS from aggregating. To test whether this is the case, 280 μM pre-formed fibrils of apo-β-PV were added to 70 μM αS. Apo-β-PV fibrils also displayed an inhibitory behavior on αS aggregation (Figure 21B). Since amyloid fibril formation can be inhibited at many different stages, the question arises as to whether the apo-β-PV fibrils interact with monomeric or assembled pre-fibrillar αS species. Since αS does not display secondary nucleation at pH 7.4, and fibril growth occurs by monomer addition (295), one might expect all observed non-β-PV kinetics to be due to elongation. To probe this, 1 and 5 % pre-formed αS fibrils were added to a solution containing 280 μM apo-β-PV and 70 μM αS. Interestingly, the observed kinetics are identical to those of apo-β-PV monomers for longer than 20-30 hours, followed by an increase of ThT fluorescence intensity, which is attributed to αS aggregation (Figure 21C). These results indicate that apo-β-PV fibrils are capable of slowing down the elongation rate of αS, likely by sequestering monomers from the solution. However, the aggregation of αS after about 25 h is difficult to explain, as one might expect that any elongation should occur at a constant rate due

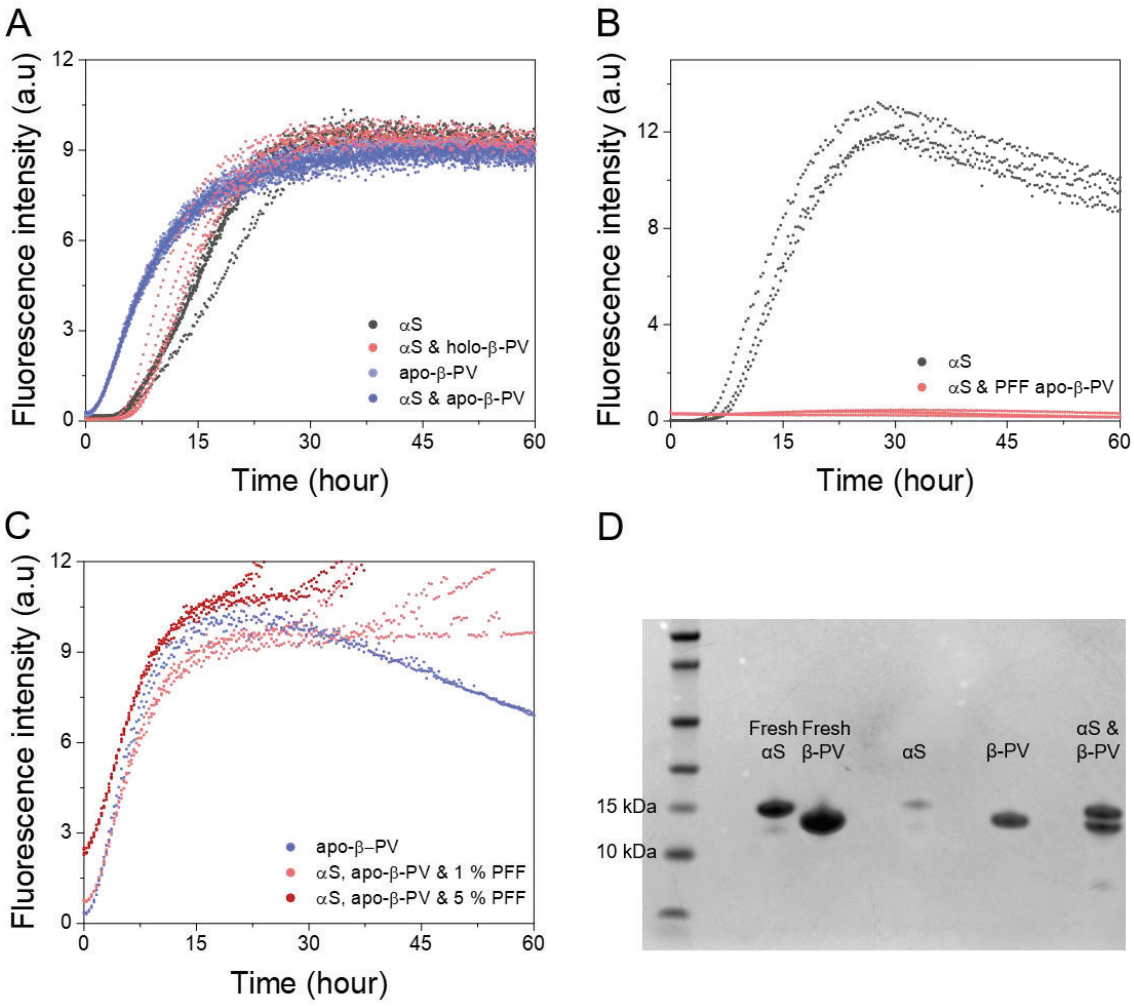

Figure 21 ThT aggregation kinetics of 70 μM αS and 280 μM apo-β-PV under agitation with 2 mm beads at 37 ˚C (150 mM NaCl, 1 mM $CaCl_2$, 5 mM EDTA (for apo) and 25 mM Tris-HCl, pH 7.4). Pre-formed fibrils (PFF) of 280 μM apo-β-PV in (B) and αS PFF in (C). (D) SDS-PAGE analysis after aggregation in (A).

to an equilibrium of monomeric αS release from the apo-β-PV fibrils. In addition, adding 1 mM Ca^{2+} to αS inhibited by β-PV fibrils appears to induce αS aggregation (**paper III**). This effect might be due to direct interaction of Ca^{2+} with either β-PV or αS. The amyloid fibril core of β-PV does not incorporate the Ca^{2+} binding loops (151, 177), and if αS interacts with these, Ca^{2+} might interfere. On the other hand, direct interaction of Ca^{2+} with αS in the C-terminal and part of the NAC-region has been shown (110), and should αS interact with β-PV fibrils through these domains, Ca^{2+} might shift the equilibrium towards released αS.

To investigate whether αS remains in a soluble non-fibrillar state when incubated together with apo-β-PV (Figure 21D), as the ThT experiments suggest, as well as whether the aggregation end-product morphology supports the ThT experiments, SDS-PAGE and AFM were used. SDS-PAGE shows that while soluble αS is clearly diminished in samples without apo-β-PV, it remains in a soluble form to a far greater degree in the presence of apo-β-PV (Figure 21D).

To verify that αS binds the β-PV fibrils, transmission electron microscopy together with immunogold staining was used, by employing non-conformationally specific αS reactive antibodies. From these images it can clearly be seen that while αS

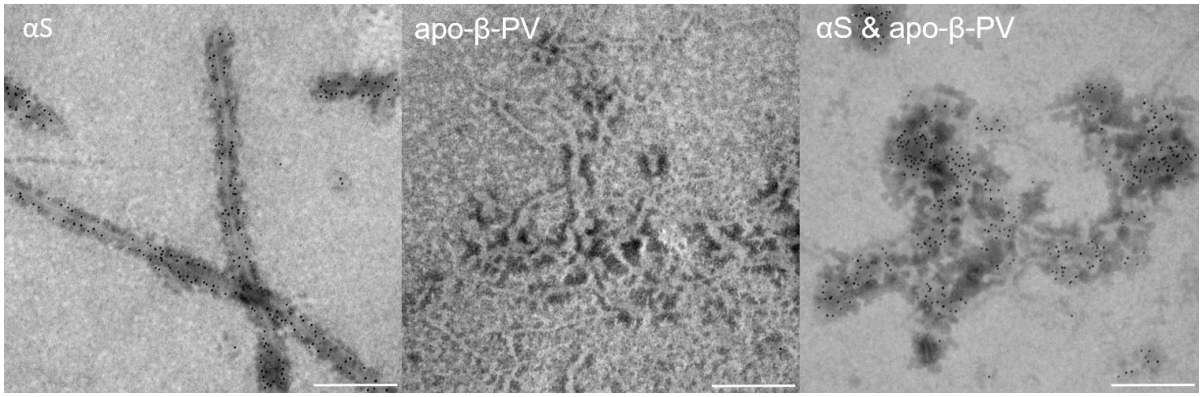

Figure 22 Transmission electron microscopy images of fibrils incubated with non-conformationally specific anti-αS antibodies and 2˚ antibodies coupled to gold nanoparticles.

fibrils are readily recognized by the antibodies, the β-PV fibrils are not. However, in the samples where αS has been incubated together with apo-β-PV, epitope reactivity can be observed for fibrils displaying β-PV morphology (Figure 22).

These results show that β-PV fibrils are capable of inhibiting αS amyloid fibril formation, likely involving monomeric αS binding to β-PV fibrils, thus sequestering αS. Although, the data do not fully exclude potential interaction with oligomeric αS, where the interaction could *e.g.* disassemble the oligomeric species. The binding location of αS is likely the surface of the β-PV fibrils, as the kinetics of the latter are unaffected by the presence of the former. From a physiological standpoint, considering the wide tissue expression of αS, including the gastrointestinal system (98, 101-103) where misfolded αS has been found (21, 22), as well as the apparent prevalence of an enteric origin in PD (18-20), β-PV would not be required to cross the blood-brain barrier for any potential interaction with αS. In addition, since there are indications that β-PV is capable of transcellular transport (178), β-PV might instead act directly in the gut, where PD triggering events might occur, thus preventing misfolding of αS. However, this is purely speculative at this point, as these findings are in a highly simplified *in vitro* system, and must thus be followed up with *in vivo* data prior to any conclusion. Nevertheless, the data are interesting from a purely molecular perspective, where the amyloid fibril of one protein appears to inhibit the amyloid fibril formation of another; in this case by αS binding to the surface of β-PV fibrils.

4.3 Copper chaperone Atox1 blocks amyloid formation of α-synuclein

Copper is one of the most abundant redox-active metal ions in humans, and is capable of generating reactive oxygen species through Fenton/Haber-Weiss reactions, that may then react with and damage lipids, proteins and DNA (296). Due to this toxic nature, virtually no free copper ions exists within the cell (297). Cells have instead developed sophisticated regulatory functions involved in the import, compartmentalization, transport and export of copper ions. After import of Cu^+ by the transmembrane high-affinity copper uptake protein 1 (298), Cu^+ is distributed to the copper chaperones antioxidant 1 copper chaperone (Atox1), cytochrome c oxidase copper chaperone and copper chaperone for superoxide dismutase (299). While αS is capable of binding copper ions, and has been implicated to both act as a ferrireductase (123) and depend on copper ions to modulate its cell membrane binding (122), the αS copper ion binding is relatively weak compared to the high affinity copper ion-binding proteins. Thus, any cytosolic copper ion-dependent activity would likely require the transfer of copper ions from another protein, if such a function exists. One such candidate could be the copper chaperone, Atox1.

To probe the effect of Atox1 on αS aggregation, ThT assay with several conditions was undertaken. Addition of either equimolar apo- or Cu^+-Atox1 to 70 μM αS results in a delayed aggregation (Figure 23A). To investigate whether αS remains in a soluble non-fibrillar state, SDS-PAGE was used to analyze the samples after the aggregation. As can be seen, while soluble αS in samples incubated with apo-Atox1 was significantly reduced, samples with Cu^+-Atox1 retained a large degree of soluble αS. Inhibition of αS aggregation by Cu^+-Atox1 was further confirmed by SEC, where a significant fraction of monomeric αS was detected after the ThT assay (Figure 23B). To directly test whether Cu^+-Atox1 is capable of binding αS, SPR was used, wherein biotinylated αS (maleimide conjugated through Ala107Cys mutation) was immobilized. Confirming the previous results, Cu^+-Atox1 was found to bind αS in a concentration-dependent manner, with a detected dissociation constant of ~5 μM, whereas no interaction with apo-Atox1 was detected (Figure 23C). To further probe the αS and Cu^+-Atox1 interaction, a fresh mixture of the proteins was run through SEC. Cu^+ bound to Atox1 results in absorption at 254 nm, and relating it to the 280 nm protein absorbance, relative Cu^+ loading of Atox1 can be measured. While no complex was observed, it could be seen that Cu^+ had been removed from Atox1, as the 254/280 nm ratio was reduced. As this ratio cannot be used to determine αS copper ion binding, the αS fraction was analyzed by inductively coupled plasma mass spectrometry for elemental analysis, which revealed elevated copper ion levels, suggesting transfer of copper from Atox1 to αS.

In an attempt to probe the Atox1 binding site, the C-terminal truncated αS variant (αS 1-97) was incubated together with Cu^+-Atox1. As the 1-97 αS amyloid fibril formation was inhibited by Cu^+-Atox1 as well, the likely site of interaction is at the αS N-terminal, which is the location of the dominant copper ion-binding site (Figure 24A).

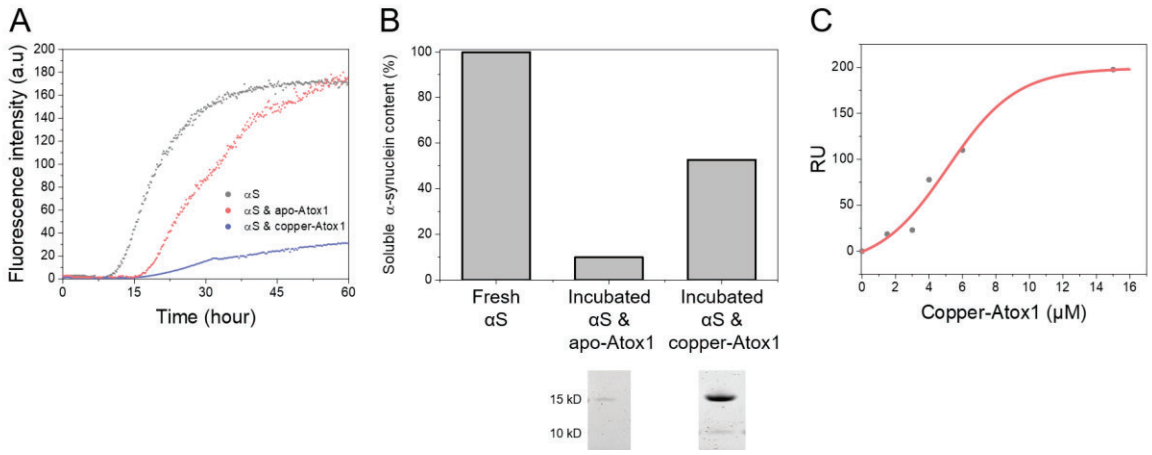

Figure 23 (A) ThT aggregation kinetics of 70 μM αS and 70 μM Atox1 under agitation with 2 mm beads at 37 ˚C (150 mM NaCl and 50 mM Tris-HCl, pH 7.4). (B) Size exclusion chromatography (top) and SDS-PAGE analysis of soluble αS after (A). (C) Surface plasmon resonance analysis of Cu^{+}-Atox1 binding to immobilized αS in 150 mM NaCl and 10 mM HEPES pH 7.4

To test whether this effect is generic to copper chaperones, copper chaperone for superoxide dismutase was incubated together with αS, resulting in no observable effect on the aggregation of αS (Figure 24B). Thus, it would appear that Atox1 specifically is capable of interacting with αS.

As can be ascertained by these results, Cu^{+}-Atox1 is capable of directly interacting with αS, thereby preventing its aggregation, whereas apo-Atox1 is not. The inhibition of 1-97 αS aggregation together with the copper ion transfer to αS indicates that a ternary complex is formed at the N-terminal of αS, bridged by Cu^{+}, which was further confirmed by a subsequent study that showed that primarily the N-terminal, up to Gln24, is involved in the binding to Atox1 (300). Furthermore, as copper chaperone for superoxide dismutase was not capable of influencing the aggregation of αS, it would appear that the interaction is specific for Atox1, and not strictly facilitated by copper ions. A subsequent study showed that Cu^{+}-Atox1 is also capable of inhibiting the aggregation of the physiologically relevant ^{NAc}αS, in addition to evidence suggesting

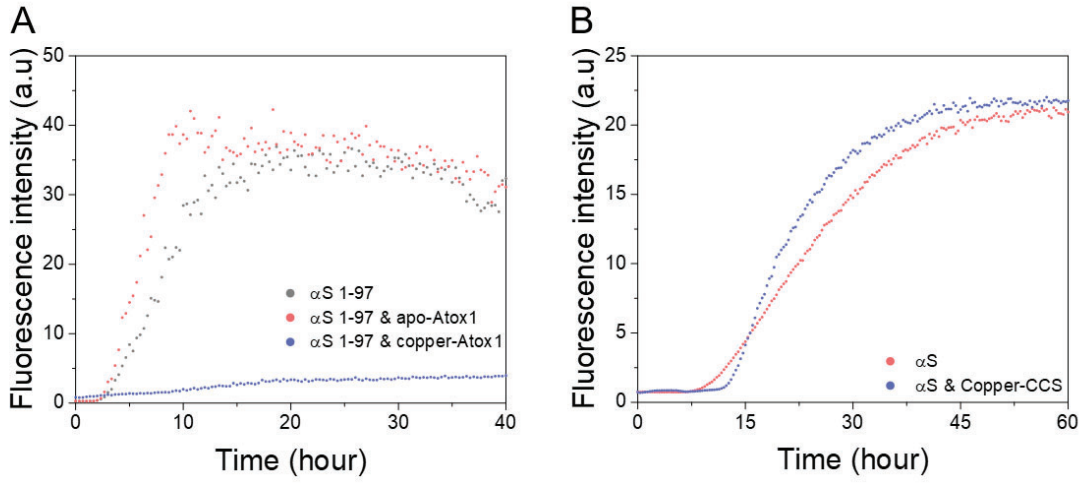

Figure 24 ThT aggregation kinetics of 70 μM αS 1-97 and 70 μM Atox1 (A), and 70 μM αS and 70 μM copper loaded copper chaperone for superoxide dismutase under agitation with 2 mm beads at 37 ˚C (150 mM NaCl and 50 mM Tris-HCl, pH 7.4).

direct interaction between the two proteins in cells (300). However, the study showed by NMR that copper ion transfer did not occur. It is interesting to speculate whether Atox1 possesses a modulating effect on αS activity through direct interaction using a copper ion as a bridge, *e.g.* modulating αS vesicle/membrane binding, or even act as an additional proteostasis component by preventing the misfolding of αS *in vivo*.

5. Concluding remarks

Through medical advances, resulting in an ever-increasing life expectancy, an increasing number of debilitating diseases related to amyloid fibrils follows. The consequences of these diseases are major reductions to quality of life as well as heavy financial costs to both private and national economy. Despite tremendous efforts into understanding these diseases, no cure exists; in part due to the multifactorial nature of their origin and complex molecular mechanisms. The complexity of the diseases has hampered our attempts to understand them, and it is therefore important to build our knowledge to better understand how and through which processes these diseases arise, so that we may rationally devise preventative measures and treatments. The work in this thesis can be divided into two main amyloid fibril related themes: (1) providing a deeper fundamental knowledge of amyloid fibril formation mechanisms, which will help guide future research and treatment efforts; (2) investigate αS interaction partners in order to provide more specific and applicable directions on future PD treatments.

The study of the amyloid fibril formation mechanism of the folded protein β-PV provided insights into the role of intermolecular interactions in protein aggregation (or fibrillization). The protein, upon losing its ligand Ca^{2+}, dimerizes through the formation of disulfide bonds followed by subsequent nucleation and amyloid fibril elongation. These findings demonstrate a system that becomes amyloidogenic through a two-step

process and is initiated by the formation of a covalent bond known to stabilize protein structures. Ligand loss could occur *in vivo* for many proteins, as a result of *e.g.* metal ion dyshomeostasis, or other conditions where proteins are unable to access crucial interaction partners, thus leading to their destabilization and amyloid fibril formation. Such an event has been demonstrated for other proteins, as in the case of demetallation of the disease related superoxide dismutase, which results in protein aggregation. Furthermore, the subsequent cross-linking of the cysteine residues, thus forming the amyloidogenic β-PV dimers, could be mirrored in amyloidoses where oxidative stress is a common feature. Subsequent templating of monomers demonstrates a potentially cascading pathogenic event where the cells end up with toxic and difficult to clear aggregates. Additionally, the otherwise protective cellular conditions of macromolecular crowding and stabilizing osmolytes, that result in excluded volume and osmophobic effect, respectively, were shown to exacerbate the amyloid fibril formation of β-PV once it was triggered.

Although amyloid fibrils are associated with diseases, they can also provide beneficial functions. β-PV in an amyloid fibril form was found to inhibit αS amyloid fibril formation, likely through sequestration onto the β-PV fibril surface. αS is expressed in the gastrointestinal tract, from which many PD incidences have been implicated to have originated. As β-PV forms amyloid fibrils in the gut, which then confers proteolytic protection, and tissue transit has been suggested, this fish protein could potentially be protective against PD. In fact, I set up a preliminary cell study using an enteroendocrine cell line and investigated potential uptake of fluorophore labeled β-PV by confocal microscopy. This study showed that while monomers were not taken up, fibrils were internalized at a very rapid rate, at lower concentrations than what the stomach concentration of β-PV would be after a meal of fish.

The putative interaction between the endogenous copper chaperone Atox1 and αS was investigated, which showed that Cu^{+}-Atox1, but not apo-Atox1, is capable of binding αS monomers and prevent their amyloid fibril formation. Additionally, it does not appear to be a generic copper chaperone effect, as copper chaperone for superoxide dismutase had no effect on the aggregation of αS. This interaction could be important *in vivo*, as it has been observed that the affected brain regions in PD have a reduced copper concentration. Such metal dyshomeostasis might then prevent the interaction of Cu^{+}-Atox1 with αS, thus facilitating the progression of PD.

The work in this thesis can be concluded as follows, based on the themes described in the first paragraph. (1) The combined effects of ligand loss and oxidative stress may induce amyloid fibril formation, and cellular environments, *i.e.* macromolecular crowding and stabilizing osmolytes are important, but often ignored, factors to consider. (2) β-PV is a potentially protective protein in fish that might prevent PD. However, physiological interaction still needs to be proven. First steps to elucidate this could be to investigate by which mechanism β-PV is taken up and whether it can gain access to the cytosol, if it is *e.g.* trapped in endosomes, in addition to studying a potential interaction between αS and β-PV in the cell. It is also an interesting general study for uptake mechanisms of amyloid fibrils, as it is unexpected that such large structures without endogenous origin would be taken up. The potential link between

αS copper binding capacity and the copper chaperone Atox1 should be followed up by expanding the study with more copper binding proteins to investigate whether more interactions exist. Research into understanding why the copper deficiency occurs is another important aspect, which may shed light on potential future therapies that may limit PD progression. For example, if the issue lies with faulty copper transporter expression or localization, one could work towards alleviating this. Alternatively, one could investigate delivery of copper, which is an approach that has indeed been initiated, with a synthetic compound known as CuATSM, and is currently undergoing clinical trials (301).

6. Acknowledgements

I would like to give my thanks to several people involved in the work presented in the thesis, directly and indirectly.

Firstly, I would like to express my thanks to my supervisor, **Pernilla**, for always being ready to give quick support and guidance no matter the time throughout my entire PhD. I am glad to have been given the scientific freedom to explore and grow as a scientist.

I would also like to express my gratitude to my co-supervisors, **Istvan** and **Sandra**, for always taking time to support, guide and discuss everything, relevant or not to the work, and all the proof-reading of the thesis.

A special thanks to **Elin** as well, for taking time out of your busy schedule to help and support. I cannot think of a better study director.

Stefan, my examiner and our head of department, you were very busy but nevertheless always ready to listen.

All the current and former lab group members. **Kumar**, I enjoyed our discussions and thank you for your support. **Ranjeet**, I would like to thank you for your support, always being ready to help and your flexibility. **Stephanie**, there were a lot of fun discussions in our office. **Xiaolu**, thank you for your optimism and helpful nature.

David, I appreciate our interesting and fruitful discussions, and thank you **Nima** for your dedication, it will be interesting to see the outcome of our joint project. I would also like to thank **Emanuele** for all the help and fantastic conversations.

I would like to thank all my colleagues at **Chemical biology, Physical chemistry** and **GU people** for creating a great and friendly environment, many interesting discussions and events.

Lastly, I would like to express my gratitude to my previous supervisors, who played crucial parts in shaping me as a researcher. **Eva Albers**, for truly opening my eyes to the greatness of science and guiding my curiosity with a lot of freedom, the importance of which cannot be overstated. **Elisabeth Hansson**, for taking in an engineer with no previous cell work and allowing me to experience the world of neurobiology, with great help and discussions during the time. **Maurizio Bettiga**, for your contagious enthusiasm, the trust you gave me and your support both within and beyond the project.

7. References

1. G. Egger, In search of a germ theory equivalent for chronic disease. *Prev Chronic Dis* **9**, E95 (2012).
2. Anonymous, 2016 Alzheimer's disease facts and figures. *Alzheimers Dement* **12**, 459-509 (2016).
3. J. Q. Trojanowski, M. Goedert, T. Iwatsubo, V. M. Y. Lee, Fatal attractions: abnormal protein aggregation and neuron death in Parkinson's disease and Lewy body dementia. *Cell Death Differ.* **5**, 832-837 (1998).
4. G. J. S. Cooper *et al.*, Purification and characterization of a peptide from amyloid-rich pancreases of type-2 diabetic-patients. *Proc. Natl. Acad. Sci. U. S. A.* **84**, 8628-8632 (1987).
5. A. Solomon, B. Frangione, E. C. Franklin, Bence-Jones proteins and light-chains of immunoglobulins - preferential association of the v-lambdavi subgroup of human light-chains with amyloidosis al(lambda). *J. Clin. Invest.* **70**, 453-460 (1982).
6. D. M. Fowler *et al.*, Functional amyloid formation within mammalian tissue. *PLoS. Biol.* **4**, 100-107 (2006).
7. L. P. Blanco, M. L. Evans, D. R. Smith, M. P. Badtke, M. R. Chapman, Diversity, biogenesis and function of microbial amyloids. *Trends Microbiol.* **20**, 66-73 (2012).
8. R. Virchow, Ueber eine im Gehirn und Rückenmark des Menschen aufgefundene Substanz mit der chemischen Reaction der Cellulose. *Archiv für pathologische Anatomie und Physiologie und für klinische Medicin* **6**, 135-138 (1854).
9. C. J. Eberth, Zur Amyloidfrage. *Archiv für pathologische Anatomie und Physiologie und für klinische Medicin* **84**, 111-118 (1881).
10. J. D. Sipe, A. S. Cohen, Review: History of the amyloid fibril. *J. Struct. Biol.* **130**, 88-98 (2000).
11. A. S. Cohen, E. Calkins, Electron microscopic observations on a fibrous component in amyloid of diverse origins. *Nature* **183**, 1202-1203 (1959).
12. M. Ankarcrona *et al.*, Current and future treatment of amyloid diseases. *J. Intern. Med.* **280**, 177-202 (2016).
13. Y. Q. Wong, K. J. Binger, G. J. Howlett, M. D. W. Griffin, Methionine oxidation induces amyloid fibril formation by full-length apolipoprotein A-I. *Proc. Natl. Acad. Sci. U. S. A.* **107**, 1977-1982 (2010).
14. T. Koudelka, F. C. Dehle, I. F. Musgrave, P. Hoffmann, J. A. Carver, Methionine Oxidation Enhances kappa-Casein Amyloid Fibril Formation. *J. Agric. Food Chem.* **60**, 4144-4155 (2012).
15. V. N. Uversky, J. Li, A. L. Fink, Pesticides directly accelerate the rate of alpha-synuclein fibril formation: a possible factor in Parkinson's disease. *FEBS Lett.* **500**, 105-108 (2001).
16. C. Garza-Lombo, Y. Posadas, L. Quintanar, M. E. Gonsebatt, R. Franco, Neurotoxicity Linked to Dysfunctional Metal Ion Homeostasis and Xenobiotic Metal Exposure: Redox Signaling and Oxidative Stress. *Antioxidants & Redox Signaling* **28**, 1669-1703 (2018).
17. F. Chiti, C. M. Dobson, "Protein Misfolding, Amyloid Formation, and Human Disease: A Summary of Progress Over the Last Decade" in Annual Review of

Biochemistry, Vol 86*,* R. D. Kornberg, Ed. (Annual Reviews, Palo Alto, 2017), vol. 86, pp. 27-68.
18. E. Svensson *et al.*, Vagotomy and subsequent risk of Parkinson's disease. *Ann Neurol* **78**, 522-529 (2015).
19. H. Braak *et al.*, Staging of brain pathology related to sporadic Parkinson's disease. *Neurobiol. Aging* **24**, 197-211 (2003).
20. M. E. Johnson, B. Stecher, V. Labrie, L. Brundin, P. Brundin, Triggers, Facilitators, and Aggravators: Redefining Parkinson's Disease Pathogenesis. *Trends Neurosci.* **42**, 4-13 (2019).
21. S. J. Chung *et al.*, Alpha-synuclein in gastric and colonic mucosa in Parkinson's disease: Limited role as a biomarker. *Mov. Disord.* **31**, 241-249 (2016).
22. B. A. Killinger *et al.*, The vermiform appendix impacts the risk of developing Parkinson's disease. *Sci. Transl. Med.* **10**, 15 (2018).
23. A. Bloch, A. Probst, H. Bissig, H. Adams, M. Tolnay, alpha-Synuclein pathology of the spinal and peripheral autonomic nervous system in neurologically unimpaired elderly subjects. *Neuropathol. Appl. Neurobiol.* **32**, 284-295 (2006).
24. E. Bianconi *et al.*, An estimation of the number of cells in the human body. *Ann. Hum. Biol.* **40**, 463-471 (2013).
25. J. D. Bloom, F. H. Arnold, In the light of directed evolution: Pathways of adaptive protein evolution. *Proc. Natl. Acad. Sci. U. S. A.* **106**, 9995-10000 (2009).
26. H. R. Qin *et al.*, Activation of signal transducer and activator of transcription 3 through a phosphomimetic serine 727 promotes prostate tumorigenesis independent of tyrosine 705 phosphorylation. *Cancer Res* **68**, 7736-7741 (2008).
27. A. Quintas, D. C. Vaz, I. Cardoso, M. J. M. Saraiva, R. M. M. Brito, Tetramer dissociation and monomer partial unfolding precedes protofibril formation in amyloidogenic transthyretin variants. *J. Biol. Chem.* **276**, 27207-27213 (2001).
28. C. B. Anfinsen, Principles that govern the folding of protein chains. *Science* **181**, 223-230 (1973).
29. G. N. Ramachandran, C. Ramakrishnan, V. Sasisekharan, Stereochemistry of polypeptide chain configurations. *J. Mol. Biol.* **7**, 95-& (1963).
30. L. Pauling, R. B. Corey, H. R. Branson, The structure of proteins; two hydrogen-bonded helical configurations of the polypeptide chain. *Proc Natl Acad Sci U S A* **37**, 205-211 (1951).
31. C. Nick Pace, J. M. Scholtz, G. R. Grimsley, Forces stabilizing proteins. *FEBS Lett.* **588**, 2177-2184 (2014).
32. P. A. Thompson *et al.*, The helix-coil kinetics of a heteropeptide. *J. Phys. Chem. B* **104**, 378-389 (2000).
33. G. Aronsson, A. C. Brorsson, L. Sahlman, B. H. Jonsson, Remarkably slow folding of a small protein. *FEBS Lett.* **411**, 359-364 (1997).
34. D. Barrick, What have we learned from the studies of two-state folders, and what are the unanswered questions about two-state protein folding? *Phys. Biol.* **6**, 9 (2009).
35. C. Levinthal, Are there pathways for protein folding. *J. Chim. Phys.-Chim. Biol.* **65**, 44-+ (1968).
36. A. Sali, E. Shakhnovich, M. Karplus, How does a protein fold. *Nature* **369**, 248-251 (1994).
37. E. Shakhnovich, G. Farztdinov, A. M. Gutin, M. Karplus, Protein folding bottlenecks - a lattice monte-carlo simulation. *Phys. Rev. Lett.* **67**, 1665-1668 (1991).

38. S. W. Englander, L. Mayne, The nature of protein folding pathways. *Proc. Natl. Acad. Sci. U. S. A.* **111**, 15873-15880 (2014).
39. K. Kuwajima, The Molten Globule, and Two-State vs. Non-Two-State Folding of Globular Proteins. *Biomolecules* **10**, 407 (2020).
40. P. G. Wolynes, J. N. Onuchic, D. Thirumalai, Navigating the folding routes. *Science* **267**, 1619-1620 (1995).
41. P. E. Wright, H. J. Dyson, Intrinsically disordered proteins in cellular signalling and regulation. *Nat Rev Mol Cell Biol* **16**, 18-29 (2015).
42. F. U. Hartl, A. Bracher, M. Hayer-Hartl, Molecular chaperones in protein folding and proteostasis. *Nature* **475**, 324-332 (2011).
43. M. P. Torrente, J. Shorter, The metazoan protein disaggregase and amyloid depolymerase system. *Prion* **7**, 457-463 (2013).
44. W. E. Balch, R. I. Morimoto, A. Dillin, J. W. Kelly, Adapting proteostasis for disease intervention. *Science* **319**, 916-919 (2008).
45. M. S. Hipp, P. Kasturi, F. U. Hartl, The proteostasis network and its decline in ageing. *Nat. Rev. Mol. Cell Biol.* **20**, 421-435 (2019).
46. H. Cui, Y. Kong, H. Zhang, Oxidative stress, mitochondrial dysfunction, and aging. *J Signal Transduct* **2012**, 646354-646354 (2012).
47. M. Sunde, C. Blake, "The structure of amyloid fibrils by electron microscopy and X-ray diffraction" in Advances in Protein Chemistry, Vol 50: Protein Misassembly, R. Wetzel, Ed. (Elsevier Academic Press Inc, San Diego, 1997), vol. 50, pp. 123-159.
48. M. Sunde *et al.*, Common core structure of amyloid fibrils by synchrotron X-ray diffraction. *J. Mol. Biol.* **273**, 729-739 (1997).
49. B. P. Ren *et al.*, Fundamentals of cross-seeding of amyloid proteins: an introduction. *J. Mat. Chem. B* **7**, 7267-7282 (2019).
50. W. Tony, I. Horvath, P. Wittung-Stafshede, Crosstalk Between Alpha-Synuclein and Other Human and Non-Human Amyloidogenic Proteins: Consequences for Amyloid Formation in Parkinson's Disease. *J. Parkinsons Dis.* **10**, 819-830 (2020).
51. L. Goldschmidt, P. K. Teng, R. Riek, D. Eisenberg, Identifying the amylome, proteins capable of forming amyloid-like fibrils. *Proc. Natl. Acad. Sci. U. S. A.* **107**, 3487-3492 (2010).
52. D. S. Eisenberg, M. R. Sawaya, "Structural Studies of Amyloid Proteins at the Molecular Level" in Annual Review of Biochemistry, Vol 86, R. D. Kornberg, Ed. (Annual Reviews, Palo Alto, 2017), vol. 86, pp. 69-95.
53. S. L. Shammas *et al.*, Perturbation of the stability of amyloid fibrils through alteration of electrostatic interactions. *Biophys. J.* **100**, 2783-2791 (2011).
54. Z. L. Almeida, R. M. M. Brito, Structure and Aggregation Mechanisms in Amyloids. *Molecules* **25**, 30 (2020).
55. M. Fandrich *et al.*, Amyloid fibril polymorphism: a challenge for molecular imaging and therapy. *J. Intern. Med.* **283**, 218-237 (2018).
56. M. Arrasate, S. Mitra, E. S. Schweitzer, M. R. Segal, S. Finkbeiner, Inclusion body formation reduces levels of mutant huntingtin and the risk of neuronal death. *Nature* **431**, 805-810 (2004).
57. M. M. Tompkins, W. D. Hill, Contribution of somal Lewy bodies to neuronal death. *Brain Res.* **775**, 24-29 (1997).
58. P. J. Muchowski, J. L. Wacker, Modulation of neurodegeneration by molecular chaperones. *Nat. Rev. Neurosci.* **6**, 11-22 (2005).

59. A. Y. Chen, P. Wilburn, X. Hao, T. Tully, Walking deficits and centrophobism in an alpha-synuclein fly model of Parkinson's disease. *Genes Brain Behav.* **13**, 812-820 (2014).
60. K. Wakabayashi, K. Matsumoto, K. Takayama, M. Yoshimoto, H. Takahashi, NACP, a presynaptic protein, immunoreactivity in Lewy bodies in Parkinson's disease. *Neurosci. Lett.* **239**, 45-48 (1997).
61. K. Wakabayashi *et al.*, The Lewy Body in Parkinson's Disease and Related Neurodegenerative Disorders. *Mol. Neurobiol.* **47**, 495-508 (2013).
62. H. C. Cheng, C. M. Ulane, R. E. Burke, Clinical Progression in Parkinson Disease and the Neurobiology of Axons. *Ann. Neurol.* **67**, 715-725 (2010).
63. G. W. Ross *et al.*, Parkinsonian signs and substantia nigra neuron density in decendents elders without PD. *Ann. Neurol.* **56**, 532-539 (2004).
64. T. R. Sampson *et al.*, A gut bacterial amyloid promotes alpha-synuclein aggregation and motor impairment in mice. *eLife* **9**, 19 (2020).
65. M. F. Sun, Y. Q. Shen, Dysbiosis of gut microbiota and microbial metabolites in Parkinson's Disease. *Ageing Res. Rev.* **45**, 53-61 (2018).
66. J. M. Kim *et al.*, Association between hepatitis C virus infection and Parkinson's disease. *Mov. Disord.* **31**, 1584-1585 (2016).
67. E. Stolzenberg *et al.*, A Role for Neuronal Alpha-Synuclein in Gastrointestinal Immunity. *J. Innate Immun.* **9**, 456-463 (2017).
68. C. T. Dow, M. paratuberculosis and Parkinson's disease - Is this a trigger. *Med. Hypotheses* **83**, 709-712 (2014).
69. R. L. Jayaraj, E. A. Rodriguez, Y. Wang, M. L. Block, Outdoor Ambient Air Pollution and Neurodegenerative Diseases: the Neuroinflammation Hypothesis. *Current environmental health reports* **4**, 166-179 (2017).
70. L. G. Gunnarsson, L. Bodin, Parkinson's disease and occupational exposures: a systematic literature review and meta-analyses. *Scand. J. Work Environ. Health* **43**, 197-209 (2017).
71. P. Dusek *et al.*, The neurotoxicity of iron, copper and manganese in Parkinson's and Wilson's diseases. *J. Trace Elem. Med. Biol.* **31**, 193-203 (2015).
72. A. Camacho-Soto *et al.*, Traumatic brain injury in the prodromal period of Parkinson's disease: A large epidemiological study using medicare data. *Ann. Neurol.* **82**, 744-754 (2017).
73. F. Barreau, J. P. Hugot, Intestinal barrier dysfunction triggered by invasive bacteria. *Curr. Opin. Microbiol.* **17**, 91-98 (2014).
74. D. M. da Fonseca *et al.*, Microbiota-Dependent Sequelae of Acute Infection Compromise Tissue-Specific Immunity. *Cell* **163**, 354-366 (2015).
75. V. N. Uversky, J. Li, A. L. Fink, Metal-triggered structural transformations, aggregation, and fibrillation of human alpha-synuclein - A possible molecular link between Parkinson's disease and heavy metal exposure. *J. Biol. Chem.* **276**, 44284-44296 (2001).
76. M. T. Baltazar *et al.*, Pesticides exposure as etiological factors of Parkinson's disease and other neurodegenerative diseases-A mechanistic approach. *Toxicol. Lett.* **230**, 85-103 (2014).
77. E. M. Rocha, B. De Miranda, L. H. Sanders, Alpha-synuclein: Pathology, mitochondrial dysfunction and neuroinflammation in Parkinson's disease. *Neurobiol. Dis.* **109**, 249-257 (2018).
78. I. Peter *et al.*, Anti-Tumor Necrosis Factor Therapy and Incidence of Parkinson Disease Among Patients With Inflammatory Bowel Disease. *JAMA Neurol.* **75**, 939-946 (2018).

79. P. Weimers *et al.*, Inflammatory Bowel Disease and Parkinson's Disease: A Nationwide Swedish Cohort Study. *Inflamm. Bowel Dis.* **25**, 111-123 (2019).
80. J. C. Lin, C. S. Lin, C. W. Hsu, C. L. Lin, C. H. Kao, Association Between Parkinson's Disease and Inflammatory Bowel Disease: a Nationwide Taiwanese Retrospective Cohort Study. *Inflamm. Bowel Dis.* **22**, 1049-1055 (2016).
81. M. Villumsen, S. Aznar, B. Pakkenberg, T. Jess, T. Brudek, Inflammatory bowel disease increases the risk of Parkinson's disease: a Danish nationwide cohort study 1977-2014. *Gut* **68**, 18-24 (2019).
82. L. Thoo, M. Noti, P. Krebs, Keep calm: the intestinal barrier at the interface of peace and war. *Cell Death Dis.* **10**, 13 (2019).
83. S. F. Assimakopoulos, I. Papageorgiou, A. Charonis, Enterocytes' tight junctions: From molecules to diseases. *World J Gastrointest Pathophysiol* **2**, 123-137 (2011).
84. S. K. Biswas, Does the Interdependence between Oxidative Stress and Inflammation Explain the Antioxidant Paradox? *Oxidative Med. Cell. Longev.* **2016**, 9 (2016).
85. M. H. Polymeropoulos *et al.*, Mutation in the alpha-synuclein gene identified in families with Parkinson's disease. *Science* **276**, 2045-2047 (1997).
86. J. C. Bridi, F. Hirth, Mechanisms of alpha-Synuclein Induced Synaptopathy in Parkinson's Disease. *Front. Neurosci.* **12**, 18 (2018).
87. A. Iwai *et al.*, The precursor protein of non-a-beta component of alzheimers-disease amyloid is a presynaptic protein of the central-nervous-system. *Neuron* **14**, 467-475 (1995).
88. Y. T. Asi *et al.*, Alpha-synuclein mRNA expression in oligodendrocytes in MSA. *Glia* **62**, 964-970 (2014).
89. L. Maroteaux, J. T. Campanelli, R. H. Scheller, Synuclein - a neuron-specific protein localized to the nucleus and presynaptic nerve-terminal. *J. Neurosci.* **8**, 2804-2815 (1988).
90. J. Burre, The Synaptic Function of alpha-Synuclein. *J. Parkinsons Dis.* **5**, 699-713 (2015).
91. M. Zaltieri *et al.*, alpha-synuclein and synapsin III cooperatively regulate synaptic function in dopamine neurons. *J. Cell Sci.* **128**, 2231-2243 (2015).
92. S. Chandra, G. Gallardo, R. Fernandez-Chacon, O. M. Schluter, T. C. Sudhof, alpha-synuclein cooperates with CSP alpha in preventing neurodegeneration. *Cell* **123**, 383-396 (2005).
93. J. Burre *et al.*, alpha-Synuclein Promotes SNARE-Complex Assembly in Vivo and in Vitro. *Science* **329**, 1663-1667 (2010).
94. F. Miraglia, A. Ricci, L. Rota, E. Colla, Subcellular localization of alpha-synuclein aggregates and their interaction with membranes. *Neural Regen. Res.* **13**, 1136-1144 (2018).
95. N. M. Bonini, B. I. Glasson, Snaring the function of alpha-synuclein. *Cell* **123**, 359-361 (2005).
96. J. J. Diao *et al.*, Native alpha-synuclein induces clustering of synaptic-vesicle mimics via binding to phospholipids and synaptobrevin-2/VAMP2. *eLife* **2**, 17 (2013).
97. J. Burre, M. Sharma, T. C. Sudhof, alpha-Synuclein assembles into higher-order multimers upon membrane binding to promote SNARE complex formation. *Proc. Natl. Acad. Sci. U. S. A.* **111**, E4274-E4283 (2014).

98. N. P. Alza, P. A. I. Gonzalez, M. A. Conde, R. M. Uranga, G. A. Salvador, Lipids at the Crossroad of alpha-Synuclein Function and Dysfunction: Biological and Pathological Implications. *Front. Cell. Neurosci.* **13**, 17 (2019).
99. A. A. Surguchev, A. Surguchov, Synucleins and Gene Expression: Ramblers in a Crowd or Cops Regulating Traffic? *Front. Molec. Neurosci.* **10**, 11 (2017).
100. F. N. Emamzadeh, Alpha-synuclein structure, functions, and interactions. *J. Res. Med. Sci.* **21**, 165-173 (2016).
101. S. J. Gardai *et al.*, Elevated Alpha-Synuclein Impairs Innate Immune Cell Function and Provides a Potential Peripheral Biomarker for Parkinson's Disease. *Plos One* **8**, 21 (2013).
102. J. Burre, M. Sharma, T. C. Sudhof, Cell Biology and Pathophysiology of alpha-Synuclein. *Cold Spring Harb. Perspect. Med.* **8**, 28 (2018).
103. R. Chandra, A. Hiniker, Y. M. Kuo, R. L. Nussbaum, R. A. Liddle, alpha-Synuclein in gut endocrine cells and its implications for Parkinson's disease. *JCI Insight* **2**, 13 (2017).
104. W. S. Davidson, A. Jonas, D. F. Clayton, J. M. George, Stabilization of alpha-synuclein secondary structure upon binding to synthetic membranes. *J. Biol. Chem.* **273**, 9443-9449 (1998).
105. M. Zhu, A. L. Fink, Lipid binding inhibits alpha-synuclein fibril formation. *J. Biol. Chem.* **278**, 16873-16877 (2003).
106. G. Fusco *et al.*, Direct observation of the three regions in alpha-synuclein that determine its membrane-bound behaviour. *Nat. Commun.* **5**, 8 (2014).
107. O. M. A. El-Agnaf *et al.*, Aggregates from mutant and wild-type alpha-synuclein proteins and NAC peptide induce apoptotic cell death in human neuroblastoma cells by formation of beta-sheet and amyloid-like filaments. *FEBS Lett.* **440**, 71-75 (1998).
108. J. A. Rodriguez *et al.*, Structure of the toxic core of alpha-synuclein from invisible crystals. *Nature* **525**, 486-+ (2015).
109. V. N. Uversky, A. Fink, Amino acid determinants of alpha-synuclein aggregation: putting together pieces of the puzzle. *FEBS Lett.* **522**, 9-13 (2002).
110. J. Lautenschlager *et al.*, C-terminal calcium binding of alpha-synuclein modulates synaptic vesicle interaction. *Nat. Commun.* **9**, 13 (2018).
111. A. Binolfi, L. Quintanar, C. W. Bertoncini, C. Griesinger, C. O. Fernandez, Bioinorganic chemistry of copper coordination to alpha-synuclein: Relevance to Parkinson's disease. *Coordination Chemistry Reviews* **256**, 2188-2201 (2012).
112. A. Binolfi *et al.*, Exploring the Structural Details of Cu(I) Binding to α-Synuclein by NMR Spectroscopy. *J. Am. Chem. Soc.* **133**, 194-196 (2011).
113. F. Camponeschi *et al.*, Copper(I)-α-synuclein interaction: structural description of two independent and competing metal binding sites. *Inorg Chem* **52**, 1358-1367 (2013).
114. E. Atrian-Blasco *et al.*, Cu and Zn coordination to amyloid peptides: From fascinating chemistry to debated pathological relevance. *Coord. Chem. Rev.* **371**, 38-55 (2018).
115. A. Ohrfelt *et al.*, Identification of Novel alpha-Synuclein Isoforms in Human Brain Tissue by using an Online NanoLC-ESI-FTICR-MS Method. *Neurochem. Res.* **36**, 2029-2042 (2011).
116. J. P. Anderson *et al.*, Phosphorylation of Ser-129 is the dominant pathological modification of alpha-synuclein in familial and sporadic Lewy body disease. *J. Biol. Chem.* **281**, 29739-29752 (2006).

117. M. C. Miotto *et al.*, Copper Binding to the N-Terminally Acetylated, Naturally Occurring Form of Alpha-Synuclein Induces Local Helical Folding. *J. Am. Chem. Soc.* **137**, 6444-6447 (2015).
118. G. M. Moriarty, C. Minetti, D. P. Remeta, J. Baum, A Revised Picture of the Cu(II)-alpha-Synuclein Complex: The Role of N-Terminal Acetylation. *Biochemistry* **53**, 2815-2817 (2014).
119. R. J. Mason, A. R. Paskins, C. F. Dalton, D. P. Smith, Copper Binding and Subsequent Aggregation of alpha-Synuclein Are Modulated by N-Terminal Acetylation and Ablated by the H50Q Missense Mutation. *Biochemistry* **55**, 4737-4741 (2016).
120. M. C. Miotto *et al.*, Copper binding to the N-terminally acetylated, naturally occurring form of alpha-synuclein induces local helical folding. *J Am Chem Soc* **137**, 6444-6447 (2015).
121. P. Faller, C. Hureau, G. La Penna, Metal Ions and Intrinsically Disordered Proteins and Peptides: From Cu/Zn Amyloid-beta to General Principles. *Accounts Chem. Res.* **47**, 2252-2259 (2014).
122. X. Y. Wang, D. Moualla, J. A. Wright, D. R. Brown, Copper binding regulates intracellular alpha-synuclein localisation, aggregation and toxicity. *J. Neurochem.* **113**, 704-714 (2010).
123. P. Davies, D. Moualla, D. R. Brown, Alpha-synuclein is a cellular ferrireductase. *PLoS One* **6**, e15814 (2011).
124. N. D'Ambrosi, L. Rossi, Copper at synapse: Release, binding and modulation of neurotransmission. *Neurochem. Int.* **90**, 36-45 (2015).
125. K. Yamada, T. Iwatsubo, Extracellular alpha-synuclein levels are regulated by neuronal activity. *Mol. Neurodegener.* **13**, 8 (2018).
126. Y. P. Cao, R. Mezzenga, Food protein amyloid fibrils: Origin, structure, formation, characterization, applications and health implications. *Adv. Colloid Interface Sci.* **269**, 334-356 (2019).
127. C. Veerman, H. Baptist, L. M. C. Sagis, E. Van der Linden, A new multistep Ca2+-Induced cold gelation process for beta-lactoglobulin. *J. Agric. Food Chem.* **51**, 3880-3885 (2003).
128. Y. Shen *et al.*, Amyloid fibril systems reduce, stabilize and deliver bioavailable nanosized iron. *Nat. Nanotechnol.* **12**, 642-+ (2017).
129. M. Mohammadian, A. Madadlou, Characterization of fibrillated antioxidant whey protein hydrolysate and comparison with fibrillated protein solution. *Food Hydrocolloids* **52**, 221-230 (2016).
130. B. Hu *et al.*, Polyphenol-Binding Amyloid Fibrils Self-Assemble into Reversible Hydrogels with Antibacterial Activity. *ACS Nano* **12**, 3385-3396 (2018).
131. F. C. Dehle, H. Ecroyd, I. F. Musgrave, J. A. Carver, alpha B-Crystallin inhibits the cell toxicity associated with amyloid fibril formation by kappa-casein and the amyloid-beta peptide. *Cell Stress Chaperones* **15**, 1013-1026 (2010).
132. Y. M. Xing *et al.*, Transmission of mouse senile amyloidosis. *Lab. Invest.* **81**, 493-499 (2001).
133. D. Cui, H. Kawano, Y. Hoshii, Y. Liu, T. Ishihara, Acceleration of murine AA amyloid deposition by bovine amyloid fibrils and tissue homogenates. *Amyloid-J. Protein Fold. Disord.* **15**, 77-83 (2008).
134. R. Sanchez *et al.*, The amyloid fold of Gad m 1 epitopes governs IgE binding. *Sci Rep* **6**, 10 (2016).

135. R. S. Brown, A. J. Bennet, H. Slebockatilk, Recent perspectives concerning the mechanism of h3o+-promoted and oh--promoted amide hydrolysis. *Accounts Chem. Res.* **25**, 481-488 (1992).
136. H. X. Zhou, X. D. Pang, Electrostatic Interactions in Protein Structure, Folding, Binding, and Condensation. *Chem. Rev.* **118**, 1691-1741 (2018).
137. F. Dong, H. X. Zhou, Electrostatic contributions to T4 lysozyme stability: Solvent-exposed charges versus semi-buried salt bridges. *Biophys. J.* **83**, 1341-1347 (2002).
138. J. S. Harrison *et al.*, Role of Electrostatic Repulsion in Controlling pH-Dependent Conformational Changes of Viral Fusion Proteins. *Structure* **21**, 1085-1096 (2013).
139. S. M. Loveday, S. G. Anema, H. Singh, beta-Lactoglobulin nanofibrils: The long and the short of it. *Int. Dairy J.* **67**, 35-45 (2017).
140. S. M. Loveday *et al.*, Tuning the properties of beta-lactoglobulin nanofibrils with pH, NaCl and CaCl2. *Int. Dairy J.* **20**, 571-579 (2010).
141. A. K. Buell *et al.*, Electrostatic Effects in Filamentous Protein Aggregation. *Biophys. J.* **104**, 1116-1126 (2013).
142. S. E. Radford, W. S. Gosal, G. W. Platt, Towards an understanding of the structural molecular mechanism of beta(2)-microglobulin amyloid formation in vitro. *BBA-Proteins Proteomics* **1753**, 51-63 (2005).
143. C. Lara, S. Gourdin-Bertin, J. Adamcik, S. Bolisetty, R. Mezzenga, Self-Assembly of Ovalbumin into Amyloid and Non-Amyloid Fibrils. *Biomacromolecules* **13**, 4213-4221 (2012).
144. J. Zidar, F. Merzel, Probing Amyloid-Beta Fibril Stability by Increasing Ionic Strengths. *J. Phys. Chem. B* **115**, 2075-2081 (2011).
145. A. Abelein, J. Jarvet, A. Barth, A. Graslund, J. Danielsson, Ionic Strength Modulation of the Free Energy Landscape of A beta(40) Peptide Fibril Formation. *J. Am. Chem. Soc.* **138**, 6893-6902 (2016).
146. J. D. Flynn, R. P. McGlinchey, R. L. Walker, J. C. Lee, Structural features of alpha-synuclein amyloid fibrils revealed by Raman spectroscopy. *J. Biol. Chem.* **293**, 767-776 (2018).
147. P. J. Marek, V. Patsalo, D. F. Green, D. P. Raleigh, Ionic Strength Effects on Amyloid Formation by Amylin Are a Complicated Interplay among Debye Screening, Ion Selectivity, and Hofmeister Effects. *Biochemistry* **51**, 8478-8490 (2012).
148. G. I. Makhatadze, P. L. Privalov, Contribution of hydration to protein-folding thermodynamics .1. the enthalpy of hydration. *J. Mol. Biol.* **232**, 639-659 (1993).
149. P. L. Privalov, G. I. Makhatadze, Contribution of hydration to protein-folding thermodynamics .2. The entropy and gibbs energy of hydration. *J. Mol. Biol.* **232**, 660-679 (1993).
150. S. M. Loveday, X. L. Wang, M. A. Rao, S. G. Anema, H. Singh, beta-Lactoglobulin nanofibrils: Effect of temperature on fibril formation kinetics, fibril morphology and the rheological properties of fibril dispersions. *Food Hydrocolloids* **27**, 242-249 (2012).
151. J. Martinez *et al.*, Fish beta-parvalbumin acquires allergenic properties by amyloid assembly. *Swiss Med. Wkly.* **145**, 11 (2015).
152. B. Schwaller, The continuing disappearance of "pure" Ca2+ buffers. *Cell. Mol. Life Sci.* **66**, 275-300 (2009).
153. J. G. Henrotte, A crystalline constituent from myogen of carp muscles. *Nature* **169**, 968-969 (1952).

154. R. H. Kretsinger, C. E. Nockolds, Carp muscle calcium-binding protein .2. structure determination and general description. *J. Biol. Chem.* **248**, 3313-3326 (1973).
155. E. S. Lander *et al.*, Initial sequencing and analysis of the human genome. *Nature* **409**, 860-921 (2001).
156. M. Goodman, J.-F. Pechére, The evolution of muscular parvalbumins investigated by the maximum parsimony method. *Journal of Molecular Evolution* **9**, 131-158 (1977).
157. J. A. Cox, I. Durussel, D. J. Scott, M. W. Berchtold, Remodeling of the AB site of rat parvalbumin and oncomodulin into a canonical EF-hand. *Eur. J. Biochem.* **264**, 790-799 (1999).
158. E. Babini *et al.*, Solution structure of human beta-parvalbumin and structural comparison with its paralog alpha-parvalbumin and with their rat orthologs. *Biochemistry* **43**, 16076-16085 (2004).
159. J. A. Cox, M. Milos, J. P. MacManus, Calcium- and magnesium-binding properties of oncomodulin. Direct binding studies and microcalorimetry. *J Biol Chem* **265**, 6633-6637 (1990).
160. M. T. Henzl, J. J. Tanner, Solution structure of Ca2+-free rat beta-parvalbumin (oncomodulin). *Protein Sci.* **16**, 1914-1926 (2007).
161. M. T. Henzl, J. J. Tanner, Solution structure of Ca2+-free rat alpha-parvalbumin. *Protein Sci.* **17**, 431-438 (2008).
162. L. K. Climer, A. M. Cox, T. J. Reynolds, D. D. Simmons, Oncomodulin: The Enigmatic Parvalbumin Protein. *Front. Molec. Neurosci.* **12**, 18 (2019).
163. J. Haiech, J. Derancourt, J. F. Pechere, J. G. Demaille, Magnesium and calcium-binding to parvalbumins - evidence for differences between parvalbumins and an explanation of their relaxing function. *Biochemistry* **18**, 2752-2758 (1979).
164. A. Kuehn, T. Scheuermann, C. Hilger, F. Hentges, Important Variations in Parvalbumin Content in Common Fish Species: A Factor Possibly Contributing to Variable Allergenicity. *Int. Arch. Allergy Immunol.* **153**, 359-366 (2010).
165. C. A. McPhalen, A. R. Sielecki, B. D. Santarsiero, M. N. James, Refined crystal structure of rat parvalbumin, a mammalian alpha-lineage parvalbumin, at 2.0 A resolution. *J Mol Biol* **235**, 718-732 (1994).
166. U. G. Fohr *et al.*, Human alpha-parvalbumins and beta-parvalbumins - structure and tissue-specific expression. *Eur. J. Biochem.* **215**, 719-727 (1993).
167. D. D. Simmons, B. Tong, A. D. Schrader, A. J. Hornak, Oncomodulin Identifies Different Hair Cell Types in the Mammalian Inner Ear. *J. Comp. Neurol.* **518**, 3785-3802 (2010).
168. N. Sakaguchi, M. T. Henzl, I. Thalmann, R. Thalmann, B. A. Schulte, Oncomodulin is expressed exclusively by outer hair cells in the organ of Corti. *J. Histochem. Cytochem.* **46**, 29-39 (1998).
169. Y. Q. Yin *et al.*, Oncomodulin links inflammation to optic nerve regeneration. *Proc. Natl. Acad. Sci. U. S. A.* **106**, 19587-19592 (2009).
170. J. P. Macmanus, L. M. Brewer, J. F. Whitfield, The widely-distributed tumor protein, oncomodulin, is a normal constituent of human and rodent placentas. *Cancer Lett.* **27**, 145-151 (1985).
171. Y. Ogawa, M. Tanokura, Kinetic-studies of calcium-binding to parvalbumins from bullfrog skeletal-muscle. *J. Biochem.* **99**, 81-89 (1986).

172. H. J. Moeschler, J. J. Schaer, J. A. Cox, A thermodynamic analysis of the binding of calcium and magnesium-ions to parvalbumin. *Eur. J. Biochem.* **111**, 73-78 (1980).
173. J. A. Rall, Role of parvalbumin in skeletal muscle relaxation. *News Physiol. Sci.* **11**, 249-255 (1996).
174. T. T. Hou, J. D. Johnson, J. A. Rall, Effect of temperature on relaxation rate and ca2+, mg2+ dissociation rates from parvalbumin of frog-muscle fibers. *J. Physiol.-London* **449**, 399-410 (1992).
175. Y. Jiang, J. D. Johnson, J. A. Rall, Parvalbumin relaxes frog skeletal muscle when sarcoplasmic reticulum Ca2+-ATPase is inhibited. *Am. J. Physiol.-Cell Physiol.* **270**, C411-C417 (1996).
176. M. T. Henzl, S. Agah, J. D. Larson, Association of the AB and CD-EF domains from rat alpha- and beta-parvalbumin. *Biochemistry* **43**, 10906-10917 (2004).
177. M. Castellanos, A. Torres-Pardo, R. Rodriguez-Perez, M. Gasset, Amyloid Assembly Endows Gad m 1 with Biomineralization Properties. *Biomolecules* **8**, 11 (2018).
178. N. Scheers, H. Lindqvist, A. M. Langkilde, I. Undeland, A. S. Sandberg, Vitamin B12 as a potential compliance marker for fish intake. *Eur J Nutr* **53**, 1327-1333 (2014).
179. P. Arosio, T. P. Knowles, S. Linse, On the lag phase in amyloid fibril formation. *Phys Chem Chem Phys* **17**, 7606-7618 (2015).
180. F. Bemporad, F. Chiti, Protein misfolded oligomers: experimental approaches, mechanism of formation, and structure-toxicity relationships. *Chem Biol* **19**, 315-327 (2012).
181. F. Chiti, C. M. Dobson, Amyloid formation by globular proteins under native conditions. *Nat. Chem. Biol.* **5**, 15-22 (2009).
182. G. Meisl *et al.*, Molecular mechanisms of protein aggregation from global fitting of kinetic models. *Nat. Protoc.* **11**, 252-272 (2016).
183. F. U. Hartl, M. Hayer-Hartl, Converging concepts of protein folding in vitro and in vivo. *Nat. Struct. Mol. Biol.* **16**, 574-581 (2009).
184. P. J. Muchowski *et al.*, Hsp70 and Hsp40 chaperones can inhibit self-assembly of polyglutamine proteins into amyloid-like fibrils. *Proc. Natl. Acad. Sci. U. S. A.* **97**, 7841-7846 (2000).
185. P. Arosio *et al.*, Kinetic analysis reveals the diversity of microscopic mechanisms through which molecular chaperones suppress amyloid formation. *Nat. Commun.* **7**, 9 (2016).
186. F. A. Aprile *et al.*, Inhibition of alpha-Synuclein Fibril Elongation by Hsp70 Is Governed by a Kinetic Binding Competition between alpha-Synuclein Species. *Biochemistry* **56**, 1177-1180 (2017).
187. D. A. Parsell, A. S. Kowal, M. A. Singer, S. Lindquist, Protein disaggregation mediated by heat-shock protein hsp104. *Nature* **372**, 475-478 (1994).
188. J. Shorter, The Mammalian Disaggregase Machinery: Hsp110 Synergizes with Hsp70 and Hsp40 to Catalyze Protein Disaggregation and Reactivation in a Cell-Free System. *Plos One* **6**, 12 (2011).
189. J. R. Glover, S. Lindquist, Hsp104, Hsp70, and Hsp40: A novel chaperone system that rescues previously aggregated proteins. *Cell* **94**, 73-82 (1998).
190. J. Shorter, Hsp104: A weapon to combat diverse neurodegenerative disorders. *Neurosignals* **16**, 63-74 (2008).
191. X. C. Gao *et al.*, Human Hsp70 Disaggregase Reverses Parkinson's-Linked alpha-Synuclein Amyloid Fibrils. *Mol. Cell* **59**, 781-793 (2015).

192. I. Horvath, P. Wittung-Stafshede, Cross-talk between amyloidogenic proteins in type-2 diabetes and Parkinson's disease. *Proc. Natl. Acad. Sci. U. S. A.* **113**, 12473-12477 (2016).
193. J. X. Lu *et al.*, Structural basis of the interplay between ?-synuclein and Tau in regulating pathological amyloid aggregation. *J. Biol. Chem.* **295**, 7470-7480 (2020).
194. J. Koppen *et al.*, Amyloid-Beta Peptides Trigger Aggregation of Alpha-Synuclein In Vitro. *Molecules* **25**, 18 (2020).
195. K. Ono, R. Takahashi, T. Ikeda, M. Yamada, Cross-seeding effects of amyloid beta-protein and alpha-synuclein. *J. Neurochem.* **122**, 883-890 (2012).
196. X. Yu *et al.*, Cross-seeding and Conformational Selection between Three- and Four-repeat Human Tau Proteins. *J. Biol. Chem.* **287**, 14950-14959 (2012).
197. H. Kumar, J. B. Udgaonkar, Mechanistic and Structural Origins of the Asymmetric Barrier to Prion-like Cross-Seeding between Tau-3R and Tau-4R. *J. Mol. Biol.* **430**, 5304-5312 (2018).
198. D. Thacker *et al.*, The role of fibril structure and surface hydrophobicity in secondary nucleation of amyloid fibrils. *Proc Natl Acad Sci U S A* **117**, 25272-25283 (2020).
199. S. M. Johnson *et al.*, Native state kinetic stabilization as a strategy to ameliorate protein misfolding diseases: A focus on the transthyretin amyloidoses. *Accounts Chem. Res.* **38**, 911-921 (2005).
200. M. S. Rotunno, D. A. Bosco, An emerging role for misfolded wild-type SOD1 in sporadic ALS pathogenesis. *Front. Cell. Neurosci.* **7**, 16 (2013).
201. S. S. Ray, R. J. Nowak, R. H. Brown, P. T. Lansbury, Small-molecule-mediated stabilization of familial amyotrophic lateral sclerosis-linked superoxide dismutase mutants against unfolding and aggregation. *Proc. Natl. Acad. Sci. U. S. A.* **102**, 3639-3644 (2005).
202. G. Soldi, G. Plakoutsi, N. Taddei, F. Chiti, Stabilization of a native protein mediated by ligand binding inhibits amyloid formation independently of the aggregation pathway. *J. Med. Chem.* **49**, 6057-6064 (2006).
203. S. Giorgetti, C. Greco, P. Tortora, F. A. Aprile, Targeting Amyloid Aggregation: An Overview of Strategies and Mechanisms. *Int. J. Mol. Sci.* **19**, 27 (2018).
204. D. E. Ehrnhoefer *et al.*, EGCG redirects amyloidogenic polypeptides into unstructured, off-pathway oligomers. *Nat. Struct. Mol. Biol.* **15**, 558-566 (2008).
205. Y. X. Mo, J. T. Lei, Y. X. Sun, Q. W. Zhang, G. H. Wei, Conformational Ensemble of hIAPP Dimer: Insight into the Molecular Mechanism by which a Green Tea Extract inhibits hIAPP Aggregation. *Sci Rep* **6**, 11 (2016).
206. S. H. Wang, X. Y. Dong, Y. Sun, Thermodynamic Analysis of the Molecular Interactions between Amyloid beta-Protein Fragments and (-)-Epigallocatechin-3-gallate. *J. Phys. Chem. B* **116**, 5803-5809 (2012).
207. F. L. Palhano, J. Lee, N. P. Grimster, J. W. Kelly, Toward the Molecular Mechanism(s) by Which EGCG Treatment Remodels Mature Amyloid Fibrils. *J. Am. Chem. Soc.* **135**, 7503-7510 (2013).
208. C. Kayatekin, J. A. Zitzewitz, C. R. Matthews, Zinc Binding Modulates the Entire Folding Free Energy Surface of Human Cu,Zn Superoxide Dismutase. *J. Mol. Biol.* **384**, 540-555 (2008).
209. J. M. McCord, I. Fridovich, Superoxide dismutase. An enzymic function for erythrocuprein (hemocuprein). *J Biol Chem* **244**, 6049-6055 (1969).

210. A. Kerman *et al.*, Amyotrophic lateral sclerosis is a non-amyloid disease in which extensive misfolding of SOD1 is unique to the familial form. *Acta Neuropathol.* **119**, 335-344 (2010).
211. V. K. Mulligan *et al.*, Early Steps in Oxidation-Induced SOD1 Misfolding: Implications for Non-Amyloid Protein Aggregation in Familial ALS. *J. Mol. Biol.* **421**, 631-652 (2012).
212. M. F. Calabrese, C. M. Eakin, J. M. Wang, A. D. Miranker, A regulatable switch mediates self-association in an immunoglobulin fold. *Nat. Struct. Mol. Biol.* **15**, 965-971 (2008).
213. C. D. Syme, J. H. Viles, Solution 1H NMR investigation of Zn2+ and Cd 2+ binding to amyloid-beta peptide (Aβ) of Alzheimer's disease. *Biochimica et Biophysica Acta - Proteins and Proteomics* **1764**, 246-256 (2006).
214. C. J. Sarell, S. R. Wilkinson, J. H. Viles, Substoichiometric levels of Cu2+ ions accelerate the kinetics of fiber formation and promote cell toxicity of amyloid-β from Alzheimer disease. *J. Biol. Chem.* **285**, 41533-41540 (2010).
215. W. T. Chen, Y. H. Liao, H. M. Yu, I. H. Cheng, Y. R. Chen, Distinct effects of Zn2+, Cu2+, Fe3+, and Al3+ on amyloid-β stability, oligomerization, and aggregation: Amyloid-β destabilization promotes annular protofibril formation. *J. Biol. Chem.* **286**, 9646-9656 (2011).
216. D. L. Abeyawardhane *et al.*, Iron Redox Chemistry Promotes Antiparallel Oligomerization of alpha-Synuclein. *J. Am. Chem. Soc.* **140**, 5028-5032 (2018).
217. F. E. Ali, K. J. Barnham, C. J. Barrow, F. Separovic, Metal catalyzed oxidation of tyrosine residues by different oxidation systems of copper/hydrogen peroxide. *J. Inorg. Biochem.* **98**, 173-184 (2004).
218. Y. K. Al-Hilaly *et al.*, The involvement of dityrosine crosslinking in alpha-synuclein assembly and deposition in Lewy Bodies in Parkinson's disease. *Sci Rep* **6**, 13 (2016).
219. I. M. Kuznetsova, K. K. Turoverov, V. N. Uversky, What Macromolecular Crowding Can Do to a Protein. *Int. J. Mol. Sci.* **15**, 23090-23140 (2014).
220. R. J. Ellis, A. P. Minton, Cell biology - Join the crowd. *Nature* **425**, 27-28 (2003).
221. M. Leeman, J. Choi, S. Hansson, M. U. Storm, L. Nilsson, Proteins and antibodies in serum, plasma, and whole blood-size characterization using asymmetrical flow field-flow fractionation (AF4). *Anal. Bioanal. Chem.* **410**, 4867-4873 (2018).
222. M. M. Gao *et al.*, Crowders and CosolventsMajor Contributors to the Cellular Milieu and Efficient Means to Counteract Environmental Stresses. *ChemPhysChem* **18**, 2951-2972 (2017).
223. V. N. Uversky, E. M. Cooper, K. S. Bower, J. Li, A. L. Fink, Accelerated alpha-synuclein fibrillation in crowded milieu. *FEBS Lett.* **515**, 99-103 (2002).
224. Z. Zhou *et al.*, Crowded Cell-like Environment Accelerates the Nucleation Step of Amyloidogenic Protein Misfolding. *J. Biol. Chem.* **284**, 30148-30158 (2009).
225. L. A. Munishkina, A. Ahmad, A. L. Fink, V. N. Uversky, Guiding protein aggregation with macromolecular crowding. *Biochemistry* **47**, 8993-9006 (2008).
226. T. R. Jahn, S. E. Radford, The Yin and Yang of protein folding. *Febs J.* **272**, 5962-5970 (2005).
227. S. Mittal, L. R. Singh, Macromolecular crowding decelerates aggregation of a beta-rich protein, bovine carbonic anhydrase: a case study. *J. Biochem.* **156**, 273-282 (2014).

228. X. D. Luo, F. L. Kong, H. B. Dang, J. Chen, Y. Liang, Macromolecular crowding favors the fibrillization of beta(2)-microglobulin by accelerating the nucleation step and inhibiting fibril disassembly. *BBA-Proteins Proteomics* **1864**, 1609-1619 (2016).
229. D. M. Hatters, A. P. Minton, G. J. Howlett, Macromolecular crowding accelerates amyloid formation by human apolipoprotein C-II. *J. Biol. Chem.* **277**, 7824-7830 (2002).
230. J. Seeliger, A. Werkmuller, R. Winter, Macromolecular Crowding as a Suppressor of Human IAPP Fibril Formation and Cytotoxicity. *Plos One* **8**, 11 (2013).
231. P. H. Yancey, Organic osmolytes as compatible, metabolic and counteracting cytoprotectants in high osmolarity and other stresses. *J. Exp. Biol.* **208**, 2819-2830 (2005).
232. Z. Ignatova, L. M. Gierasch, Inhibition of protein aggregation in vitro and in vivo by a natural osmoprotectant. *Proc. Natl. Acad. Sci. U. S. A.* **103**, 13357-13361 (2006).
233. S. Sukenik, L. Sapir, R. Gilman-Politi, D. Harries, Diversity in the mechanisms of cosolute action on biomolecular processes. *Faraday Discuss.* **160**, 225-237 (2013).
234. R. Gilman-Politi, D. Harries, Unraveling the Molecular Mechanism of Enthalpy Driven Peptide Folding by Polyol Osmolytes. *J. Chem. Theory Comput.* **7**, 3816-3828 (2011).
235. R. Politi, D. Harries, Enthalpically driven peptide stabilization by protective osmolytes. *Chem. Commun.* **46**, 6449-6451 (2010).
236. M. Auton, J. Rosgen, M. Sinev, L. M. F. Holthauzen, D. W. Bolen, Osmolyte effects on protein stability and solubility: A balancing act between backbone and side-chains. *Biophys. Chem.* **159**, 90-99 (2011).
237. F. Rodriguez-Ropero, P. Rotzscher, N. F. A. van der Vegt, Comparison of Different TMAO Force Fields and Their Impact on the Folding Equilibrium of a Hydrophobic Polymer. *J. Phys. Chem. B* **120**, 8757-8767 (2016).
238. J. Mondal, G. Stirnemann, B. J. Berne, When Does Trimethylamine N-Oxide Fold a Polymer Chain and Urea Unfold It? *J. Phys. Chem. B* **117**, 8723-8732 (2013).
239. Y. T. Liao, A. C. Manson, M. R. DeLyser, W. G. Noid, P. S. Cremer, Trimethylamine N-oxide stabilizes proteins via a distinct mechanism compared with betaine and glycine. *Proc. Natl. Acad. Sci. U. S. A.* **114**, 2479-2484 (2017).
240. J. Q. Ma, I. M. Pazos, F. Gai, Microscopic insights into the protein-stabilizing effect of trimethylamine N-oxide (TMAO). *Proc. Natl. Acad. Sci. U. S. A.* **111**, 8476-8481 (2014).
241. Z. Q. Su, F. Mahmoudinobar, C. L. Dias, Effects of Trimethylamine-N-oxide on the Conformation of Peptides and its Implications for Proteins. *Phys. Rev. Lett.* **119**, 6 (2017).
242. M. C. Owen *et al.*, Effects of in vivo conditions on amyloid aggregation. *Chem. Soc. Rev.* **48**, 3946-3996 (2019).
243. A. Arora, C. Ha, C. B. Park, Inhibition of insulin amyloid formation by small stress molecules. *FEBS Lett.* **564**, 121-125 (2004).
244. F. Scaramozzino *et al.*, TMAO promotes fibrillization and microtubule assembly activity in the C-terminal repeat region of tau. *Biochemistry* **45**, 3684-3691 (2006).

245. V. N. Uversky, J. Li, A. L. Fink, Trimethylamine-N-oxide-induced folding of alpha-synuclein. *FEBS Lett* **509**, 31-35 (2001).
246. D. S. Yang, C. M. Yip, T. H. Huang, A. Chakrabartty, P. E. Fraser, Manipulating the amyloid-beta aggregation pathway with chemical chaperones. *J Biol Chem* **274**, 32970-32974 (1999).
247. J. Seeliger, K. Estel, N. Erwin, R. Winter, Cosolvent effects on the fibrillation reaction of human IAPP. *Phys. Chem. Chem. Phys.* **15**, 8902-8907 (2013).
248. M. M. Gao *et al.*, Modulation of human IAPP fibrillation: cosolutes, crowders and chaperones. *Phys. Chem. Chem. Phys.* **17**, 8338-8348 (2015).
249. G. L. Rosano, E. A. Ceccarelli, Recombinant protein expression in Escherichia coli: advances and challenges. *Front. Microbiol.* **5**, 17 (2014).
250. S. Tabor, C. C. Richardson, A BACTERIOPHAGE-T7 RNA-POLYMERASE PROMOTER SYSTEM FOR CONTROLLED EXCLUSIVE EXPRESSION OF SPECIFIC GENES. *Proc. Natl. Acad. Sci. U. S. A.* **82**, 1074-1078 (1985).
251. B. L. Wanner, R. Kodaira, F. C. Neidhardt, REGULATION OF LAC OPERON EXPRESSION - REAPPRAISAL OF THEORY OF CATABOLITE REPRESSION. *J. Bacteriol.* **136**, 947-954 (1978).
252. H. G. Pontis, "Chapter 3 - Protein and Carbohydrate Separation and Purification" in Methods for Analysis of Carbohydrate Metabolism in Photosynthetic Organisms, H. G. Pontis, Ed. (Academic Press, Boston, 2017), https://doi.org/10.1016/B978-0-12-803396-8.00003-X, pp. 45-63.
253. E. Hallgren, F. Kalman, D. Farnan, C. Horvath, J. Stahlberg, Protein retention in ion-exchange chromatography: effect of net charge and charge distribution. *J. Chromatogr. A* **877**, 13-24 (2000).
254. J. R. Lakowicz, *Principles of fluorescence spectroscopy* (Springer science & business media, 2013).
255. G. D. Fasman, *Circular dichroism and the conformational analysis of biomolecules* (Springer Science & Business Media, 2013).
256. G. Binnig, C. F. Quate, C. Gerber, Atomic force microscope. *Phys Rev Lett* **56**, 930-933 (1986).
257. C. Moller, M. Allen, V. Elings, A. Engel, D. J. Muller, Tapping-mode atomic force microscopy produces faithful high-resolution images of protein surfaces. *Biophys. J.* **77**, 1150-1158 (1999).
258. P. J. Goodhew, J. Humphreys, *Electron microscopy and analysis* (CRC Press, 2000).
259. R. Erni, M. D. Rossell, C. Kisielowski, U. Dahmen, Atomic-Resolution Imaging with a Sub-50-pm Electron Probe. *Phys. Rev. Lett.* **102**, 4 (2009).
260. S. De Carlo, J. R. Harris, Negative staining and cryo-negative staining of macromolecules and viruses for TEM. *Micron* **42**, 117-131 (2011).
261. E. Stenberg, B. Persson, H. Roos, C. Urbaniczky, Quantitative-determination of surface concentration of protein with surface-plasmon resonance using radiolabeled proteins. *J. Colloid Interface Sci.* **143**, 513-526 (1991).
262. K. J. Barnham, C. L. Masters, A. I. Bush, Neurodegenerative diseases and oxidative stress. *Nat. Rev. Drug Discov.* **3**, 205-214 (2004).
263. R. P. Robertson, Chronic oxidative stress as a central mechanism for glucose toxicity in pancreatic islet beta cells in diabetes. *J. Biol. Chem.* **279**, 42351-42354 (2004).
264. E. R. Stadtman, R. L. Levine, Free radical-mediated oxidation of free amino acids and amino acid residues in proteins. *Amino Acids* **25**, 207-218 (2003).

265. Y. K. Al-Hilaly *et al.*, A central role for dityrosine crosslinking of Amyloid-beta in Alzheimer's disease. *Acta Neuropathol. Commun.* **1**, 17 (2013).
266. J. M. Souza, B. I. Giasson, Q. P. Chen, V. M. Y. Lee, H. Ischiropoulos, Dityrosine cross-linking promotes formation of stable alpha-synuclein polymers - Implication of nitrative and oxidative stress in the pathogenesis of neurodegenerative synucleinopathies. *J. Biol. Chem.* **275**, 18344-18349 (2000).
267. M. Chattopadhyay *et al.*, Initiation and elongation in fibrillation of ALS-linked superoxide dismutase. *Proc. Natl. Acad. Sci. U. S. A.* **105**, 18663-18668 (2008).
268. T. Eneqvist *et al.*, Disulfide-bond formation in the transthyretin mutant Y114C prevents amyloid fibril formation in vivo and in vitro. *Biochemistry* **41**, 13143-13151 (2002).
269. A. Karlsson, A. Olofsson, T. Eneqvist, A. E. Sauer-Eriksson, Cys114-linked dimers of transthyretin are compatible with amyloid formation. *Biochemistry* **44**, 13063-13070 (2005).
270. C. Gobl *et al.*, Cysteine oxidation triggers amyloid fibril formation of the tumor suppressor p16(INK4A). *Redox Biol.* **28**, 14 (2020).
271. B. O'Nuallain *et al.*, Amyloid beta-protein dimers rapidly form stable synaptotoxic protofibrils. *J Neurosci* **30**, 14411-14419 (2010).
272. M. Pivato *et al.*, Covalent alpha-synuclein dimers: chemico-physical and aggregation properties. *PLoS One* **7**, e50027 (2012).
273. W. B. Zhou, C. R. Freed, Tyrosine-to-cysteine modification of human alpha-synuclein enhances protein aggregation and cellular toxicity. *J. Biol. Chem.* **279**, 10128-10135 (2004).
274. A. H. Moraes *et al.*, Solution and high-pressure NMR studies of the structure, dynamics, and stability of the cross-reactive allergenic cod parvalbumin Gad m 1. *Proteins* **82**, 3032-3042 (2014).
275. D. Cavallini, C. De Marco, S. Dupré, Luminol chemiluminescence studies of the oxidation of cysteine and other thiols to disulfides. *Arch Biochem Biophys* **124**, 18-26 (1968).
276. G. A. Bagiyan, I. K. Koroleva, N. V. Soroka, A. V. Ufimtsev, Oxidation of thiol compounds by molecular oxygen in aqueous solutions. *Russian Chemical Bulletin* **52**, 1135-1141 (2003).
277. D. S. Rehder, C. R. Borges, Cysteine sulfenic acid as an intermediate in disulfide bond formation and nonenzymatic protein folding. *Biochemistry* **49**, 7748-7755 (2010).
278. T. M. Clayshulte, D. F. Taylor, M. T. Henzl, Reactivity of cysteine 18 in oncomodulin. *J Biol Chem* **265**, 1800-1805 (1990).
279. T. Krick *et al.*, Amino Acid metabolism conflicts with protein diversity. *Mol Biol Evol* **31**, 2905-2912 (2014).
280. C. E. Paulsen, K. S. Carroll, Cysteine-mediated redox signaling: chemistry, biology, and tools for discovery. *Chem Rev* **113**, 4633-4679 (2013).
281. S. K. Powers, M. J. Jackson, Exercise-induced oxidative stress: cellular mechanisms and impact on muscle force production. *Physiol Rev* **88**, 1243-1276 (2008).
282. Y. J. Wang, H. W. He, S. Li, Effect of Ficoll 70 on Thermal Stability and Structure of Creatine Kinase. *Biochem.-Moscow* **75**, 648-654 (2010).
283. A. A. Fodeke, A. P. Minton, Quantitative characterization of polymer-polymer, protein-protein, and polymer-protein interaction via tracer sedimentation equilibrium. *J Phys Chem B* **114**, 10876-10880 (2010).

284. D. L. Zhang, L. J. Wu, J. Chen, Y. Liang, Effects of macromolecular crowding on the structural stability of human α-lactalbumin. *Acta Biochim Biophys Sin (Shanghai)* **44**, 703-711 (2012).
285. D. A. White, A. K. Buell, T. P. J. Knowles, M. E. Welland, C. M. Dobson, Protein Aggregation in Crowded Environments. *J. Am. Chem. Soc.* **132**, 5170-5175 (2010).
286. N. Lorenzen *et al.*, Role of elongation and secondary pathways in S6 amyloid fibril growth. *Biophys J* **102**, 2167-2175 (2012).
287. F. Sofi, F. Cesari, R. Abbate, G. F. Gensini, A. Casini, Adherence to Mediterranean diet and health status: meta-analysis. *Bmj* **337**, a1344 (2008).
288. A. König *et al.*, A quantitative analysis of fish consumption and coronary heart disease mortality. *Am J Prev Med* **29**, 335-346 (2005).
289. C. Bouzan *et al.*, A quantitative analysis of fish consumption and stroke risk. *Am J Prev Med* **29**, 347-352 (2005).
290. R. P. Friedland, Fish consumption and the risk of Alzheimer disease: is it time to make dietary recommendations? *Arch Neurol* **60**, 923-924 (2003).
291. G. M. Cole, Q. L. Ma, S. A. Frautschy, Omega-3 fatty acids and dementia. *Prostaglandins Leukot Essent Fatty Acids* **81**, 213-221 (2009).
292. E. Sydenham, A. D. Dangour, W. S. Lim, Omega 3 fatty acid for the prevention of cognitive decline and dementia. *Cochrane Database Syst Rev* 10.1002/14651858.CD005379.pub3, Cd005379 (2012).
293. P. W. Lee, J. A. Nordlee, S. J. Koppelman, J. L. Baumert, S. L. Taylor, Measuring parvalbumin levels in fish muscle tissue: Relevance of muscle locations and storage conditions. *Food Chem.* **135**, 502-507 (2012).
294. A. Jahan-Mihan, B. L. Luhovyy, D. El Khoury, G. H. Anderson, Dietary Proteins as Determinants of Metabolic and Physiologic Functions of the Gastrointestinal Tract. *Nutrients* **3**, 574-603 (2011).
295. A. K. Buell *et al.*, Solution conditions determine the relative importance of nucleation and growth processes in alpha-synuclein aggregation. *Proc. Natl. Acad. Sci. U. S. A.* **111**, 7671-7676 (2014).
296. J. Prousek, Fenton chemistry in biology and medicine. *Pure Appl. Chem.* **79**, 2325-2338 (2007).
297. T. D. Rae, P. J. Schmidt, R. A. Pufahl, V. C. Culotta, T. V. O'Halloran, Undetectable intracellular free copper: The requirement of a copper chaperone for superoxide dismutase. *Science* **284**, 805-808 (1999).
298. M. J. Petris, The SLC31 (Ctr) copper transporter family. *Pflugers Arch* **447**, 752-755 (2004).
299. J. H. Kaplan, E. B. Maryon, How Mammalian Cells Acquire Copper: An Essential but Potentially Toxic Metal. *Biophys. J.* **110**, 7-13 (2016).
300. I. Horvath *et al.*, Interaction between Copper Chaperone Atox1 and Parkinson's Disease Protein α-Synuclein Includes Metal-Binding Sites and Occurs in Living Cells. *ACS Chemical Neuroscience* **10**, 4659-4668 (2019).
301. K. McFarthing *et al.*, Parkinson's Disease Drug Therapies in the Clinical Trial Pipeline: 2020. *J Parkinsons Dis* **10**, 757-774 (2020).